OK1DNZ's
Low-Loss
145/222 MHz
Diplexer

QEX

INCLUDING: COMMUNICATIONS QUARTERLY

About the Cover

Pavel Zanek uses only transmission lines in his new diplexer; story on p 23.

Features

Columns

May/Jun 2004 *QEX* Advertising Index

Empirical Outlook

History Often Gets It Wrong

It's nothing short of uncanny how some books attribute certain inventions or discoveries to the wrong person. Many myths propagate indefinitely because unwitting teachers reprogram each new class with the same questionable assertions. Physics, mathematics, astronomy and communications are replete with examples, some of which we shall mention here; but any field involving discovery or invention seems to suffer as much.

Ask anyone, "Who discovered America?" Those who have an answer are likely to say it was Christopher Columbus: It's in the history books. We even have a national holiday for the man although those same history books clearly relate that he was greeted by native Caribbeans on his arrival! It seems one cannot argue that he was the first European here, either.

The answer to "Who invented radio?" usually is "Marconi" and we know that is incorrect. Ask "Who invented the light bulb?" and you will get "Edison"—wrong. Who discovered Halley's comet, Edmund Halley? Nope. Who discovered Simpson's rule? Definitely not Thomas Simpson. It was known long before he was born. Who discovered Taylor series? Not Brook Taylor, but probably James Gregory. Maclaurin series? Not Colin Maclaurin. Cramer's rule? It was Maclaurin!

Who discovered the calculus, Newton or Leibniz? Now this is where we come to the crux of the matter. Isaac Newton almost certainly had the thing before Gottfried Leibniz, *but Leibniz published it first*, well before Newton did. Ordinarily that would be enough to establish priority, but Newton was President of the Royal Society in Great Britain and was surrounded by friends who attested that he discovered it first. The ensuing row shook European scientific communities to their foundations. Had Leibniz not published, he might have been forgotten despite his brilliance.

Why are our historical accounts so tainted? What is it about human nature that assigns credit where seemingly undue? Well, it is not really undue at all. In each case above, who got the credit was the one who took the concept to fruition and brought it to the people. Guglielmo Marconi and Thomas Edison were marketing geniuses as well as immensely capable engineers. Halley used theory to predict the orbit and return of that comet —a famous feat. Simpson and Maclaurin wrote popular books, expounding on equations that today bear their names. Newton's place in scientific history is firmly cemented but Leibniz gets his spot, too.

Write and write well. If you do it, you will not be forgotten.

In This Issue

Dick Lichtel, KD4JP, shows us how to build, program and operate a USB 1.1 interface. USB is one up-to-date way to make connections to your software radios, test equipment and other computer-controlled projects. Glen Gardner Jr, AA8C, brings us his receiver preamplifier based on the Mini-Circuits MAR-6. It is a reasonably easy construction project that performs.

Paolo Antoniazzi, IW2ACD, and Marco Arecco, IK2WAQ, return with their measurements of 2.4-GHz helical antennas. They include information about building a slotted-line coupler, allowing you to make return-loss measurements. Pavel Zanek, OK1DNZ, is back with another two-band diplexer. This one is for 2 m and 1.25 m.

Bill Rynone writes about ground planes made of composite materials such as metal-mesh and carbon-fiber cloth. Bob Zavrel, W7SX, takes a look at the relations among antenna aperture, gain and directivity. Bob focuses on equations that reveal what happens between two antennas.

Chris Sieg, WA3LDI, presents his "Uncoder," a nifty accessory for those 2-m and other rigs that don't have CTCSS, also known as PL or "private line." Neat features include automatic detection and setting of PL frequencies. Andrew Roos, ZS1AN, adds to the international flavor of this issue with his reduced-height vertical array. Analysis and optimization accompany construction details.

In *RF*, Contributing Editor Zack Lau, W1VT, tells how to stack 2-m Yagis for good performance—*Doug Smith, KF6DX,* **kf6dx@ arrl.org**.□□

Implementing a USB Equipment Interface Using the Microchip PIC16C745

COM ports are becoming scarce. Come learn how to interface projects the modern way with USB.

By Dick Lichtel, KD4JP

Since the advent of personal computers, Amateur Radio has striven to connect equipment to them. The primary interface has been the ubiquitous serial port. Intel developed the Universal Serial Bus[1] (USB) in the early 90s, and while many PC peripherals now support this interface, Amateur Radio experimenters and equipment manufacturers have not kept up with the technology. Owners of newer PCs have found the number of parallel and serial ports has dwindled down to one of each, while the number of available USB ports has substantially increased (there are six

[1]Notes appear on page 8.

6545 Canal Rd.
Melbourne Village, FL 32904-3622
rlichtel@cfl.rr.com

on my PC). It is likely that PCs in the future will contain no EIA-232 serial ports. The legacy-free system-requirements section of the PC2001 system design specification requires the removal of serial and parallel ports (among other legacy ports) from the PC hardware.[2] As part of the specification, USB ports are required on new machines. Each USB port can support up to 127 devices.

Many believe that a strong knowledge of *Windows* programming, down to the device-driver level, is needed to support USB in their equipment. This article attempts to show that this is simply not true. *Windows* provides default drivers that we can use and that will take most of the work out of programming the *Windows* interface.

Microchip has several parts that include hardware support for USB 1.1.

Microchip provides sample PIC code that implements the USB 1.1 protocol.[3] In this article, I will explain how to utilize the Microchip PIC16C745 microcontroller and discuss methods for communicating with this device. I have also included functional source code for the PIC firmware as well as PC based code to communicate with the PIC.[4]

Microchip PIC16C7X5 Controllers

In 2000, Microchip introduced the PIC16C745[5] and PIC16C765 8-bit microcontrollers with USB. These controllers are similar in architecture and instruction set to other PIC16C and PIC16F series microcontrollers, which are used in many Amateur Radio projects. This compatibility should make it easier to adapt many existing

projects over to this PIC.

The PIC16C745/765 microcontroller features 8 kB of program memory and 256 8-bit memory registers, 11 interrupt sources, 22 ports (33 for the 765), three timers, five 8-bit A/D (eight for the 765) as well a USART and USB interface. The PIC16C765 also offers a parallel slave port.

Microchip supplies the development tools needed to develop applications for their microcontrollers for free.[6] The tools include a macro assembler, linker, librarian and *MPLab* Integrated Development Environment (IDE). The IDE also includes a PIC simulator and debugger. Microchip sells a *C* language compiler. There are third-party *C* compilers such as Hi-Tech (**www.htsoft.com**) that are supported by the *MPLab* IDE.

Microchip also sells PIC programmers; however, they are much more expensive than third-party programmers, such as the Newfound Electronics WARP-13a programmer (**www. newfoundelectronics.com**). The WARP-13a programmer is also compatible with the Microchip PICStart Plus! Programmer, so microcontrollers can be programmed

inside of the *MPLab* IDE.

Microchip has written example source code for the PIC16C7X5, which provides the protocol for USB 1.1 in both assembly and *C*.[7] The example source code is not immediately useful since the routine necessary for bi-directional communications with the device is commented out. The documentation supplied with the source code describes how the firmware implementation works and documents the software methods.

In conjunction with this article, I have supplied functioning firmware, source code and *MPLab* project files that support bi-directional communications with the PIC16C745. Because the assembler is free and the *C* compiler is not, the source code for the firmware is in assembly.

Communicating with the PC

Once your PIC is programmed with the supplied firmware, the PIC will simply await reception of eight bytes of data and echo them back to the PC. The number of bytes sent and received is a function of a pair of variables set in the firmware and is of fixed size. One of the files included with the firm-

ware is a linker definition file that has been adapted for this project; the default linker file provided by Microchip with *MPLab* will not work with this firmware.

To adapt this assembly code to work with your specific project, you may need to make a couple of changes in *descript.asm* that depend upon your implementation. Change only these fields!

First, you must decide whether the PIC is to be powered from an external supply or from the USB connection. If powered by the USB bus, you must know how much current it will draw. If the PIC circuitry will be self-powered, set the hex values to 0. If it is to be powered from the USB bus, leave its value at 0x80 and change the subsequent hex value of 0x0D (26 mA) to the maximum current your circuit will draw.

$$Value \quad \frac{MaxCurrent}{2} \qquad \text{(Eq 1)}$$

Current is expressed in milliamperes, with a maximum draw of 100 mA. These variables are found in the routine "Config1" as shown in Code D.

Second, you should decide how
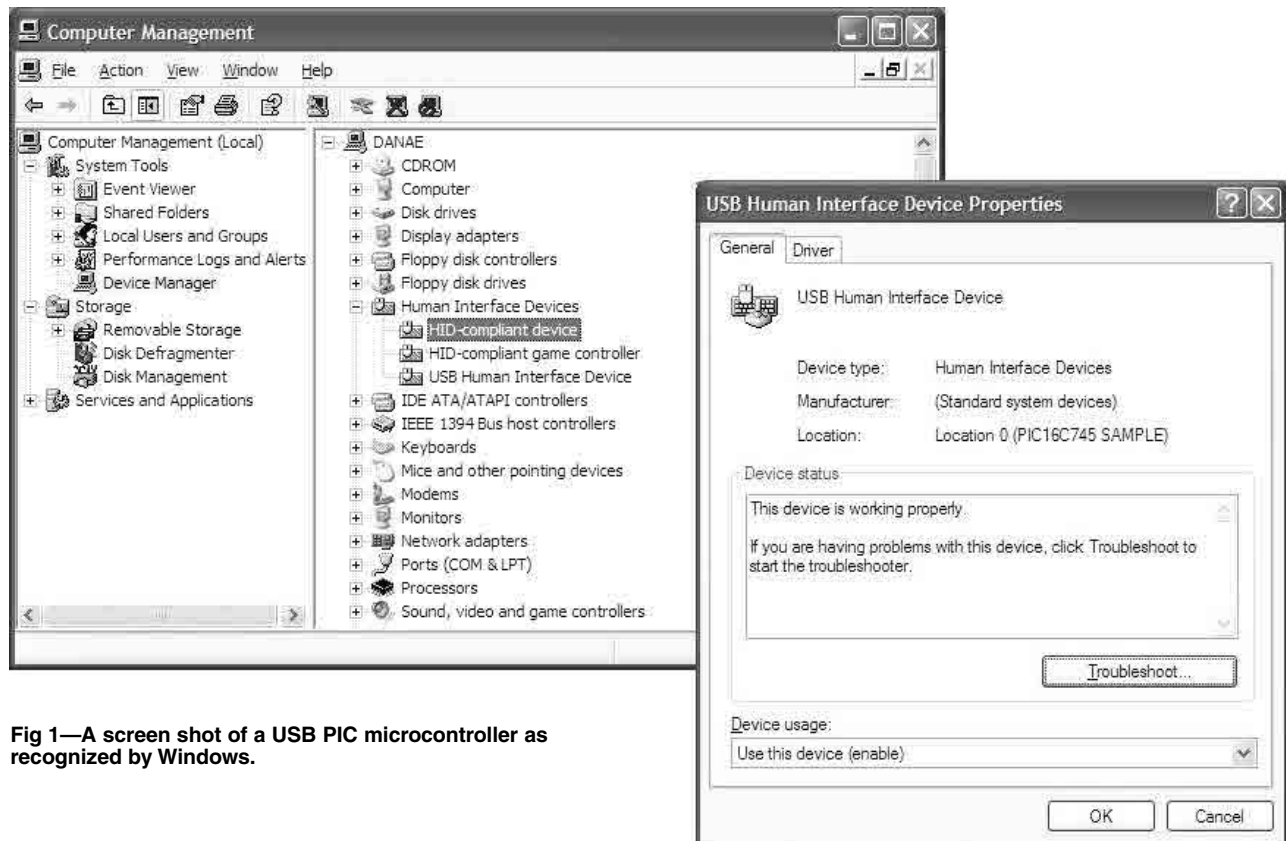
Fig 1—A screen shot of a USB PIC microcontroller as recognized by Windows.

Code A

```
pagesel      InitUSB                ; These lines of code show the appropriate
call         InitUSB                ;  way to initialize the USB. First, initialize

ConfiguredUSB    ; wait until the enumeration process is
                                          complete.

CheckEP1                            ; Check Endpoint 1 for an OUT transaction
    bankisel  Buffer                ; point to lower banks
    pagesel   GetEP1
    banksel   Buffer
    movlw     Buffer                ; Data to be recv'd will be put in Buffer
    movwf     FSR                   ; Point FSR to our buffer
    call      GetEP1                ; if data is ready, it will be copied.
    Pagesel   CheckEP1
    btfss     STATUS,C              ; was there any data for us?
    goto      CheckEP1              ; Nope, check again.

PutBuffer
    bankisel  Buffer                ; point to lower banks
    pagesel   PutEP1
    movlw     Buffer
    movwf     FSR                   ; Point FSR to our buffer
    movlw     0x08                  ; send 8 bytes to the Host
    call      PutEP1
    pagesel   PutBuffer
    btfss     STATUS,C              ; was it successful?
    goto      PutBuffer             ; No: try again until successful
    pagesel   CheckEP1
    goto      CheckEP1              ; Yes: restart loop
```

Code B

```
char HIDDevicePath[]=
"\\?\hid#vid_04D8&pid_1234#7&1bf5e077&0&0000#{4d1e55b2-f16f-11cf-88cb-001111000030}";
FileHandle=CreateFile (HIDDevicePath,
      GENERIC_READ|GENERIC_WRITE,
      FILE_SHARE_READ|FILE_SHARE_WRITE,
      (LPSECURITY_ATTRIBUTES)NULL,
      OPEN_EXISTING,
      0,
      NULL);
```

Code C

```
// default data size is 9 (8 data bytes + 1 for the report #)
CHIDDevice HIDDevice;
//The ID, product ID & version# are from the PIC firmware
DWORD dwVendorID(0x04D8),dwProductID(0x1234),dwVersionNumber(0x0079);
if(HIDDevice.Connect(&dwVendorID,&dwProductID,&dwVersionNumber))
{
      byte abytes[9];
      memset(abytes,0,sizeof(bytes));
      memcpy(abytes+1,"1234",4);        // Byte[0] must always be 0
      HIDDevice.Write(abytes);
      HIDDevice.Read(abytes);
      // HIDDevice automatically closes the device when it goes out of scope
} //end if
```

large the data packet size needs to be. Data exchanged between the PC and the microcontroller is a fixed size. The supplied code assumes the data arrives and is sent in eight-byte blocks. If you change the block size, two instances of "report Count" need to be changed. These values are found in the routine "ReportDescriptor" in descript.asm as shown in Code F. Low-speed devices like this one are limited to a maximum of eight-byte blocks.

Next, change the hex values for the idVendor(0x4D8), idProduct(0x1234) and bdcDevice(0x0079) values in descript.asm as shown in Code E. These don't really need to be changed unless they conflict with other USB devices in your system or you plan on mass-producing the part. If you are an equipment manufacturer, you will need to purchase your own unique Vendor ID. More information on obtaining a Vendor ID can be found at **www.usb.org/ developers/vendor/**. The default idVendor is 0x04D8 and is the Microchip Vendor ID. These values are found in the routine "DeviceDescriptor."

Finally, you will want to change the string descriptors, which designate the product name and version of your PIC (shown in Code G). You can also add support for different languages. The product name shows up in the *Windows* Device Manager when you display the properties for the device. The version string is useful if you want to poll the firmware for version number. These variables are found in the "String" routines at the end of the module (descript.asm).

The lines that can be changed are noted with identifying comments; search the file for the string "****Change."

The documentation supplied with the Microchip sample code details the USB methods. There are really only two routines of interest to the programmer: PutEP1 and GetEP1. These methods send and receive data from the PC host. Of secondary importance are InitUSB and ConfiguredUSB. These methods initialize the PIC and have it wait for the device to be connected to a host computer. Until the PIC is connected to a computer, the code will stay in a loop inside of ConfiguredUSB. Code A is a snippet of code from *main.asm* that shows how to read data from the PC and send it back.

I have added a little more code in my version of *main.asm*; if the PIC is sent "?V" (without quotes), the firmware will return the firmware version string.

While the PIC16C745 runs off an external 6 MHz clock, the PIC must

be configured to run internally at 24 MHz for the device to function properly running the USB firmware. Do this by setting the PIC configuration bit E4_OSC if you are using a clock generator, or H4 if you are using a crystal oscillator. The USB specific code consumes about 1 kB of the 8 kB program memory and 40 bytes of memory in Bank 2.

Communicating with the Microcontroller

Microchip implemented the USB protocol so that the device appears as a Human Interface Device (HID). This is the same class of device as mouse, joystick or keyboard. *Windows* provides native support for HID devices.[8] If the firmware is implemented correctly, when the device is plugged into a PC *Windows* will recognize a new device and automatically install the HID driver (if its not already installed). If you open the *Windows* Device Manager you will see your device under the HID device(s). Fig 1 shows the microcontroller as listed in the *Windows* Device

Manager. This microcontroller is also recognized by *LINUX* as an HID device. The methodology for communicating with this device under Windows should also apply to *LINUX*.

To communicate with the microcontroller, you need to know the path to the device. Once this path is known, the microcontroller can be opened as a file; you then can read/write to the device just like any other file.

There are two ways of finding the path to the microcontroller. The first method involves using the Microchip developed HIDComm.ocx[9] Active-X control. This control provides a method that browses the HID devices, displaying a dialog that allows the user to pick the device and returns the full path to the device. It also supplies methods to search for the device based upon vendor and product IDs (among other fields). These are the variables you may have changed when you created the firmware. The Active-X control is most useful to *BASIC* programmers. It can also be used with *C* and *C++*; but some of the other meth-
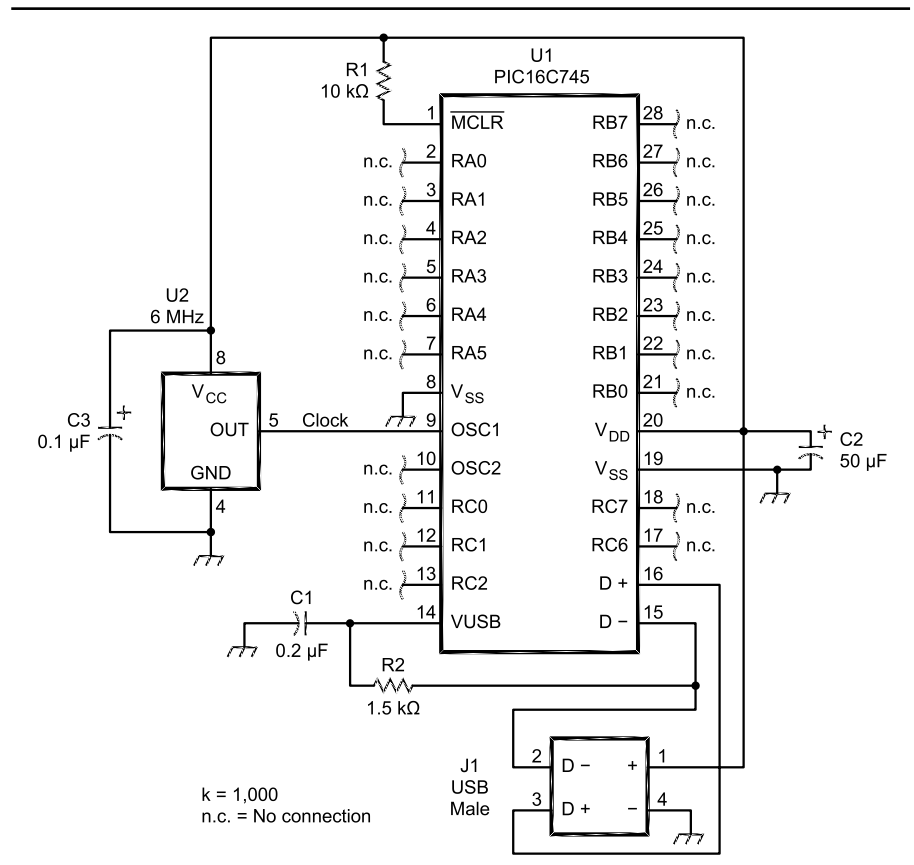
Fig 2—PIC16C745 schematic, USB powered.

U1—PIC16C745, Digi-key part #PIC16C745/ JW-ND
J1—USB 4P Male Type B Connector, Digi-key part #AE1085-ND

U2—6 MHz Epson Electronics CMOS/TTL Oscillator, Digi-Key part #SE1206-ND

ods require data conversion to adjust for the way strings are implemented in *BASIC*, which is very tedious for *C/C++* programmers.

The second method, which is probably more appealing to *C/C++* programmers, utilizes a couple of routines from the *Windows* Driver Development Kit (DDK). It involves enumerating the HID devices, searching the list for your device, and then getting the path. The *Windows* DDK is free (nearly) from Microsoft (**www.microsoft.com/ddk/**). The DDK itself is free but Microsoft insists on charging $15 for priority shipping.

Once you know the path to device, a *Windows* API call can be used to connect to the device. Notice in snippet Code B, that the path is rather complex. Also note that the vendor and product IDs (from the firmware) show up in the path.

I have included a *C++* class devel-oped for communicating with the PIC microcontroller. Along with the *C++* class, I have included the HID library(hid.lib) and header file(hid.h) which are needed to use the *C++* class. Since the DDK library only supports *C*, I have adapted the hid.h header file so it can be used with both *C* and *C++*. Code C shows how to use my *C++* class for communicating with the PIC.

While the firmware is configured to send and receive eight bytes, the USB protocol requires an additional byte for the report number. The firmware expects the report number as the first byte and for it to always be 0. So, the PC needs to send nine bytes, the first byte always being 0 and the remaining eight bytes being your data. The PC will receive nine bytes with the first byte being 0 and the remaining eight bytes containing the data.

Another important consideration when sending multiple byte numbers to the PIC is that the PC formats numbers in Little Endian format[10] and the equipment you have interfaced to the PIC may expect numbers in Big Endian format.

Fig 2 shows a schematic for a self-powered PIC16C745. Because the device operates as a slow-speed USB device, D– (pin 15) is tied to VUSB (pin 14) via R2. The power coming from the PC can be rather noisy, so a large capacitor is used across the supply. R1 is not strictly necessary and $\overline{\text{MCLR}}$ could be tied directly to VCC.

I wrote a benchmark program to measure the data rate for sending and receiving eight bytes of data (18 bytes total exchanged including the report-number byte) over 1000 cycles. The data rate was calculated a little more than 2 kB/s. Because the PIC is a low-speed USB device, this is the maximum data rate.

Code D

```
Config1 ...
    retlw 0x80 ; bmAttributes attributes - bus powered ****Change this to 0 if your device is self powered
    retlw 0x0D ; MaxPower 26 mA from the bus. ****Change this to match the current drawn by your circuit.
    ; Do not exceed 100mA otherwise Windows might not accept your device. The value is the max current/2.
```

Code E

```
StartDevDescr
    ....
    DT 0xD8,0x04 ; idVendor 0x04D8 ****Change this to uniquely ID your PIC. Note low order byte 1st
    DT 0x34,0x12 ; idProduct 0x1234 ****Change this to uniquely ID your PIC. Note low order byte 1st
    DT 0x79,0x00 ; bcdDevice 0x0079 ****Change this to uniquely ID your PIC (device version#) low byte 1st
```

Code F

```
ReportDescriptor
    ...
    DT 0x95,0x08 ; report count (8) (fields) .. ****Change 0x08 to the # of bytes you need, max of 8 ...
    DT 0x95,0x08 ; report Count (8) (fields).. ****Change 0x08 to the # of bytes you need, max of 8
```

Code G

```
String1_l1
        retlw String2_l1-String1_l1 ; length of string
        DT 0x03 ; string descriptor type 3
        DT'M',0x00,'i',0x00,'c',0x00,'r',0x00,'o',0x00,'c',0x00,'h',0x00,'i',0x00,'p',0x00

String2_l1 ;****Change this string to match your product name
        retlw String3_l1-String2_l1 ;
        DT 0x03
        DT  'P',0x00,'I',0x00,'C',0x00,'1',0x00,'6',0x00,'C',0x00,'7',0x00,'4',0x00,'5',0x00,' ',0x00
        DT  'S',0x00,'A',0x00,'M',0x00,'P',0x00,'L',0x00,'E',0x00
        global String3_l1

String3_l1 ;****Change this string to match your product version
        retlw String4_l1-String3_l1
        DT 0x03
        DT  'V',0x00,'1',0x00,'.',0x00,'0',0x00,'0',0x00
```

Summary

In summary, this paper has provided the reader with basic information for integrating a USB interface into Amateur Radio hardware. Our goal as Amateur Radio operators has always been to develop hardware and software that furthers the state of the art; but in this area, we have clearly fallen somewhat behind. I hope this paper has shown that USB can be easily adopted, and that programming for USB is not all that difficult. With the supplied PIC firmware and *Windows C++* class, the task of developing the hardware and software to utilize the USB PC interface has been made even easier. Finally, I hope this article also inspires the major equipment manufacturers to stop relying on serial ports for their PC interfaces and begin to integrate USB technology into their products.

Notes

[1] A good overview of the Universal Serial Port Implementation can be found at **www.quatech.com/support/techoverview. php.**

[2] Intel and Microsoft Corporation, *PC 2001 V 10*, Chapter 3.

[3] The USB 1.1 and 2.0 specifications can be found at **www.usb.org/developers/docs/**.

[4] You can download this package from the ARRLWeb **www.arrl.org/qexfiles/**. Look for 0504Lichtel.zip.

[5] Microchip, PIC16C745/765 datasheet Rev DS41124C; **www.microchip.com/1010/pline/picmicro/category/perictrl/14kbytes/devices/16c745**.

[6] Microchip development tools can be obtained from: **www.microchip.com/1010/pline/tools/picmicro/devenv/mplabi/mplab6/index.htm**.

[7] Assembly and *C* based firmware can be obtained from: **www.microchip.com/1010/pline/picmicro/category/perictrl/14kbytes/devices/16c745/index.htm**.

[8] OSR2 is required for *Win95*. *NT* 4 users should install the latest service pack.

[9] HIDComm can be obtained from **www.microchip.com/1010/suppdoc/appnote/codxamp/9073/**.

[10] Dr. W. T. Verts, "An Essay on 'Endian' Order," **www.cs.umass.edu/~verts/cs32/endian.html**, April 1996.

Dick was first licensed in 1977 and in 1999 upgraded to Extra. He is an ARRL life member. Dick graduated from Siena College in 1979 with a BS in Physics. He has worked for Harris Semiconductor and Intel and is now somewhat retired. He has authored several IEEE papers and is an inventor on four patents on semiconductor processing. Dick wrote PakTerm *(later licensed by AEA and became* PcPackratt II) *and* PcPakratt for Windows.　□□

REQUEST FOR INFORMATION ON GIGAHERTZ AND TERAHERTZ SPECTRUM

ARRL seeks information on spectrum requirements and preferred frequency bands in the spectrum above 275 GHz toward studies now underway by the United States Government and the International Telecommunication Union (ITU). The preliminary agenda for the 2010 World Radiocommunication Conference includes an item to consider frequency allocations between 275 GHz and 3000 GHz. Other studies are being conducted on bands well above 20 THz.

While no frequencies have been allocated above 275 GHz, there is growing interest, particularly for scientific and space applications. Amateurs can presently use any frequency above 300 GHz but this could eventually change if the ITU makes allocations to radio services. Amateur spectrum requirements and preferred frequency bands in the range 275-1000 GHz have been documented by the International Amateur Radio Union in **www.iaru.org/ac-spec02.html** and are being studied by the ITU along with similar information from other radio services. The preferred bands in the 275-1000 GHz range were chosen primarily because they are bands where atmospheric attenuation is low.

The need is for information on frequencies above 1000 GHz:

• What is the best scientific data available on the attenuation (or other propagation phenomena) in parts of this band? (Please see Figs 1 and 2, which pertain only to vertical paths.)
• What are the anticipated amateur and amateur-satellite uses of these bands?
• How much bandwidth is required for these uses?
• If sharing is necessary, which other radio services would be the preferred sharing partners and why?

Please provide information to ARRL Chief Technical Officer Paul Rinaldo, W4RI; e-mail **prinaldo@arrl.org**.
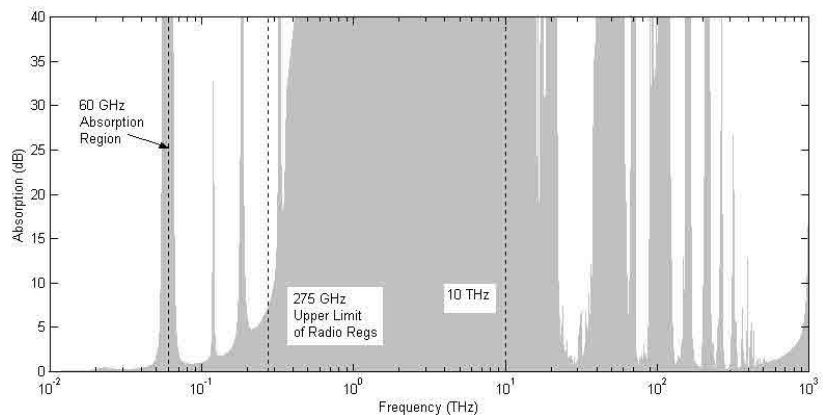
Fig 1—Absorption (shaded area) of a standard atmosphere along a vertical path.
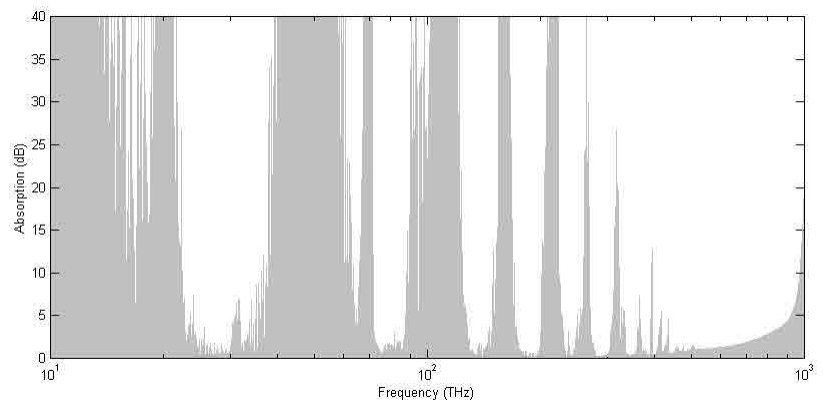
Fig 2—Absorption (shaded area) above 10 THz of a standard atmosphere along a vertical path.　□□

A Ruggedized, General Purpose 100 kHz-2 GHz Low-Noise RF Preamplifier

Good performance doesn't require many parts.

By Glen E. Gardner Jr, AA8C

Some time ago, I was experimenting with a homebrew VHF receiver for use with weak-signal over-the-horizon voice and satellite communications. Out of that project, came a number of small projects that I have since found to be very useful for my other Amateur Radio interests. One of these little bits is a wide bandwidth preamplifier that I have found to be a good performer that is very inexpensive and easy to build.

The circuit is based on the use of the MAR-6 monolithic amplifier integrated circuit made by Minicircuits. It is inexpensive, readily available from a number of sources and extremely easy to handle. The preamplifier features high gain, low noise, a regulated power supply for good isolation from external noises on the supply side, transformerless construction for good bandwidth and reverse polarity protection on the power-supply input.

Additionally, the low component count makes the project simple and easy to complete. The use of double-sided, copper-clad glass-epoxy board material for the enclosure insures low cost, lightweight and high mechanical strength while offering excellent RF integrity. A schematic, board templates, enclosure templates and component list are available in electronic format.[1]

The specifications for this preamplifier are taken to be those of the MAR-6 amplifier as stated by Minicircuits. The performance the builder achieves will depend largely on construction practice and individual variations in component tolerances. Although the equipment to perform exhaustive testing of the preamplifier was not available to me, my experience has shown that the performance claims for the MAR-6 are reasonably close to truth, and repeatability of the circuit is quite good. I have built and used several of these preamplifiers.

Theory of Operation

Please refer to the schematic in Fig 1. An operating voltage, +V, ranging from about 9.5 to 15 V dc (13.8 V dc, nominal) is applied to the anode of D1.

D1 provides reverse-polarity protection for U2 and C5. U2 is a ZR78L07 linear voltage regulator. The regulator features 200-mA current capacity with current limiting and thermal overload protection. It requires a minimum operating voltage of 8.7 V dc and tolerates a maximum input of 20 V dc. The regulator is very quiet, with a nominal noise output of

8 Parkway, Apt L
Greenbelt, MD 20770
Glen.Gardner@verizon.net

[1]You can download this package from the *ARRLWeb* **www.arrl.org/qexfiles/**. It includes full-size copies of Figs 6 and 7. Look for 0405GARDNER.ZIP.
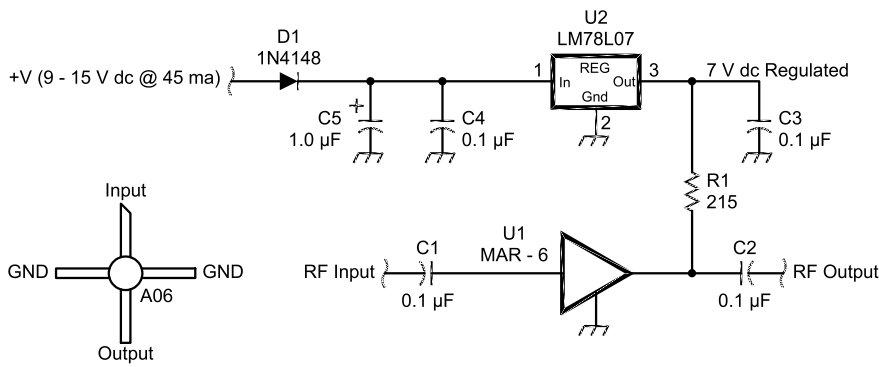
Except as indicated, decimal values of capacitance are in microfarads (μF); others are in picofarads (pF); resistances are in ohms.

Fig 1—A schematic for the preamplifier. Gain: 20 dB@100 MHz; 18.5 dB@500 MHz; 16.0 dB@1000 MHz; 11.0 dB@2000 MHz; NF 3.0 dB; IP3 +14.5 dBm; SWR<1.5:1.
C1-C4—0.1 μF 50 V dc ceramic.
C5—1.0 μF 35 V dc tantalum.
D1—1N4148.
R1—215 Ω, ⅛ W.
U1—MAR-6 monolithic amplifier.
U2—78L07 regulator, 7 V dc at 150 mA.

75 μV RMS. It provides an extremely quiet power source for the MMIC preamplifier.

Operating the preamplifier with input voltages near its maximum rating can lead to elevated operating temperatures in the regulator, so the circuit is derated conservatively to operate with a reduced maximum +V input of 15 V dc. Operating the regulator near its minimum input specification reduces the regulator's noise immunity, potentially spoiling the noise floor of the preamplifier. For these reasons, a nominal input voltage of 13.8 V dc was chosen to insure

that the regulator operates at an acceptable temperature with low-noise output. U2 provides low noise, regulated +7 V dc to R1 and also isolates the MMIC amplifier (U1) from the external power source. C3, C4 and C5 provide adequate dc transient filtering and RF decoupling to assure quiet operation of the voltage regulator.

R1 delivers power to U1 while acting to limit current and drop the supply voltage for U1 to acceptable levels for proper operation. U1 is a Minicircuits MAR-6 MMIC amplifier circuit. Normal operation requires 3.5 V at 16 mA. According to Minicircuit's lit-

erature, the value of bias resistor R1 is calculated as:

$$R1 = \frac{V_{cc} - V_d}{I_d} \qquad \text{(Eq 1)}$$

In this case, V_{cc} is 7 V dc, V_d is 3.5 V, and $I_d = 0.016$ A. Given these parameters, the ideal value is:

$$R1 = \frac{7 - 3.5}{0.016} = 218.75\,\Omega \qquad \text{(Eq 2)}$$

A slight increase in the nominal operating voltage is not detrimental, thus a value of 215 Ω was chosen from resistors in stock. This value for R1 provides an operating voltage of 3.56 V at the rated 16 mA current.

Of particular interest is the lack of a series choke between the bias resistor (R1) and the amplifier output/bias pin. This arrangement leaves the output with a minor impedance mismatch. Given the tendency of most chokes and many RF transformers to have limited usable frequency ranges and unwanted resonances, the small loss due to impedance mismatch without a choke seems trivial. Minicircuits gives the loss in power gain due to the output impedance mismatch as:

$$20\log\left(\frac{2Rbias + 50}{2Rbias}\right) \qquad \text{(Eq 3)}$$

In this case,

$$20\log\left[\frac{430 + 50}{430}\right] = 0.95\,\text{dB} \qquad \text{(Eq 4)}$$

Fig 2—The component-placement guide for the preamplifier. Be sure to carefully check the orientation of U1 and U2 prior to soldering.
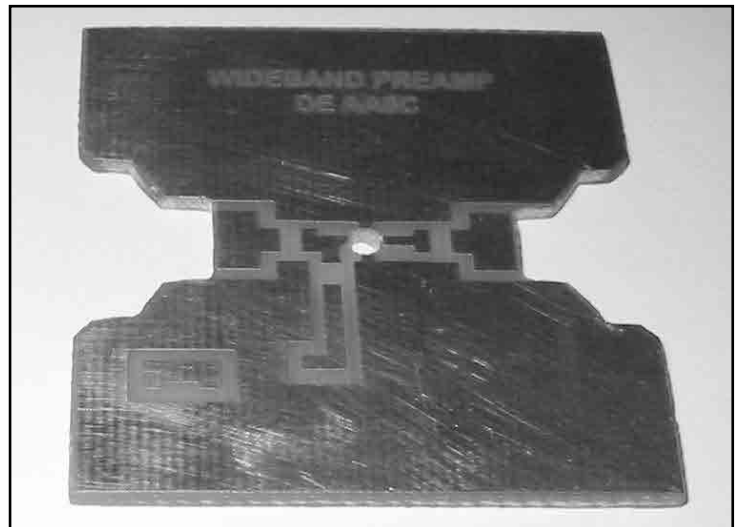
Fig 3—The fabricated board after cutting and drilling.

Thus, the 1-dB performance loss is easily tolerated in favor of simplicity, lower component count and good bandwidth performance.

C1 and C2 provide dc blocking for the input and output of the RF-amplifier circuit to assure that external dc loads or current sources do not adversely affect the proper operation of the amplifier. The 50 Ω nominal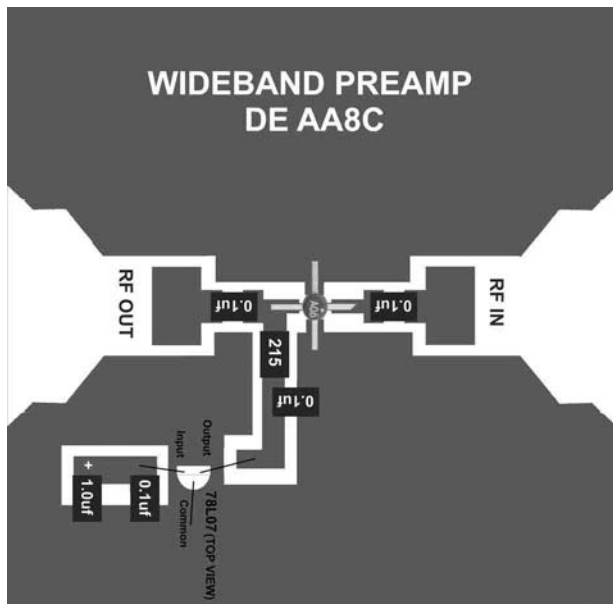 input and output impedances of U1 are low enough that the reactance of C1 and C2 roll-off the low-end frequency response of the RF amplifier is conservatively rated at 100 kHz. For this application, the 6 dB cutoff point is taken as: $Xc = 50\ \Omega$, $C = 0.1\ \mu F$ and

$$f = \left[\frac{\frac{1}{Xc}}{2\pi C}\right]^2 = \left[\frac{0.02}{6.28 \cdot 10^7}\right]^2 = 63.69\ \text{kHz} \tag{Eq 5}$$

Making the Board and Enclosure

The preamplifier circuit board was made photographically from single-sided, $1/16$-inch thick, glass-epoxy circuit-board stock.

Full size negative templates for the board (Fig 6) are available electronically for those wishing to photo-fabricate their own boards. I strongly recommend that the preamplifier board be made as a single-sided board. Experience with early prototypes suggests that using a double layer board with this design will likely degrade the noise figure and ruin the frequency response of the amplifier because of the oversized pads at the center pins of the BNC connectors.

The original enclosure was cut from double-sided glass-epoxy board stock that had been photo fabricated. Using 300 dpi templates (Fig 7). The use of good quality double-sided board stock for the enclosure is important to assure adequate mechanical strength. Full-size negative templates for the enclosure sides and enclosure top and bottom are also available in electronic format (see Note 1).

Construction Practices

The semiconductors used in this project are easily damaged by electrostatic discharge, so be sure to observe proper ESD precautions during construction and testing of the preamplifier. The components are very small, and a little precision is required to get everything to fit together, as it should. Some magnification will help. Use a temperature controlled ESD-rated soldering iron with suitably small tips. A pair of nonmagnetic tweezers is useful for handling and holding small parts. If you are new to surface-mount

technology, use a tiny amount of paste flux to adhere the parts to the board prior to soldering. This helps reduce the tendency of the components to skate around and stand on end ("tombstone") when soldering. For surface-mount resistors and capacitors, tin one pad first, then hold the opposite end of the component with nonmagnetic tweezers while soldering it in place.

Newcomers to SMT might want to practice with some scrap pc-board stock and spare parts. Once you get the hang of it, SMT is easy, but learning to solder components that are just a couple of millimeters wide can be intimidating at first.

Building the Preamplifier Board

Manufacture the preamplifier cir-
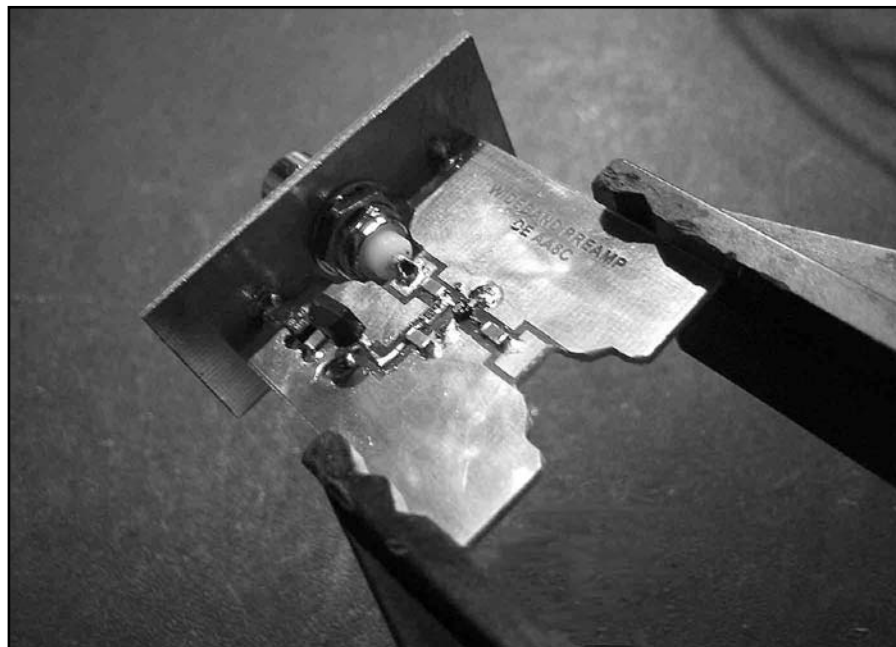
Fig 4—Fabricate the board and install the components, then install the end plates and BNC connectors. Tack solder the end plates and connector in place temporarily if needed.

Fig 5—After all the panels are in place, carefully solder and fillet all seams before installing D1 and the feedthrough filter. Solder the BNC center pins after completing the assembly of the enclosure sides to be sure of adequate stress relief for the connections.
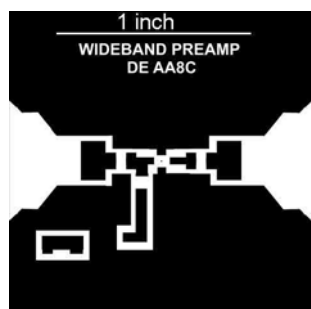
Fig 6—A negative etching template for the circuit board. It's best to use single-sided board material here.

Fig 7—A negative etching template for the enclosure sides, top and bottom. Use double-sided board material for good mechanical strength.

cuit board and cut out the clearance notches for the BNC jacks at both ends of the board (Fig 3). Test fit the end panels against the ends of the board by temporarily installing the jacks on the end panels. Work slowly, this is a cut-and-try operation. Carefully trim excess board material from the circuit board cutouts (the large end areas with no foil). Rough cut the board with a hand grinder or a nibbling tool. Fine trimming can be accomplished with a small file. Some BNC jacks are a little longer than others and require that the center pin be trimmed in order to avoid clearance issues with the 0.1 μF coupling capacitors at C1 and C2. In addition, the drop-in package of the MAR-6 requires a 5/64-inch hole drilled at the mounting point so that the amplifier can be mounted flush with the surface of the board. The surface-mount version of the MAR-6 does not require this hole.

Install the MAR-6 amplifier first, following the layout provided in Fig 2. You may need to trim the leads of the MAR-6 in order to get proper clearance for the pads at C1 and C2. Next, install the resistor and the capacitors, being careful to allow enough pad space for the tips of the chassis mounted BNC jacks near C1 and C2. Install the voltage regulator (U2) last. Be careful to install the voltage regulator close enough to the surface of the board so that the top cover can be installed when the enclosure is assembled. To prepare the regulator IC for installation, cut the leads to an appropriate length, then bend them to form small "feet" that can be soldered to the circuit board pads. Be sure the regulator's package will not interfere with the placement of the feedthrough capacitor and diode D1 when they are installed later. Don't install the BNC jacks, enclosure panels, feedthrough capacitor or diode (D1) until the board
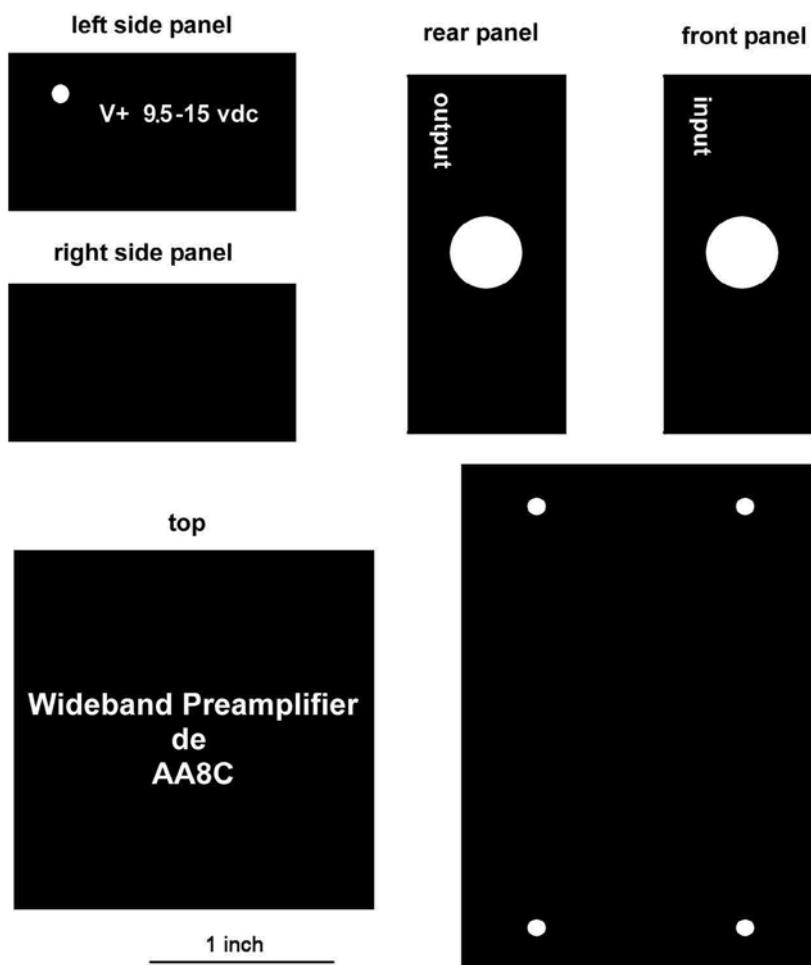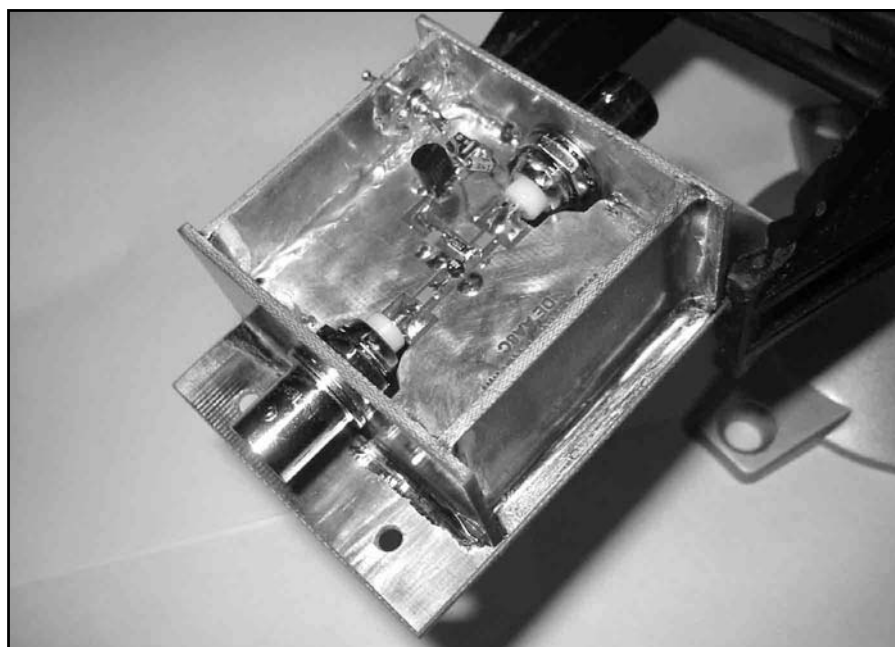
Fig 8—The completed preamplifier prior to testing and installation of the enclosure lid. Notice the long leads on D1. The long, bent leads allow for adequate stress relief in order to avoid cracking the diode with flexing of the enclosure.

is fully stuffed and the enclosure is ready for assembly.

Building the Enclosure

The enclosure for the prototype preamplifier was cut from surplus, double-sided, $1/16$-inch G-10 glass-epoxy circuit board using a small sheet metal shear. FR-4 glass-epoxy laminate is equally suitable. Phenolic resin board proved too brittle to be usable for the enclosure. Two-ounce copper board stock was used on the enclosure panels and cover plates. One-ounce per square foot copper-clad material is likely to be equally suitable, because the peel strength for copper-clad board material is about the same regardless of the copper thickness. Use good quality material for the enclosure and strength won't be a problem.

Final Assembly

Install the BNC jacks on the end panels prior to assembling the enclosure around the completed board. Test fit the end panels to the circuit board and carefully trim the preamplifier circuit board cutouts to allow proper clearance for the BNC jacks per the instructions above. Be sure that the circuit board is centered properly and sits flush against the end panels. Also, be sure the center pins of the BNC jacks are in contact with the oversized foil pads provided on the circuit board and do not interfere with C1 and C2 as discussed earlier. When done, square up the end panels with respect to the board and solder the seams where the boards meet the end panels. You can tack spots temporarily to hold things together and make the soldering easier (see Fig 4), but be sure to establish a good solder connection at every seam where one copper panel meets another. Likewise, install the side panels and solder them in place. Also, be sure that the inside and outside corners where the side panels meet the end panels are soldered. Fillet all seams and leave no unnecessary gaps (see Fig 5). If copper meets copper, solder it. This is important both for low-noise operation and good mechanical strength.

To reduce mechanical stress on the connections at the BNC jacks, do not solder the center pins to the board until the preamplifier board and enclosure side panels have been completely assembled.

When done, install a feedthrough capacitor or a through-hole filter in the hole provided for power in the side panel and install D1 carefully to allow sufficient lead length for stress relief (fiberglass enclosures flex a lot).

Next solder the center pins of the BNC jacks to the board and inspect all solder connections. The preamplifier is now ready for testing. If the test is a success give yourself a pat on the back and complete the enclosure assembly.

After inspection and testing is complete, clean the board as needed and install the top and bottom covers. Then solder all external seams carefully (see Fig 8). For those who want to remove the cover easily, I suggest tack soldering the corners of the top cover for easy removal in the event that servicing is needed at a later date.

Caveats

Very strong signals (greater than 13 dBm) will damage the MAR-6 amplifier. The addition of a pair of front-to-back small signal diodes on the input of the amplifier to limit input amplitude ought to remedy this issue at some cost to performance at VHF frequencies and above. For those needing good performance at VHF and above, I suggest arriving at some other means of resolving this issue.

Don't apply power without first properly terminating the input and output of the amplifier. I have used these preamplifiers hard and long and have not experienced any troubles with instability, but the MAR-6 is not guaranteed to be unconditionally stable. Connecting/disconnecting the input or output of this preamplifier when the power is applied could lead to instability and sudden failure of the amplifier. The same precautions should be taken with any high performance preamplifier because many high-gain preamplifiers are not unconditionally stable and may oscillate destructively if the input impedance is badly mismatched. Be sure you power down the preamplifier before connecting/disconnecting and you will avoid this issue completely.

Glen holds an AS in Natural Science and Mathematics, a BS in Geology and an MS in Geology all from Ohio University. Heathkit formerly employed him as a Senior Technician (from 11/78 to 2/84). His present employer is Global Science and Technology (GST), a contractor to NASA Goddard Space Flight Center (GSFC). He worked in the Laboratory for Extraterrestrial Physics at the NASA GSFC from April 2000 through August 2003, building payload instruments for sounding-rocket studies of the ionosphere. He presently works as a computer systems engineer in the Earth Sciences directorate NASA GSFC.

He has been an Amateur Radio operator since 1971 (originally WN8GSJ, upgraded later to WB8GSJ, then AA8C in 1977). He enjoys experimenting with electronics, especially radio circuitry and unusual/original designs. He built his first radio (with help from his father) from a Scouting Handbook when about nine years old. Al Beeler, WA8LHJ (SK), helped troubleshoot it. Glen still has the LLH Bunnel "grandfather" telegraph key Al gave him when Glen began learning the CW for the Novice license several years later. From the very first time he burned his fingers with a soldering iron, Glen knew that he wanted to build radios.

Glen's most memorable times with Amateur Radio have been: ragchewing at the low end of 40 meter CW late at night with an HW-16, working sporadic-E skip on 6 meter AM back in Ohio and tearing up the Midwestern US on 2 meter SSB when he lived in Michigan.

His present-day interests in Amateur Radio are 95% experimental ELF/VLF/HF (reception, mostly), particularly working with surface-mount technology. His latest project is a simple, completely inductorless microprocessor-controlled radio (more on this in the months ahead as time permits). □□
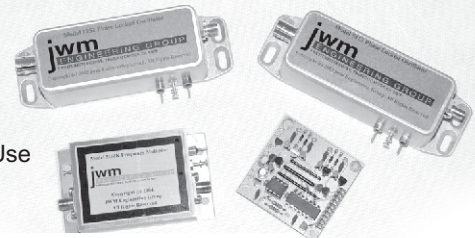
Measuring 2.4 GHz Helix Antennas

It's not very difficult to design and make a helix antenna for a specific frequency and gain. It's more difficult for the serious experimenter to make precise measurements of the finished antenna.

By Paolo Antoniazzi, IW2ACD, and Marco Arecco, IK2WAQ

In 1946, John D. Kraus invented the helical-beam antenna (or axial-mode helix).[1] Commencing with Kraus's correct hypothesis that travelling-wave structures then used in electromagnetic devices would make efficient antennas, the helix antenna has proven to be the radiator of choice for many radio astronomy and space-science applications.

The helical antenna has been carried to the Moon and Mars, and the

[1]Notes appear on page 22.

Via Roma 18
20050 Sulbiate MI, Italy
paolo.antoniazzi@tin.it

Via Luigi Einaudi 6
20093 Cologno Monzese, Italy
ik2waq@libero.it

Navstar GPS satellites use arrays of axial-mode helices. At the end of 1990s, a new interest in helix antennas was born, thanks to the AMSAT Phase 3D program (the well-known AO40 satellite with S-band down links.[2,3] It's not very difficult to design and make a specific helix for some frequency and gain. It's more difficult for the serious experimenter to make precise measurements of the finished antenna.

Network analyzers, today standard in telecom laboratories, are inaccessible to many amateur experimenters because of budget limits. We have analyzed shortly the possible use of directional couplers, but they are unsuitable because of the very high bandwidth and directivity required for precise microwave measurements. Directivity is the measure of how well

the coupler isolates two opposite-travelling (forward and reverse) signals. When measuring reflection coefficient (return loss) of a device under test, directivity is a crucial parameter[4,5] in the uncertainty of the results. For example, with a coupler directivity of 35 dB and a measured return loss of 30 dB (SWR < 1.07), the measurement error can be between –4 to +7 dB!

To use directional couplers, we need also some form of vector voltmeter (both magnitude and phase angle of the reflection coefficient) so that we can transfer the measured values to a Smith Chart for impedance analysis. At this point, we decided to design and construct a modern version of an instrument famous from early in microwave history: the slotted line.

The measurement of radiation diagrams to obtain helix directivity data

is a more conventional task with helices. In effect, the big errors related to direct-reflected wave encountered in Yagi tests[6] are not a problem with circular propagation, because the sense of the reflected wave is reversed. If the receiving antenna is of opposite sense (or the signal received via a reflective path) a signal loss of 20 dB or more results from the cross polarization.

A plane electromagnetic wave is linearly polarized when the electric field lies wholly in one plane containing the direction of propagation. The polarization is vertical when that plane is perpendicular, horizontal when it is parallel to the Earth's surface. A plane electromagnetic wave is circular polarized when the extremity of the electric vector describes a circle in a plane perpendicular to the direction of propagation, making one complete revolution in one period of the wave.

The polarization sense used by the Institute of Electrical and Electronic Engineers (IEEE) is a defacto standard: When viewing the antenna from the feed-point end, a clockwise wind results in right-hand circular polarization (RHCP), and a counterclockwise wind results in left-hand circular polarization (LHCP). When two stations use helical antennas over a nonreflective path, both must use antennas with the same polarization sense. The sense of the helix must be reversed also when feeding a parabolic dish reflector.

The Slotted Line Project

Some types of slotted lines are today available on the surplus market, for example the HP805A and 805C and General Radio type 874-B, but they are expensive. In the seventies, Hewlett Packard also built the 805C, a professional "slotted line" employing two parallel plates (slab line) instead of the normal coaxial line. The equipment, with 40-cm probe travel length, has been realized to work in the frequency range of 0.5 to 4.0 GHz.

A slotted line is essentially a precision 50-Ω, low-attenuation, low-SWR coaxial line intended for precise measurement. For those interested in the project including mechanical realization, the notes in the sidebar "the Slotted Line" are intended as a short tutorial. Our version of slotted line (Fig 1) was realized starting from a 30-cm-long brass square bar, drilled with a precision 14.00-mm hole. Two high-quality Amphenol N female connectors are fixed at the two ends of the bar. The center pins of two panel connectors support the internal precision rod (diameter = 6.08 mm for an exact 50-Ω line) made in gold-plated copper. One side of the rod is soldered, the other side is connected via a homemade spring contact. This point is very critical to obtain the targeted very low SWR. Table 1 shows the maximum permissible mechanical errors. A probe, mounted on a carriage (as shown in Fig 2), which is movable in a narrow (3 mm) slot cut longitudinally along the outer conductor, extends into the line to sample the RF field.

In the past the probe was a diode. Today the best solution is a very small loop connected via a short cable and a 6-dB attenuator to a broadband 20-dB preamplifier. The input attenuator is needed to avoid the risk of amplifier oscillations. For some tests we also used a Drake 2880 converter followed by a Boonton RF millivoltmeter, model 92B.

Possible Sources of Errors with Slotted Lines

The primary function of a slotted line is to provide a method of detecting a standing wave pattern along a transmission line. Thus, to faithfully reproduce this pattern, the critical parameters are the residual SWR and the possible irregularities. The commercial slotted lines, manufactured to work at these frequencies, have guaranteed SWR ≤ 1.04 and 0.2 dB of irregularities. A line with a perfect 50-Ω characteristic impedance is related to the fact that both SWR and impedance measurement accuracy are strictly linked to this value.

For this reason, the manufacturing phase requires attention to all possible errors caused by dimensional tolerances. They have been analyzed individually even if, at the end, their effects may overlap.

The first one is related to the ratio between the inner diameter of outer conductor D and the outer diameter of the inner conductor d that must be exactly 2.30 to have a perfect 50-Ω characteristic impedance as described by the following expression [7]:

$$Z_0 = 60 \ln\left(\frac{D}{d}\right) \qquad \text{(Eq 1)}$$

In Table 1, the slotted-line SWR changes versus mechanical data (tolerances) are shown. For instance if we consider $D = 14.00$ mm and SWR = 1.02, the d tolerance will be about ±0.10 mm. Remember that a value of SWR = 1.02 is equivalent to a resistive characteristic impedance change of ±1 Ω or ±0.5%.

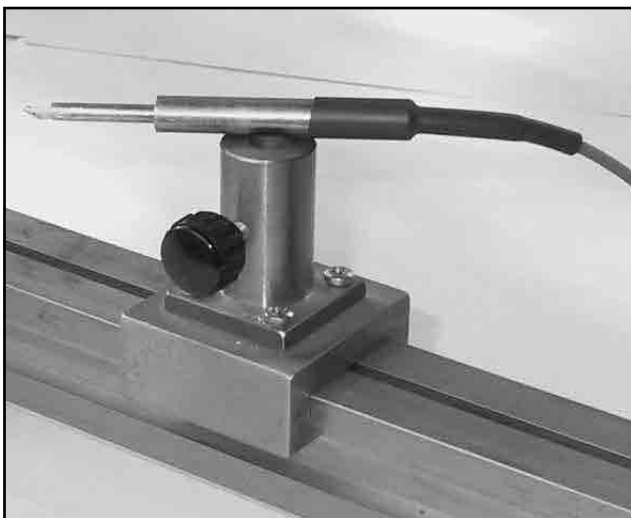Another error that prevents obtain-
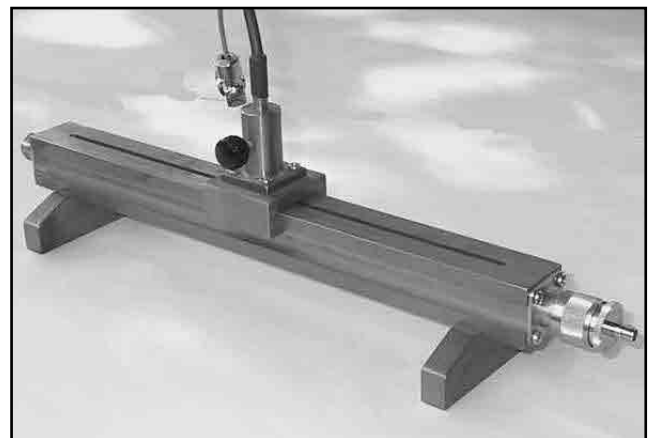

Fig 1—The complete homebrew slotted line.

Fig 2—Carriage and probe of the slotted line.

ing a perfect 50-Ω characteristic line impedance is related to the placement of the inner conductor exactly at the center of the outer one. In the ideal case, the two symmetry axes must coincide. In the following equation is reported the relation between the eccentricity c and the characteristic impedance of the line (from Note 7):

$$Z_0 = 60 \cosh^{-1}\left(\frac{\frac{D}{d} + \frac{d}{D} - \frac{4c^2}{d\,D}}{2}\right) \quad \text{(Eq 2)}$$

The change of characteristic impedance versus the eccentricity c (that is the distance between the center lines of the inner and the outer conductors) is reported in Table 1. The described values are relative to our case ($D = 14$ mm and $d = 6.08$ mm). If we consider SWR = 1.02; the maximum eccentricity allowed is 0.80 mm.

A third source of error can be the discontinuity created by the longitudinal slot on the outer conductor (to detect the field within the slotted line via a very small loop probe). Nevertheless its impact is negligible as can be seen looking at the following equation (from Note 7):

$$\Delta Z = 0.03\theta^2 \quad \text{(Eq 3)}$$

where:

ΔZ = characteristic impedance increase compared with a 50-Ω coaxial line.
θ = angular opening of the slot (in radians).

Cables and Coaxial Adapters: A Very Critical Point

One of the critical points in very low SWR measurements is the extremely high quality required of the cables and adapters.[8] The time and money spent on high-quality cables can be wasted if there are large impedance mismatches within the connectors, at the connector-cable interface and with the adapters (typically N to SMA, for the device in test). David Slack of Times Microwave Systems writes:

"…a microwave cable assembly is not just a wire. It is a passive, TEM mode, microwave component and an integral part of a system…."

Assuming a high-quality cable is used, the predominant contributor to the SWR of a cable assembly (on a 10-50 cm short assembly) is the connector. Improperly compensated geometry changes in the connector interface will exhibit very poor SWR characteristics.

In previous eras, this design was considered a "black art," and trial and error was a key component of high-performance design. Today, the computer simulation of discontinuities in connectors is an art, and the practical results are visible when the SWR performance of a very good cable assembly (N-male connectors) as that of the Times Microwave Systems is shown (Note 8). Only N and SMA connectors are used in our tests.

The characteristic impedance of the slotted line also may be affected by SWR induced by incorrect characteristic impedances of parts of the line, particularly at the transition between the inner conductor and the N-type panel connector lead that have different dimensions.

The following equation gives the SWR of the whole line when a small part of it ($L < 0.1\ \lambda$) does not match the characteristic impedance of the line under test:[9]

$$SWR = 1 + 2\pi\left(SWR_1 - \frac{1}{SWR_1}\right)\frac{L}{\lambda}$$
$$\text{(Eq 4)}$$

where:

SWR_1 = SWR of the mismatched part of the line: either Z_1/Z_0 or Z_0/Z_1 so that $SWR_1 \geq 1$.
Z_1 = characteristic impedance of the mismatched part of the line (ohms)
L = length of the mismatched part of the line (mm)
Z_0 = characteristic impedance of the main line (ohms)
λ = wavelength in the line (mm)

To clarify use of the above equation, let's perform an example.

If $Z_0 = 50\ \Omega$; $Z_1 = 35\ \Omega$; $L = 1$ mm; $\lambda = 125$ mm, the total SWR increases to 1.04:1 with a discontinuity of the characteristic impedance of only 1 mm. Analyzing the possible errors during the slotted-line manufacturing phase, it is considered a low SWR value because its worst case can increase rapidly as reported below.

Several components are used to connect the slotted line to the load: adapters, connectors and cables. These components can introduce very important impedance mismatches, and the worst-case standing wave ratio can increase rapidly, as can be seen by applying the following simple expression considering four mismatches:

$$\rho_{\text{total}} = \rho_1\rho_2\rho_3\rho_4 \quad \text{(Eq 5)}$$

A numerical example will clarify this quick SWR increase. For instance, an SWR = 1.02—that is very small—can become 1.08 considering four similar mismatch sources.

First Measurements of SWR and Impedance

The use of a slotted line is becoming a lost art; but to learn about it is not so difficult. The first suggested measurement with a new slotted line is the SWR of the system terminated on a very good commercial termination. Our first results with an old HP termination model 909A (N-male connector) were not the best, but the 909A is guaranteed no better than SWR = 1.04. The results are better using the famous Minicircuits[10] type Anne-50 with SMA-male connector (SWR = 1.03 at 3 GHz) and a good Amphenol N-male/SMA-female adapter. The

Table1

Maximum permissible mechanical errors

SWR	1.00	1.01	1.02	1.05	1.10
RL (dB)	∞	46	40	32	26
$\lvert\rho\rvert$	0	0.005	0.010	0.024	0.048
D/d	2.30	2.28	2.26	2.21	2.13
		2.32	2. 34	2.40	2.50
D (mm)	14.00	—	—	—	—
d (mm)	6.08	−0.05	−0.10	−0.24	−0.48
		+0.06	+0.11	+0.25	+0.51
D (mm)	14.00	−0.13	−0.25	−0.55	−1.04
		+0.11	+0.24	+0.60	+1.21
D (mm)	6.08	—	—	—	—
c(mm)	0	0.57	0.80	1.24	1.69

measured values on our slotted line are shown in Fig 3. For almost all tests, we used a signal generator from 2.2 to 2.6 GHz composed of a JTOS-3000 VCO followed by an MNA-6 amplifier (3´3 mm package).

Another important point: Make sure to use the correct RF signal levels during measurements. The input level from the oscillator is very high (+10 dBm), but some attenuation must be included for stability (the wide-band amplifiers oscillate very easy with loads that are not exactly 50 Ω). Using the Boonton RF Millivoltmeter (model 92B) as a detector, we have also a sensitivity attenuation of about 10 dB at 2.4 GHz

(referred to the maximum suggested operating frequency of about 1.2 GHz) and consequently the level sampled by the probe is very low (typically 0.3 to 3 mV). In future measurements, we will use a 2.2 to 2.6 GHz heterodyne system composed of a harmonic mixer and a 1.05 GHz fixed-frequency local oscillator. The IF will be in the range 100-500 MHz, limited by a 550 MHz low-pass filter. This solution is free from oscillation risks, and the gain is obtained with a simple wide-band amplifier followed by the RF millivoltmeter. In effect, it's very important to minimize the coupling of the probe to the line to obtain reliable results.

Simulation and Measurement of Helices

After a short but necessary didactical phase, we will go speedily to the helix antennas. Using *NEC* and particularly the powerful *NEC-WinPro* software[11, 12] as a simulation tool and starting from the important results obtained by the simulation work of D. T. Emerson (Fig 4)[13] we have analyzed two different antennas (Fig 5). One is a simple unit of five turns (gain = 12 dBi) and one is 16.7 turn with 14.5 dBi gain. A more complex antenna named TriHelix, a 18 dB array of 16.7 turn helices feed via three flat
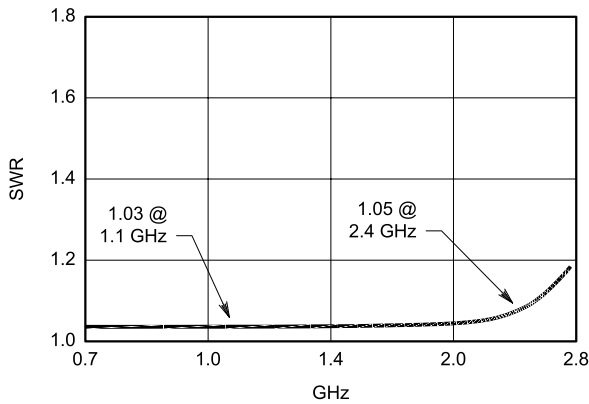

Fig 3—Measured slotted line: a very good SWR from 500 to 2800 MHz.
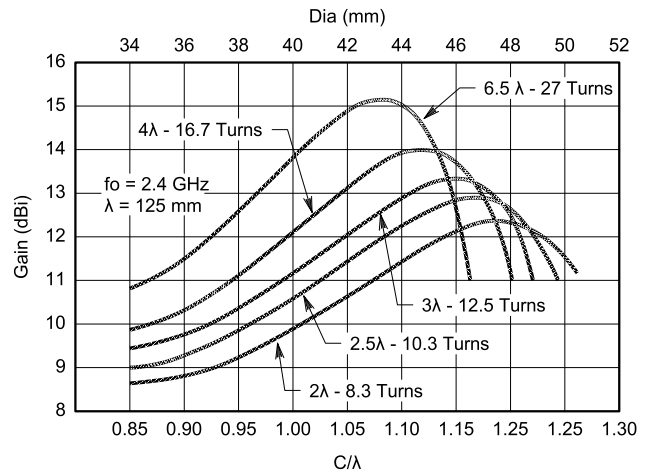

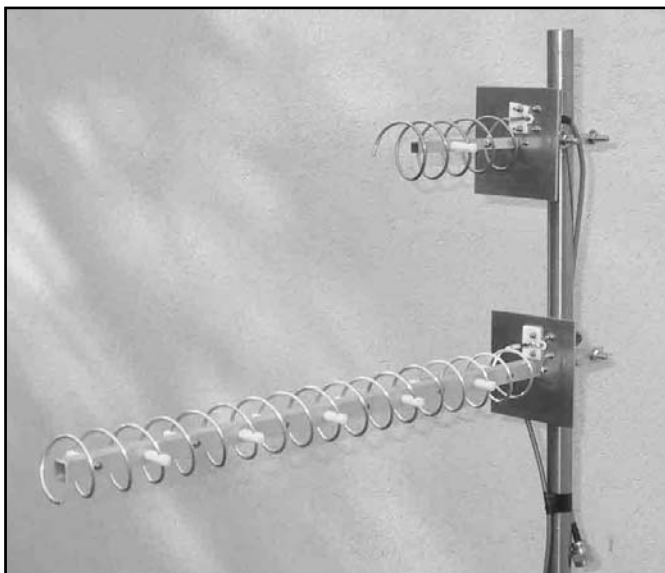Fig 4—Simulated gain versus helix diameter and C/λ at 2.4 GHz.

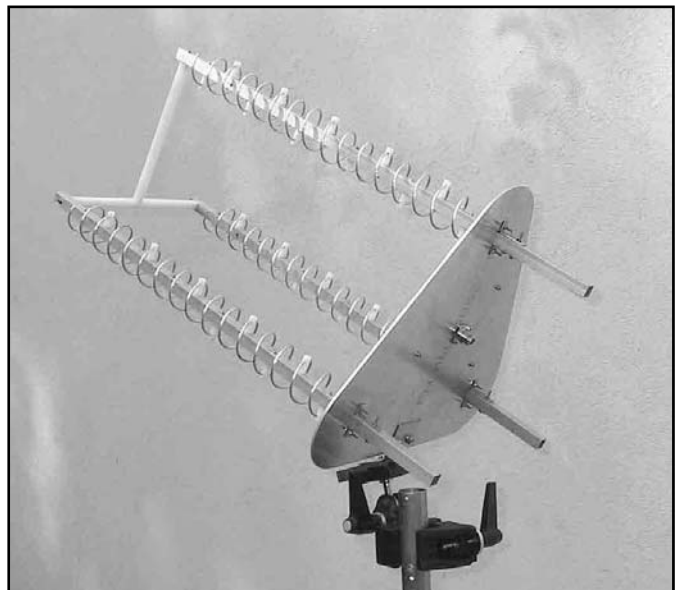Fig 5—Five turn and 16.7 turn helices in test.

Fig 6—Experimental trihelix antenna.

130-Ω air-dielectric lines (see Fig 6), is in an experimental phase.

The *NEC-Win Pro* software allows simple wire modeling of the helix antenna using the "GH" card (the name card came from *Fortran*). This card avoids the need to calculate the coordinates of each segment using a spreadsheet software (such as *Lotus 1-2-3*, *Excel* and so on) and transfer them to *NEC-Win Pro* as text with risk of errors. To describe a helix however complex, the "GH" card needs only eight parameters:

Number of segments.

Spacing between turns (0.24 λ or 30 mm at 2.4 GHz for our helices).

Helix radii in two perpendicular directions, at both the beginning and end of the winding (this feature allows us to simulate both elliptic and conical helices).

Total helix length.

Wire diameter.

To simulate the helix, we decided to use ten segments per turn as a good trade-off between the *NEC-Win Pro* rules and the need for a better description of the circular shape of the antenna. To be unidirectional, a helix needs a suitable ground plane near the feed point. It can be made with *NEC-Win Pro* using a square grid plate (125×125 mm, λ at 2.4 GHz). This kind of structure needs a number of segments given by the following general equation:

$$N \quad 2n(n+1) \qquad \text{(Eq 6)}$$

where n is the grid factor (the number of parts in which the plate is divided by the wires that compose it).

In our case, with the purpose of minimizing the current within the screen, we decided to use $n = 20$ (0.05 λ pitch between wires), and so the plate is composed of no less than 840 segments. With the same purpose of minimizing the current in the screen, a 6-mm-long stub has been added between the helix and the grid plate. This requirement for a large number of screen segments prevents use of a grid plate when the total number of segments exceeds the 2000 available with the *NEC-Win Pro* software. In this last case, it is possible to simulate it by using a perfect ground and orienting the helix symmetry axis vertically.

We tried to simulate the helices both with the grid screen and a perfect ground and the differences detected in power gain, radiation angle and feed impedance are not significant. The only big difference is the loss of the radiation pattern at the back of the antenna when using the perfect ground.
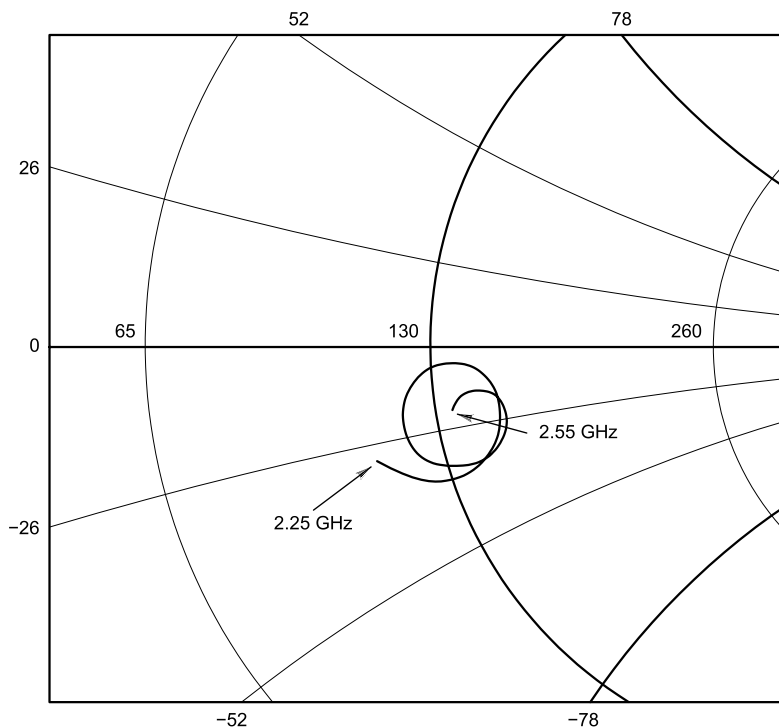
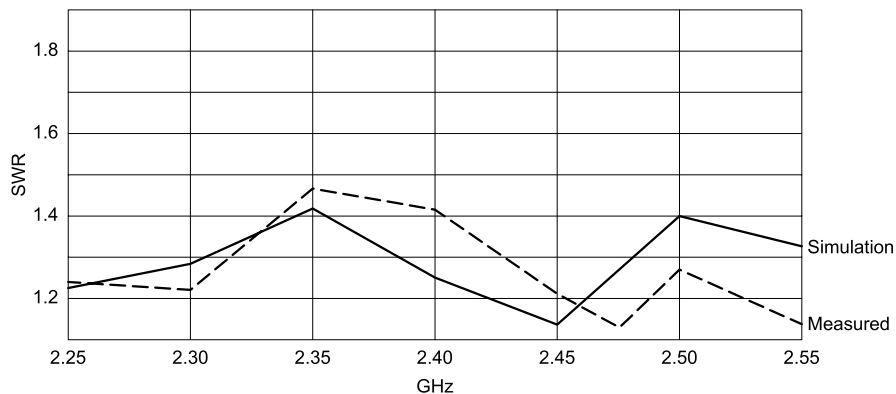**Fig 7—Simulated input impedance of the 16.7 turn helix.**

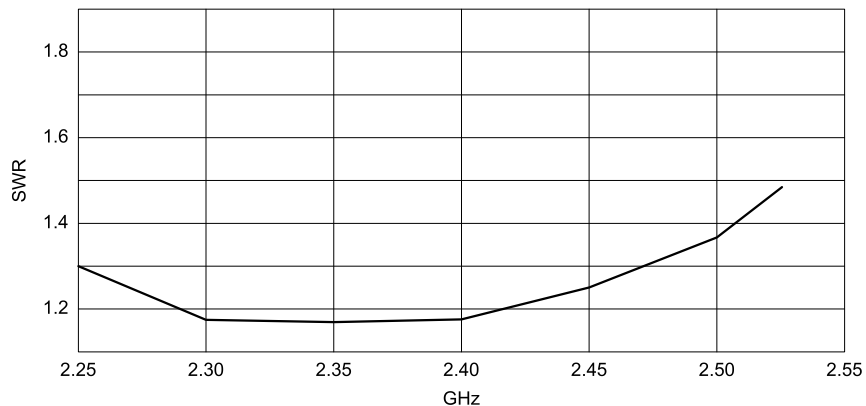**Fig 8—First approach to the SWR versus frequency of a 16.7 turn helix.**

Fig 9—Finally tuned 16.7 turn helix: measured SWR versus frequency.

Also, the screen can be simulated easier with the "GM" card that allows the repeating and the moving of the segments with only few statements, with respect to the full description of the segments.

The files of the 5 and 16.7 turn helices will be supplied to interested experimenters by e-mail on request.

The simulated values for the input impedance (referred to 130 Ω) of the 16.7 turn helix are shown in Fig 7. The simulation of SWR values and the first measured values from 2.25 to 2.55 GHz are visible in Fig 8. In Fig 9, the measured values for the finally tuned helix are shown. The matching between the 130-Ω nominal input impedance of the single helix and 50 Ω is obtained via a λ/4 transformer (Teflon support with h = 2.5 mm and line with W = 3 mm, Z = 81 Ω). The transformer layout is shown in Fig 10 (calculated using a good HP tool, *AppCad*.[14] See also the photo of Fig 11 where the real Teflon impedance adapter is shown at the beginning of the five-turn helix. The first measurements on the TriHelix antenna give a *SWR* = 1.3-1.4 at 2.4 GHz ±100 MHz. With the multiple-helix arrays the mutual impedance of adjacent helices is to be considered, but when separated by a wavelength or more, as is typical in helix arrays, the mutual impedance is only a few percent or less of the helix self impedance (130-140 Ω). Thus in designing the feed corrections for a helix array, the effect of the mutual impedance can often be neglected (see Note 1) without significant consequences.

Free Space Attenuation

To reduce the measurement errors, the distance between transmitting and receiving antennas must be considered. To determine this distance, you need to measure the signal level with a filtered RF voltmeter having a 30-40 dB dynamic range. Also, the wave reaching the receiving antenna should be as planar as possible.

The first condition can be easy established starting with the received power and calculating the attenuation experienced by the wave in the open space:

$$\alpha \quad 32.4 + 20\log(f) + 20\log(d \quad - G_t - G_r \quad \text{(Eq 7)}$$

Here, a is the attenuation in decibels, f is the frequency (megahertz), d is the distance (km), G_t is the gain of transmitting antenna (dBi) and G_r is the gain of receiving antenna (dBi) obtained by simulation.

There is also a simple, easy-to-remember method of calculating the
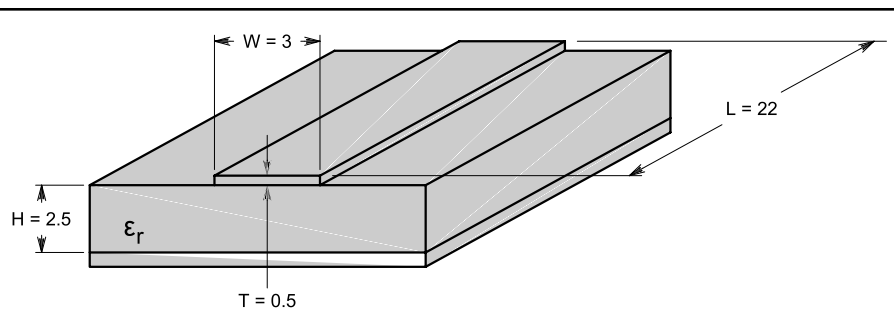

Fig 10—Layout of the λ/4 Teflon transformer calculated using HP-*AppCAD*. This is a λ/4 transformer from 130 Ω to 50 Ω. The transformer is realized using a Teflon plate (22×30 mm) and a copper strip with *W* = 3 mm and *T* = 0.5 mm at the beginning of the helix.
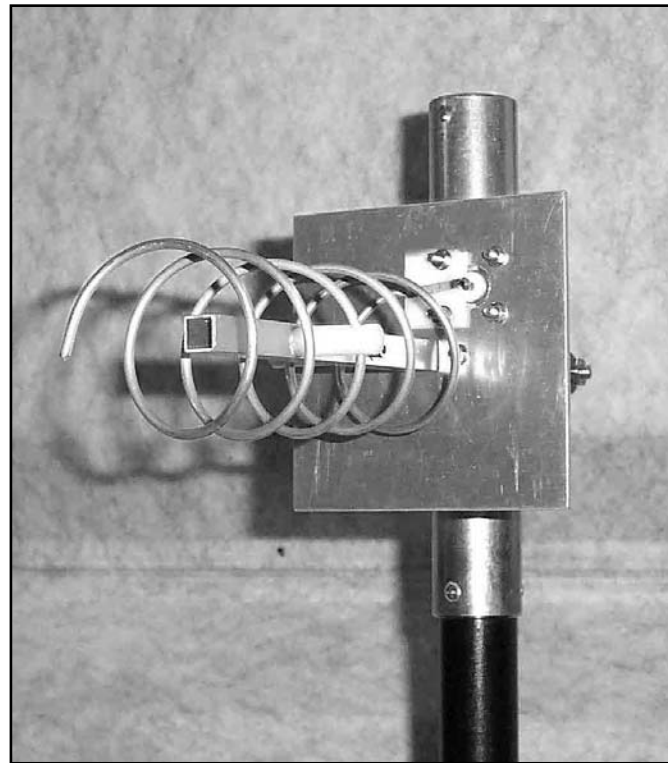

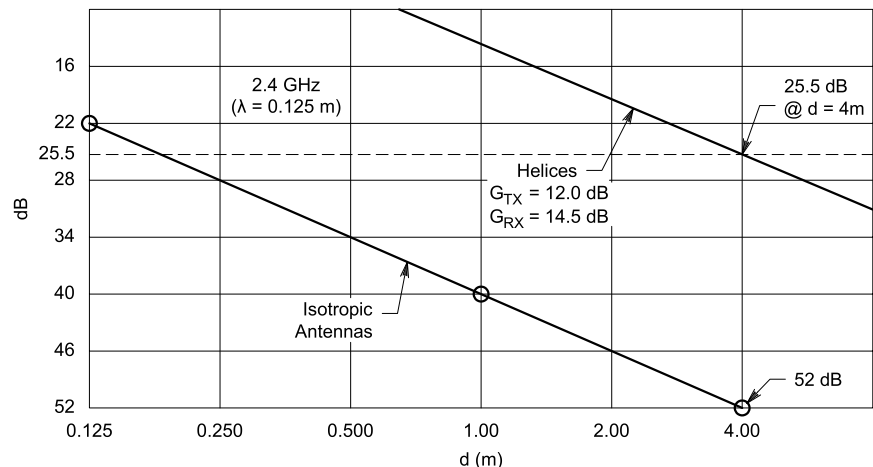Fig 11—Five turn helix (see the λ/4 79 Ω Teflon adapter).

Fig 12—Free-space attenuation at 2400 MHz.

free-space attenuation by considering the distance between the two antennas in terms of wavelengths. When $d = \lambda$, α is always 22 dB between isotropic antennas.

This equates to 12.5 cm at 2400 MHz. The attenuation increases by 6 dB for each doubling of the path distance. This means that the free space attenuation is 22 dB at 0.125 m, 28 dB at 0.25m, 34 dB at 0.5 m, etc (see the diagram of Fig 12). To make the wave reaching the receiving antenna as planar as possible, the capture area of the receiving antenna in square meters and the maximum acceptable phase error are needed:

$$\alpha \quad \frac{G_r \lambda^2}{4\pi} \qquad \text{(Eq 8)}$$

This expression is valid for an antenna with no thermal losses and was certainly useful for our experiments. Assuming that the capture area is circular, the minimum distance in meters between the antennas will be:

$$d >= \frac{n\,G_r\,\lambda}{\pi^2} \qquad \text{(Eq 9)}$$

For a maximum phase difference of 22.5°, which is usually enough, $n = 2$. If a phase error of only 5° is required, $n = 9$. In the case where one dimension prevails over the others, the maximum length, instead of the capture diameter, is used. In this case, the minimum distance in meters becomes, (Note 7)[15, 16]:

$$d >= \frac{n\,L}{\pi^2} \qquad \text{(Eq 10)}$$

where L is the maximum length in meters (50 cm for the 16.7-turn helix).

The site we selected (in the garden) is particularly useful for our measurements and equates $d = 4$ m $= 32\,\lambda$ at 2400 MHz. For a lot of very useful information on antenna measurements, see also Kraus.[17]

Radiation Diagrams, Efficiency and Gain

In Figs 13 and 14, the radiation diagrams of the 5- and the 16.7- turn helices, obtained via the *NEC-Win Pro* simulation, are shown with gains in dBi. The directivity of an antenna is based entirely on the shape of radiated power pattern and does not consider the minor lobes. In this parameter, the antenna efficiency is not involved.

The gain of an antenna is defined as a ratio of a maximum radiation intensity of the antenna to a maximum
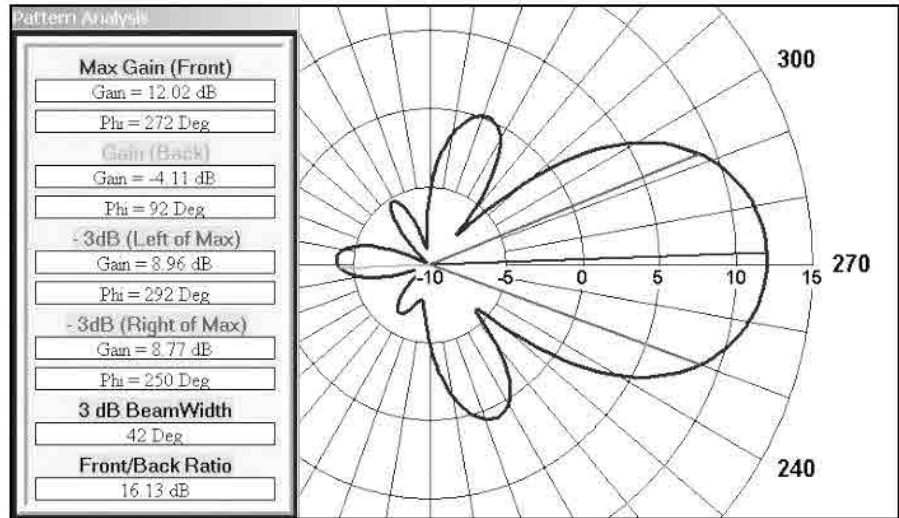

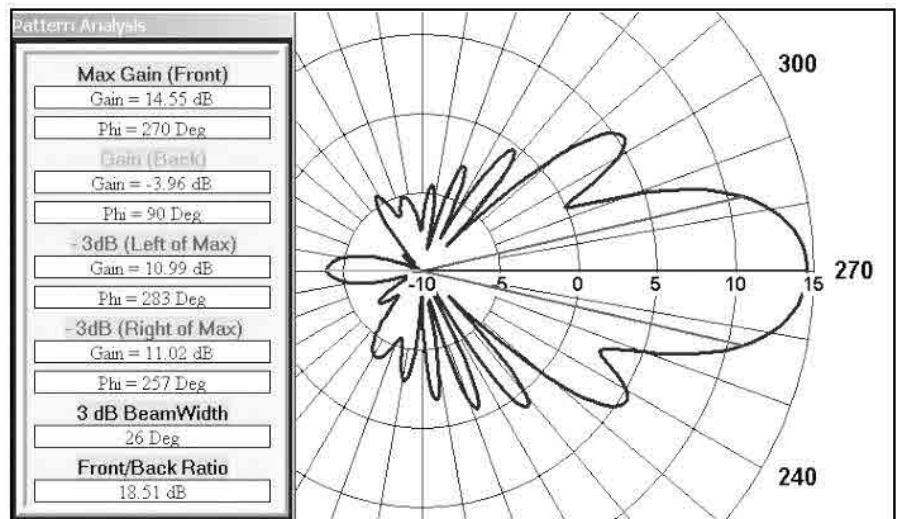Fig 13—Five turn helix radiation diagrams: simulation with *NEC-Win pro*.

Fig 14—Radiation diagrams for the 16.7 turn helix: simulation with *NEC-Win pro*.
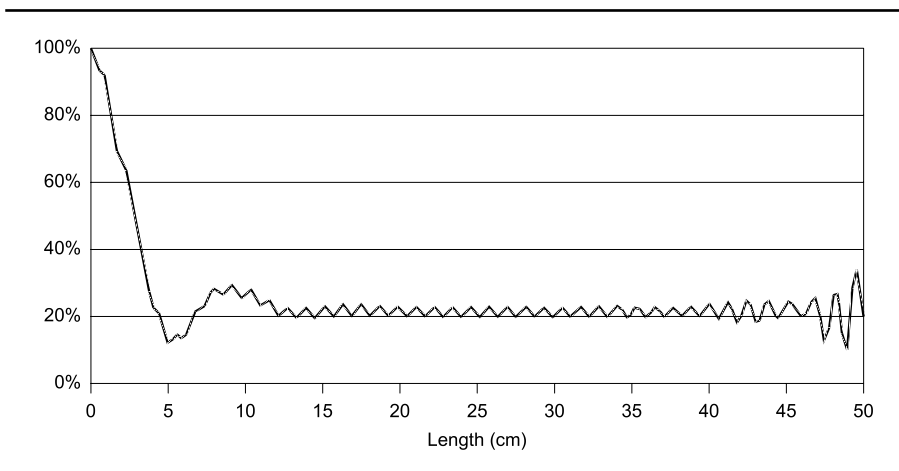

Fig 15—Simulated helix current for a 16.7 turn antenna.

Slotted Line

A "slotted line" is an air-dielectric, low-loss coaxial transmission line (<0.3 dB) having precisely 50 Ω characteristic impedance. It is 30 to 50 cm long, depending on the lowest working frequency, and at the ends it presents two connectors, generally N type, for connection to a RF generator, a load or a line to be measured. Along the outer conductor of the coaxial line is a narrow longitudinal slot, in which is placed a small probe. The penetration of the probe into the line is a tradeoff between the voltage levels to be detected and the need to minimize the perturbation of the line field in which it is immersed. An RF millivoltmeter is used to detect the field existing in the slotted line. It is connected to the probe via a shielded cable. The probe is placed on a sliding carriage that can move along the line. Its position can be read with a resolution of about 0.5 mm by a pointer moving along a suitable ruler fixed to the slotted-line body. The instrument's low-frequency limit is a function of the maximum length on which the carriage probe can travel. When a generator is connected at one end of the slotted line and a load to the other one, we have two possibilities: the load has impedance equal to the characteristic impedance (Z_0) or not. In the first case, we have no reflection from the load and the voltage detected by the probe along the line is flat. If the load impedance differs from Z_0, a standing-wave pattern occurs and moving the probe along the line we will find one or more maxima (loops) and minima (nodes). In this case, the distances between two contiguous maxima (see Fig 16) or minima is one-half wavelength, and so we are able to estimate the frequency of the RF source used to feed the load. We are also able to calculate the SWR using the following equation:

$$SWR = \frac{e_{MAX}}{e_{min}} \qquad \text{(Eq 12)}$$

or Return Loss in decibels:

$$RL = 20\,log\left(\frac{e_{MAX} + e_{min}}{e_{MAX} - e_{min}}\right) \qquad \text{(Eq 13)}$$

where

e_{MAX} = maximum voltage, measured with the probe, along the slotted line (mV).

e_{min} = minimum voltage, contiguous to the previous maximum, measured with the probe (mV).

Moreover, the slotted line gives us the capability to calculate the impedance, both real and imaginary parts, measuring the node displacement when the line is connected to the load and the load is replaced by a short circuit.

The computation of the complex impedance can be performed using the expression of the lossless line:

$$Z = Z_0 \frac{Z_L + jZ_0\,tan(\beta\,l)}{Z_0 + jZ_L\,tan(\beta\,l)} \qquad \text{(Eq 14)}$$

where

β = phase constant: $2\,\pi\,/\,\lambda$, (cm^{-1})
l = node displacement, (cm).*
λ = wavelength, (cm).

The same kind of calculation can be performed more easily with the aid of the Smith chart.

The slotted line can also be used to establish the cable attenuation, repeating the SWR measurement at both the beginning and the end of the line to be tested.

The computation of the attenuation A (in decibels) can be performed using the following equation derived from the one for lossy lines:

$$A = \left[tanh^{-1}\left(\frac{1}{\rho_1}\right) - tanh^{-1}\left(\frac{1}{\rho_2}\right) \right] 8.69 \qquad \text{(Eq 15)}$$

where
ρ_1 = SWR at the beginning of the line.
ρ_2 = SWR at the end of the line.

*Pay attention that, in the evaluation phase, the maximum displacement allowed is ±λ/4.

---

radiation intensity of a reference antenna with the same power input—in the gain the antenna efficiency is involved.

The helix antenna power gain (in dBi) can be computed using the following:

$$G = 10log_{10}\left(\frac{360^2\eta}{\pi\,\theta^2}\right)$$

$$\approx 10log_{10}\left(\frac{41{,}253\,\eta}{\theta^2}\right) \qquad \text{(Eq 11)}$$

where:
θ = main-lobe radiation angle at half power, in degrees
η = efficiency (< 1)

In Table 2, there are computations of the power gains of the 5- and 16.7-turn helices as functions of the measured radiation angles and efficiency. We can see that increasing the length
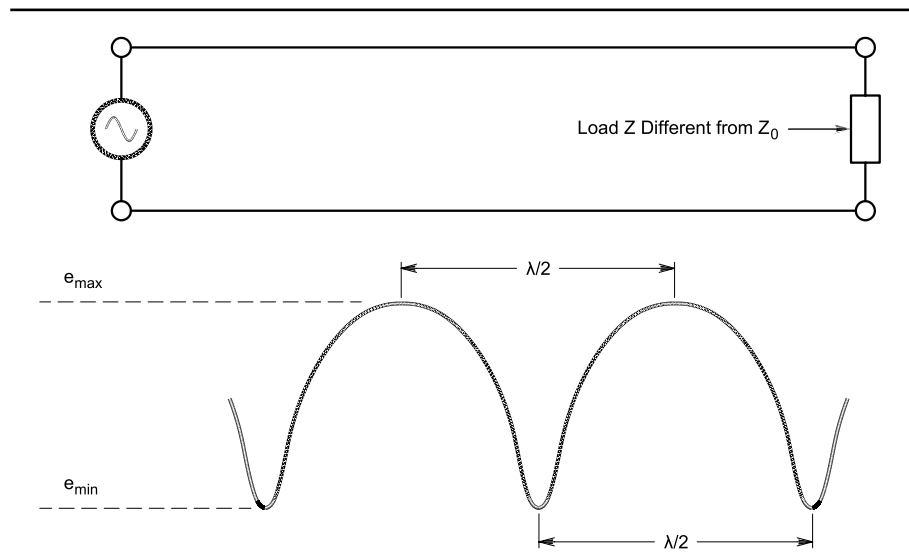

Fig 16—A standing wave on a transmission line terminated by a load impedance different from the line characteristic impedance (50 Ω in our case).

of the helix (from 150 mm to 500 mm) decreases its efficiency. The measured and simulated values of helix gain are shown in Table 3.

The measured radiation lobes (–3 dB) at 2400 MHz agree within about ±1.5 degrees with the calculated values on both the helices. The simulated behavior of the current in the helix versus antenna length is shown in Fig 15. As you can see, the current decayed exponentially near the input end; there was a standing wave over a short distance near the open end, while there was a relatively uniform current amplitude (small SWR) between the ends, which extended over most of the helix.

Notes

[1]J. D. Kraus, *Antennas*, second edition (New York: McGraw-Hill, 1988) "The Helical Antenna," pp 265-339.

[2]"Microwave Radio via AMSAT Oscar AO-40," *RadCom* (Hertfordshire, England: RSGB), Aug 2001.

[3]"A Practical Approach to Operating AO-40," *RadCom*, Nov/Dec 2001.

[4]P. Antoniazzi, "High Directivity RF Coupler," *Electronics World*, Oct 1966, pp 763-765.

[5]"HP-Dual Directional Coupler, Model 778D," technical brochure, 1982.

[6]P. Antoniazzi and M. Arecco, "Measuring Yagis," *Electronics World*, Dec 1998, pp 1002-1006.

[7]*Reference Data for Radio Engineers,* fifth edition, (Indianapolis, Indiana, USA: H. W. Sams & Co, 1989) pp 29-19 to 29-23.

[8]D. Slack, "Microwave and RF Cable Assemblies: the Neglected System Component," *Applied Microwave & Wireless*, Nov/Dec 1997, pp 36-45.

[9]M. W. Dixon (Ed), G3PFR, *Microwave Handbook* Vol 1, (RSGB, 1989) pp 5-22.

[10]**www.minicircuits.com**.

[11]*NEC-Win Pro*, release 1.4, 2002 (Nittany Scientific Inc; **www.nittany-scientific. com**).

[12]W. Walker, W5GFE, "*A Perl/Tk Package for NEC* Based Antenna Design," *QEX*, May/Jun 2001, pp 51-54.

[13]D. T. Emerson, "The Gain of the Axial-Mode Helix Antenna: A Numerical Modeling Study," March 1995, National Radio Observatory, Tucson, Arizona, USA.

[14]*AppCAD*, is a free download from Agilent. For the 14.5 MB download, visit **www. educatorscorner.com/index.cgi? CONTENT_ID=2601** and page down to "RF Cool Links." You can order the application on CD by e-mailing **semiconductorsupport@agilent.com**.

[15]*The ARRL Antenna Book*, 16th edition (Newington, Connecticut, USA: ARRL, 1992).

[16]D. R. J. White, *Electromagnetic Interference and Compatibility*, Vol 2, 1980. Published by Don White Consultants, State Rd 625, PO Box D, Gainesville, VA 22065.

[17]J. D. Kraus, *Antennas*, second edition, (McGraw-Hill, 1988) "Antenna Measurements," pp 805-843.

Paolo Antoniazzi, IW2ACD, is a Technical Information Manager in the TPA-Central Marketing department of STMicroelectronics. He has more than 35 years of experience in RF and audio applications. Paolo is a member of IEEE, RSGB, ARI (Associazione Radioamatori Italiani) and the Audio Engineering Society. He was first licensed in the early 1960s, and in February 2003 obtained a "Ruolo d' Onore ARI" (40 years of ARI membership). His amateur interests include slow CW in the LF band and simulation and tests of antennas from LF loops to VHF-µW.

Marco Areco, IK2WAQ, is a Standard Nonvolatile Memories Product Engineering Team Leader with more than 30 years experience in semiconductor manufacturing. Marco is a member of ARI. He has been licensed 10 years and his amateur interests include LF operations and VHF, UHF, µW antenna simulations and measurements.

Table 2

Helix radiation angles, efficiency and gain

Efficiency (%)	5.0 Turns, L = 150 mm (degrees)			16.7 Turns, L = 500 mm (degrees)		
	41	42	43	24	25	26
70	12.3	12.1	11.9	17.0	16.6	16.3
65	12.0	**11.8**	11.6	16.7	16.3	16.0
60	11.7	11.5	11.3	16.3	16.0	15.6
55	11.3	11.1	10.9	16.0	15.6	15.3
50	10.9	10.7	10.5	15.5	15.2	14.8
45	10.4	10.2	10.0	15.1	**14.7**	14.4
40	9.9	9.7	9.5	14.6	14.2	13.9
35	9.3	9.1	8.9	14.0	13.6	13.3
30	8.	8.5	8.3	13.3	13.0	12.6

Table 3

Comparison of simulated and measured helix gain

HELIX	L (λ)	NECWinPro Simulation (dB)	Emerson (*) Simulation (dB)	Emerson (**) Simplified Formula (dB)	Measured Values (dB)
5.0 turns	1.2	12.0	-	11.6	**12.5**
16.7 turns	4.0	14.5	14.0	14.0	**15.0**

*See Reference 13
**G = 10.25 + 1.22 L −0.00726 L^2

□□

A Low-Loss 145 MHz/ 220 MHz Diplexer

Building on his previous work, OK1DNZ makes this diplexer with transmission-line sections only, no lumped constants.

By Pavel Zanek, OK1DNZ

My previously published VHF/ UHF diplexer[1] used inductors and coaxial cables: a combination of lumped and distributed design elements. I recommend you to read that previous article to learn more about it. This current article is meant as an extension of my previous work. Let's now design a 145 MHz/220 MHz diplexer with coaxial cables only, to make things easier.

Features and Measured Data
- Characteristic impedance is 50 Ω.
- Operating frequency range: 144-148 MHz, 220-225 MHz
- Low insertion loss (IL): 0.31 dB at 145 MHz and 0.34 dB at 220 MHz.
- High isolation: Minimum 65 dB.
- All ports are well matched to 50 Ω: Maximum SWR = 1.22:1.
- All ports are dc connected.

[1]Notes appear on page 26.

Slovenska 518
Chrudim, Czech Republic 537 05
Zanek.pavel@tiscali.cz

- Maximum RF power at 145 MHz or 220 MHz or 145 MHz/ 220 MHz port: 250 W CW at 55°C.
- Fully shielded construction.
- Easy to produce, low-cost solution.

All the parameters above were measured in a laboratory on the first sample of the diplexer. The measurements were performed by means of vector network analyzer (HP8714B) with an output level of 0 dBm. Two additional 10-dB pads for transmission measurement were used to avoid mismatch error when low insertion loss (IL) was measured. The HP8714B was calibrated before the impedance measurements.

Design Requirements

First, let's define the geometric centers of wavelengths in meters for the next description. We get for the 144-148 MHz band:

$$\lambda 145\text{MHz} \quad \frac{300}{\sqrt{144 \cdot 148}} \quad 2.055\,\text{m} \tag{Eq 1}$$

and for the 220-225 MHz band:

$$\lambda 220\text{MHz} \quad \frac{300}{\sqrt{222 \cdot 225}} \quad 1.342\,\text{m} \tag{Eq 2}$$

The wavelength ratio of

$$\frac{\lambda_{145\,\text{MHz}}}{\lambda_{220\,\text{MHz}}} \quad 1.53 \tag{Eq 3}$$

is suitable for a pure distributed design (coaxial cables only) to satisfy very low IL (less than 0.40 dB) and high power handling (250 W). The practically achieved isolation must be better than 65 dB and SWR lower than 1.40:1. My design solution was analyzed and optimized by using the *SUPER COMPACT* program.[2]

Circuit Description

The operation is similar to my last design. I will write only a brief description so you can understand how to go about proper tuning and adjustment. A full electrical sche-matic diagram is shown in Fig 1. The lengths of coaxial cables (CCx) are shown in Table 1. All sections of coaxial transmission lines have a characteristic impedance of 50 Ω.

220 MHz Passband Section

The 145 MHz signals are shunted by two λ/4 coaxial cable stubs with open ends (CC1 and CC3, approximately λ/4 at 145 MHz). CC1 and CC3 have a little bit different tuning/length to satisfy the desired isolation at full range: 144-148 MHz. (See Table 1 and Fig 4.) The length of transmission line CC2 satisfies a perfect impedance matching at 220-225 MHz. The shortening of CC2 shifts the SWR minimum to higher frequencies; lengthening it lowers the minimum SWR frequency. The change of CC2 length does not affect the tuning of the CC1 and CC2 stubs. The line CC4 makes a phase shift to transform the impedance at 144-148 MHz from the top of CC3 to near infinity at the common 145 MHz/ 220 MHz port. Thus, transmission in the 145 MHz passband section is not influenced.

145 MHz Pass-band Section

The 220 MHz signals are shunted by two λ/4 coaxial cable stubs with open ends (CC5 and CC7, approximately λ/4 at 220 MHz). CC5 and CC7 have also a little bit different tuning/length to satisfy the desired isolation in the range 220-225 MHz. (See Table 1 and Fig 4.) The length of transmission line CC6 satisfies a perfect impedance match in the band 144-148 MHz. The shortening of CC6 shifts the SWR minimum to higher frequencies; lengthening it lowers the SWR minimum frequency. The change of CC6 length does not affect the tuning of the CC5 and CC7 stubs. The line CC8 makes a phase shift to transform the impedance at 220-225 MHz from the top of CC7 to near infinity at the common 145 MHz/ 220 MHz port. Thus, transmission in the 220 MHz band section is not influenced.

Voltage Analysis

This analysis was made using *SUPER COMPACT* software. A complete loss model of the diplexer was used. Let's assume that the 145 MHz port is driven by an input RF power P_{145} (W) at $f = 148.0$ MHz and the other ports are correctly terminated. Then maximum RF voltage amplitude V_{145} (V) will be at the open end of CC5:

$$V_{145} = 2.89\sqrt{50 P_{145}} \qquad \text{(Eq 4)}$$

If the 220 MHz port were driven by an input RF power P_{220} (W) at $f = 220.0$ MHz and the other ports were correctly terminated again, then a maximum RF voltage amplitude V_{220} (V) would be at the open end of CC1:

$$V_{220} = 1.96\sqrt{50 P_{220}} \qquad \text{(Eq 5)}$$

Do not touch the open cable ends of live nodes when the diplexer is carrying RF power! Use the diplexer with both covers attached and use a correctly adjusted unit.

Practical Construction

Refer to Note 1 for basic information and Figs 2 and 3 here for more details. I have used the same coaxial cable: 141-mil hand-formable semi-rigid microwave coaxial cable[3] (0.139 dB/m at 150 MHz, power handling at 40°C is 1.8 kW at 150 MHz; relative propagation velocity is 0.71 and minimum bending radius for bending once is 8 mm). The initial lengths are somewhat longer before first tuning/shortening: CC1 and CC2: 370 mm; CC5 and CC7: 240 mm.

RF Measurement and Adjustment

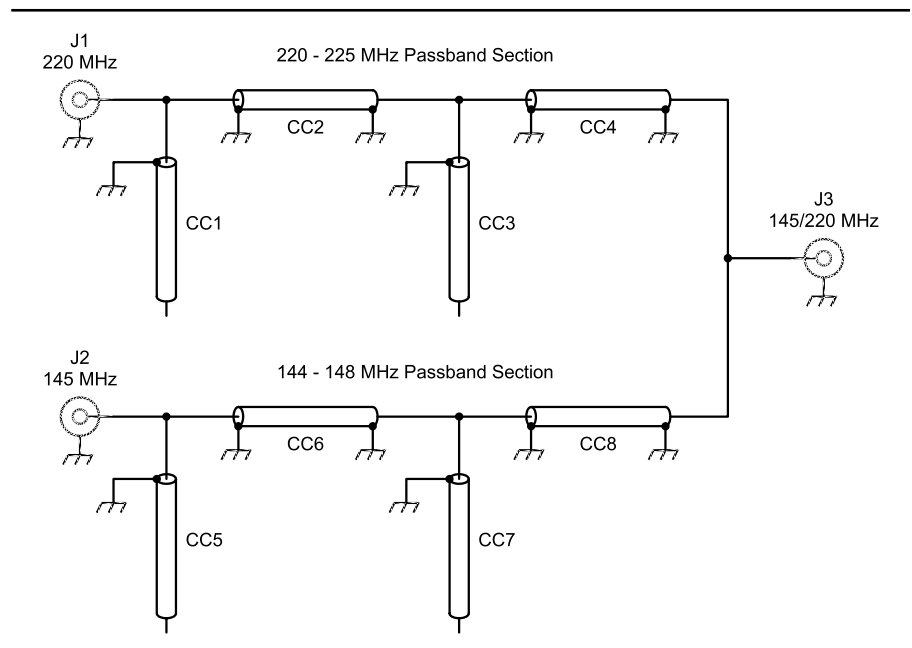RF measurements/adjustments are necessary before using the diplexer. The high performance of the diplexer, which

Fig 1—A schematic diagram of 145 MHz/ 220 MHz diplexer.

CC1-CC8—Transmission-line sections cut (see Table 1 for lengths) from 2.5 m of hand formable semi-rigid cable.

J1-J3—Panel-mount female N flange jacks (Rosenberger #53K 403-200 N3). Misc—Tinned steel box, WBG 40 DONAU, 74x148x30 mm, 0.5 mm thick.

Table 1

Cable Lengths. Physical length = 71% of electrical length for SM141 Cu.

Cable (Sucoform SM 141 Cu)	Electrical Length	Physical Length [mm]	Note
CC1	0.243 $\lambda_{145\,MHz}$	354	Must be set, start with 370 mm
CC2	0.197 $\lambda_{145\,MHz}$	288	
CC3	0.241 $\lambda_{145\,MHz}$	351	Must be set, start with 370 mm
CC4	0.248 $\lambda_{145\,MHz}$	362	
CC5	0.238 $\lambda_{220\,MHz}$	227	Must be set, start with 240 mm
CC6	0.211 $\lambda_{220\,MHz}$	201	
CC7	0.226 $\lambda_{220\,MHz}$	215	Must be set, start with 240 mm
CC8	0.244 $\lambda_{220\,MHz}$	233	

Fig 2—A photo of the 145 MHz/220 MHz diplexer.

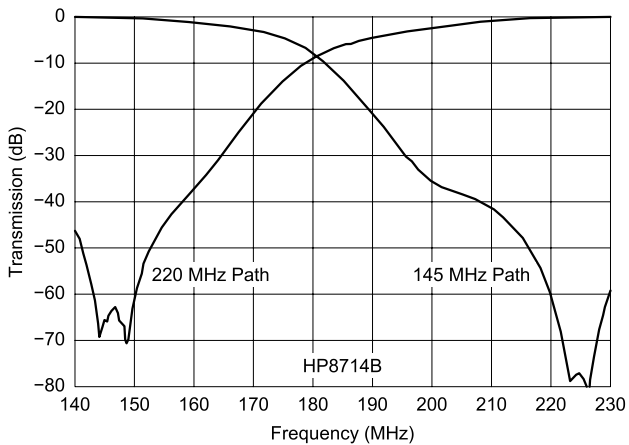Fig 3—A photo of the 145 MHz/220 MHz diplexer interior.

Fig 4—Measured transmissions of the 145 MHz and 220 MHz paths.
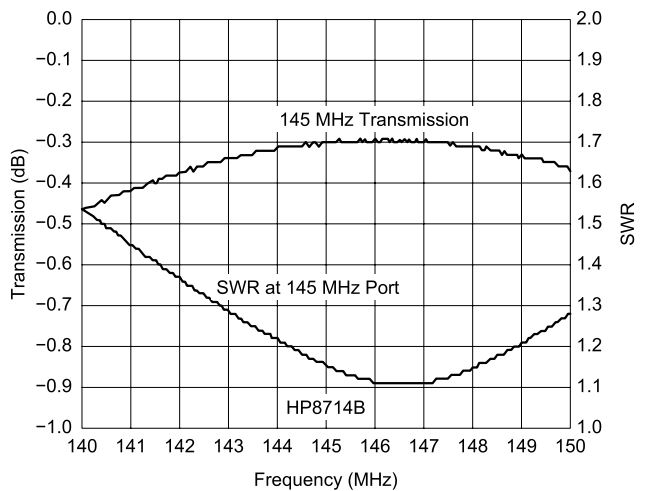

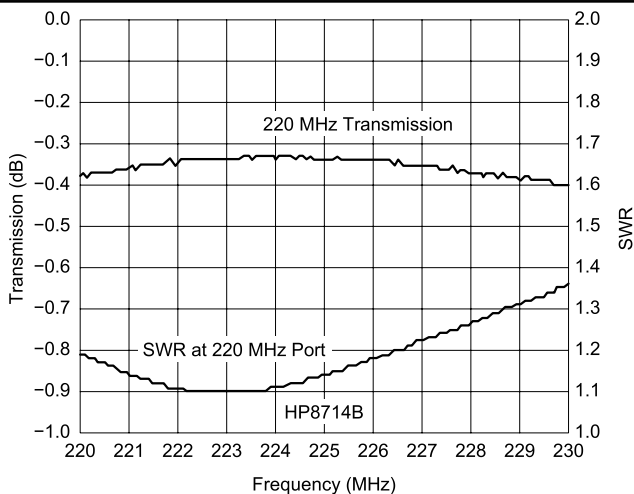Fig 5—Measured transmission and SWR of the 145 MHz path.

Fig 6—Measured transmission and SWR of the 220 MHz path.

Fig 7—The 145 MHz section under measurement.

compares well with similar professional products on the market, cannot be realized without sophisticated measurement equipment, especially when high power levels are intended.

Here are the basic steps of the adjustment procedure. A vector/scalar network analyzer or a spectrum analyzer with tracking generator and SWR bridge are required for perfect adjustment. Set a simultaneous two-channel measurement: transmission and impedance. Set the swept frequency range to 140-240 MHz. The adjustment procedure consists of the proper setting of the lengths of CC1, CC3, CC5 and CC7 and does not exceed 20 minutes.

145 MHz Passband Section Adjustment

Apply a swept RF signal to the 145 MHz port and connect the 145/220 MHz port to the receiving section of the test equipment. Terminate the 220-MHz port with a 50-Ω load. Shorten the open ends of CC5 and CC7 little by little to achieve maximum attenuation over the full 220-MHz band. It is typical for achieved attenuation to be about 70 dB (see Fig 4). Check now if the

SWR minimum is in the range 144-148 MHz. The maximum SWR in that band should be about 1.22:1 (see Fig 5). If a shift of minimum SWR toward higher frequencies is necessary, shorten the CC6 line; to shift toward lower frequencies, you would need to lengthen the line by replacing it.

220 MHz Passband Section Adjustment

Now apply a swept RF signal to the 220-MHz port and terminate the 145-MHz port with a 50-Ω load. Shorten the open ends of CC1 and CC3 little by little to achieve maximum attenuation over the full 145-MHz band. It is typical for achieved attenuation to be about 65 dB (see Fig 4). Check now if the SWR minimum is in the range 220-225 MHz. The maximum SWR should be about 1.14 (see Fig 6). If a shift of minimum SWR toward higher frequencies is necessary then shorten the CC2 line. If you can accept a narrower operating bandwidth, you may be able to achieve greater isolation.

RF Performance

The three graphs in Figs 4-6 show the RF performance achieved with my

unit. The power losses for intended input RF power of 250 W are: 17.2 W for a 145 MHz transmitter and 18.8 W for a 220 MHz transmitter.

The diplexer solution offers the following useful features. The minimum second-harmonic suppression for 220-MHz transmitter is typically 44 dB. The 145-MHz section also passes 430-440 MHz. Measured data here: insertion loss is 0.63 dB and SWR is 1.69:1. It should be acceptable for UHF receivers only, not for transmitters! DC-connected ports permit you many possibilities to get power to your receive preamplifiers.
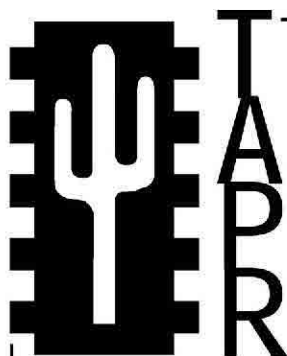
Fig 7 shows the properly adjusted 145-MHz section of the diplexer with the help of vector network analyzer Hewlett Packard HP8714B.

Notes

[1] P. Zanek, OK1DNZ, "A Low-Loss VHF/UHF Diplexer," *QEX*, Mar/Apr 2002, pp 47-51.
[2] *Super Compact* is no longer available. It evolved into some of the current software offered by Ansoft; **www.ansoft.com**.
[3] Huber & Suhner, Suhner Microwave Cable, SUCOFORM, the hand formable microwave cable, Type SM 141 Cu, article number: 22511635. □□

An Investigation of Ground Planes Constructed of Composite Materials

---

Composites are replacing aluminum for some aircraft skins, and some autos already have plastic skins. How can we establish effective ground planes?

By William Rynone (ex-WB2EIQ), PhD, PE

Where air drag is not of concern, it is common for aircraft antennas to be affixed to the outside surface of a plane, most often to the fuselage and/or vertical stabilizer. Predominately, the skins of aircraft have been made of sheet aluminum. However, the use of composites for the construction material of aircraft skins has been gaining acceptance. Some considerations that a designer must weigh while selecting the skin material include strength, cost, weight, cost of installation, maintenance and durability. The electrical characteristics of the material require consideration as well. The effects of a lightning strike, the ability of the ma-

129 Pinecrest Dr
Annapolis, MD 21403
Rynone_Eng@juno.com

terial to carry electricity as a ground conductor and the ability of the skin material to act as a ground plane for antennas are some of those concerns.

If the immediate surface area where antennas are mounted is intended to enhance the antenna's performance, it is referred to as a "ground plane." This investigation was directed towards the evaluation of various ground-plane test samples that employ treated graphite cloth as a skin material.

The aluminum sheet metal used in the majority of aircraft skins is a high-quality ground plane material because of its high electrical conductivity. Carbon fiber is a reasonably good conductor. Fiberglass is a good insulator. Where these materials are employed as a mounting surface for antennas, it is common practice to enhance the electrical conductivity in that area. Carbon fiber cloth may be covered

with an aluminum sheet, a conductive coating or special carbon fiber cloth may be purchased that has a metal mesh embedded in the cloth. Metal mesh, carbon fiber cloth is expensive and nickel electroplated carbon fiber cloth costs $490/square yard. For this reason, other methods of increasing the conductivity of the carbon fiber were investigated in this study. These included the spray coating of conducting paints or the use of conducting materials in the resin used to bind layers of carbon fiber cloth (see Table 1). The resistivity of the coating materials in addition to the thickness of the applied coat will determine the planar resistance of the final assembly. For purposes of this study, the surface resistance was measured with an ohmmeter by applying the ohmmeter probes to opposing corners of the top surface of the treated ground plane.

Also, radio frequency energy at 450 MHz was emitted from a λ/4 monopole that was mounted to the various test samples (see Fig 1). To standardize the physical characteristics of the ground planes, each was constructed of carbon fiber sheets that were one foot by one foot, but varied slightly in thickness (see Fig 2). Since the length of a λ/4 monopole is approximately seven inches at 450 MHz, the requirement that a ground plane be λ/2 across was met (pp 2-39, 18-27 and 15-3, *ARRL Antenna Book*, 15th edition). Although a low resistance reading may be indicative of superior ground plane function, it was important to evaluate this correlation via antenna performance measurements.

To perform the measurements, Mr Joseph Johoda, President of Astron Wireless, kindly consented to having his personnel obtain gain and impedance measurements (Figs 3-11) for

Table 1

Results of Test measurements.

Mat'l#	Ground Plane Construction Materials	R(Ω)
1	Copper Powder In Laminate Resin #1	∞
2	Aluminum Powder in Latex Paint Coating	∞
3	Copper Powder In Laminate Resin #2	13.6
4	Aluminum Wire Co-Woven	108
5	Copper Powder In Laminate Resin #3	2.3
6	Commercial Conductive Paint	∞
7	Cloth With Glued Aluminum Foil	0.2
8	Cloth With Laminate Resin	0.14

Notes
1. Resistance measurements were performed with a Cen-Tech P37772 Digital VOM
2. To achieve desired strength, all laminated carbon fiber samples consisted of three layers. Where embedded with resistance modifier, the first layer was altered.
3. All carbon fiber ground plane samples were approximately 12×12×3/32-inches thick.
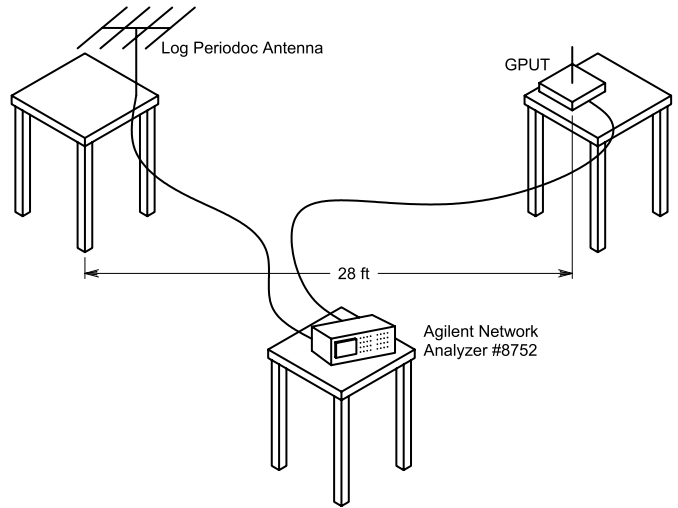4. Infinite resistance is indicative of non-contiguous conductive grain boundaries.

Fig 1—The antenna test setup. The distance between the antennas was 28 feet (≈12.8 λ), exceeding the 10 λ near-field range. Ferrite beads were used on the cables to prevent interaction.
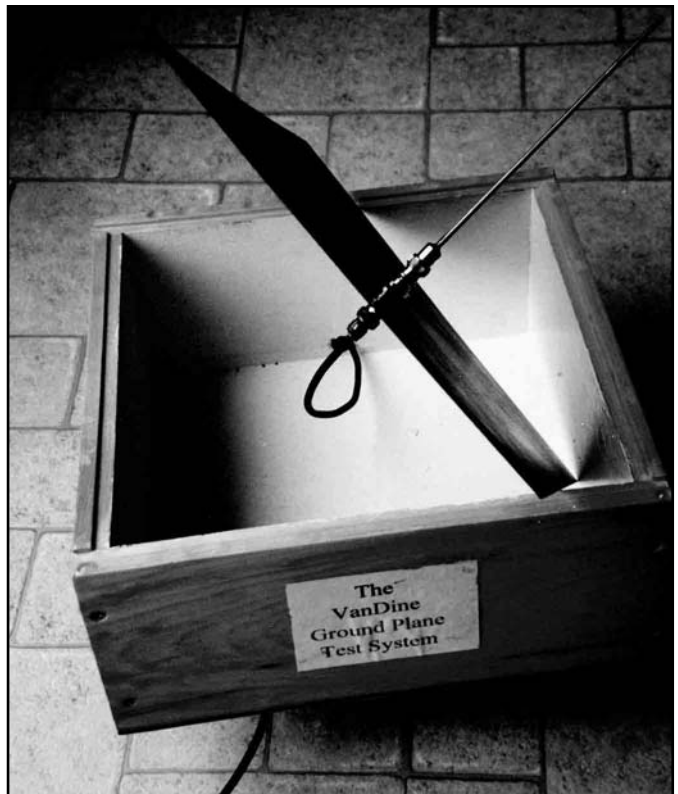

Fig 2—Photos of the test box.

each one of nine (aluminum was in- cluded) different ground-plane samples. Mr Glen Brown performed the tests. The same antenna was mounted alternately in each ground plane under test (GPUT). The spacing between the transmitter antenna mounted in the GPUT and the receiv- ing antenna was set at 28 feet, thus meeting the empirical requirement of greater than 10 λ to overcome near- field effects. The RF test equipment was an Agilent Network Analyzer #8752 used with a receiving log-peri- odic antenna having a gain of 7 dB at 450 MHz. This antenna has a reason- ably flat frequency response from 200 MHz to 1 GHz.

The source and receiving antennas were elevated from the ground via a wooden table and a wooden stand. Cables from the test set were isolated from each other and the test equip- ment using ferrite beads.
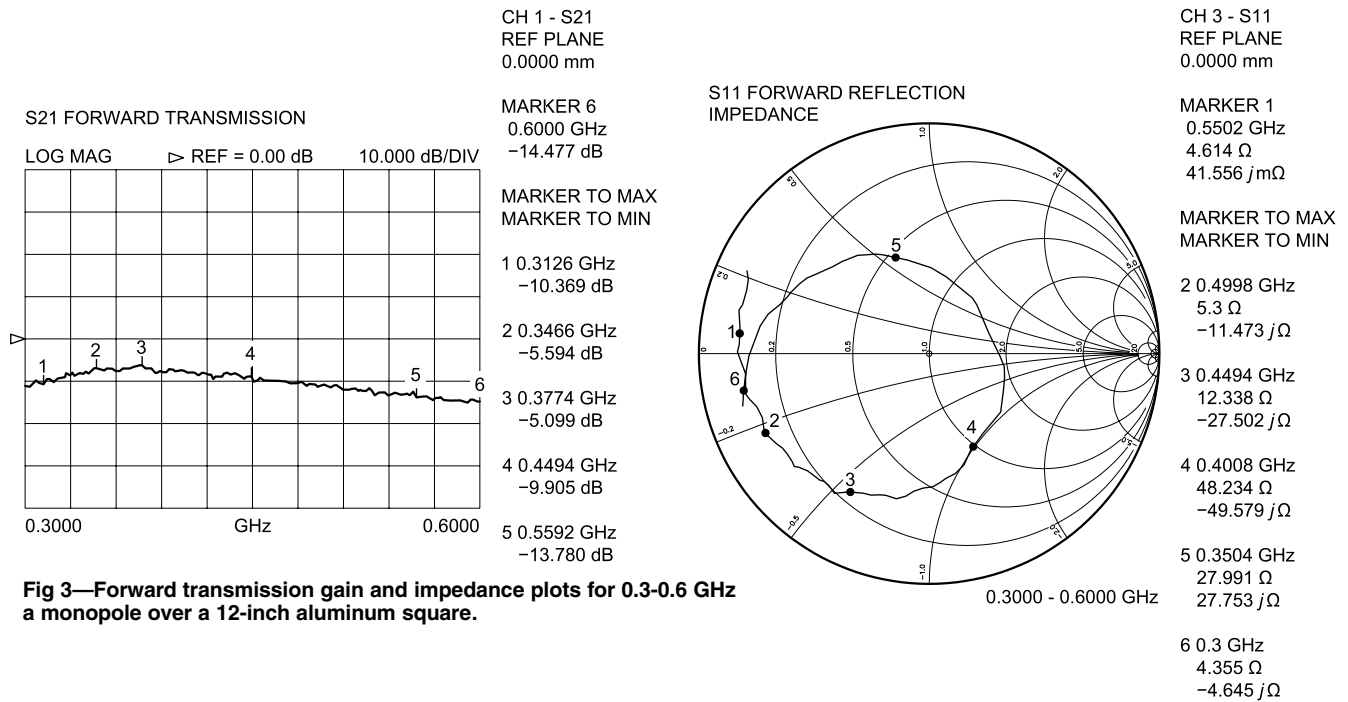
CH 1 - S21
REF PLANE
0.0000 mm

MARKER 6
0.6000 GHz
−14.477 dB

MARKER TO MAX
MARKER TO MIN

1 0.3126 GHz
−10.369 dB

2 0.3466 GHz
−5.594 dB

3 0.3774 GHz
−5.099 dB

4 0.4494 GHz
−9.905 dB

5 0.5592 GHz
−13.780 dB

S21 FORWARD TRANSMISSION

LOG MAG   ▷ REF = 0.00 dB   10.000 dB/DIV

0.3000   GHz   0.6000

S11 FORWARD REFLECTION
IMPEDANCE

0.3000 - 0.6000 GHz

CH 3 - S11
REF PLANE
0.0000 mm

MARKER 1
0.5502 GHz
4.614 Ω
41.556 jmΩ

MARKER TO MAX
MARKER TO MIN

2 0.4998 GHz
5.3 Ω
−11.473 jΩ

3 0.4494 GHz
12.338 Ω
−27.502 jΩ

4 0.4008 GHz
48.234 Ω
−49.579 jΩ

5 0.3504 GHz
27.991 Ω
27.753 jΩ

6 0.3 GHz
4.355 Ω
−4.645 jΩ

Fig 3—Forward transmission gain and impedance plots for 0.3-0.6 GHz a monopole over a 12-inch aluminum square.

CH 1 - S21
REF PLANE
0.0000 mm

MARKER 6
0.6000 GHz
−14.700 dB

MARKER TO MAX
MARKER TO MIN

1 0.3126 GHz
−9.710 dB

2 0.3466 GHz
−6.777 dB

3 0.3774 GHz
−6.168 dB

4 0.4494 GHz
−9.998 dB

5 0.5592 GHz
−13.983 dB

S21 FORWARD TRANSMISSION

LOG MAG   ▷ REF = 0.00 dB   10.000 dB/DIV

0.3000   GHz   0.6000

S11 FORWARD REFLECTION
IMPEDANCE

0.3000 - 0.6000 GHz

CH 3 - S11
REF PLANE
0.0000 mm

MARKER 1
0.5502 GHz
4.553 Ω
1.027 jΩ

MARKER TO MAX
MARKER TO MIN

2 0.4998 GHz
5.219 Ω
−10.489 jΩ

3 0.4494 GHz
11.954 Ω
−26.150 jΩ

4 0.4008 GHz
45.017 Ω
−48.191 jΩ

5 0.3504 GHz
30.042 Ω
28.189 jΩ
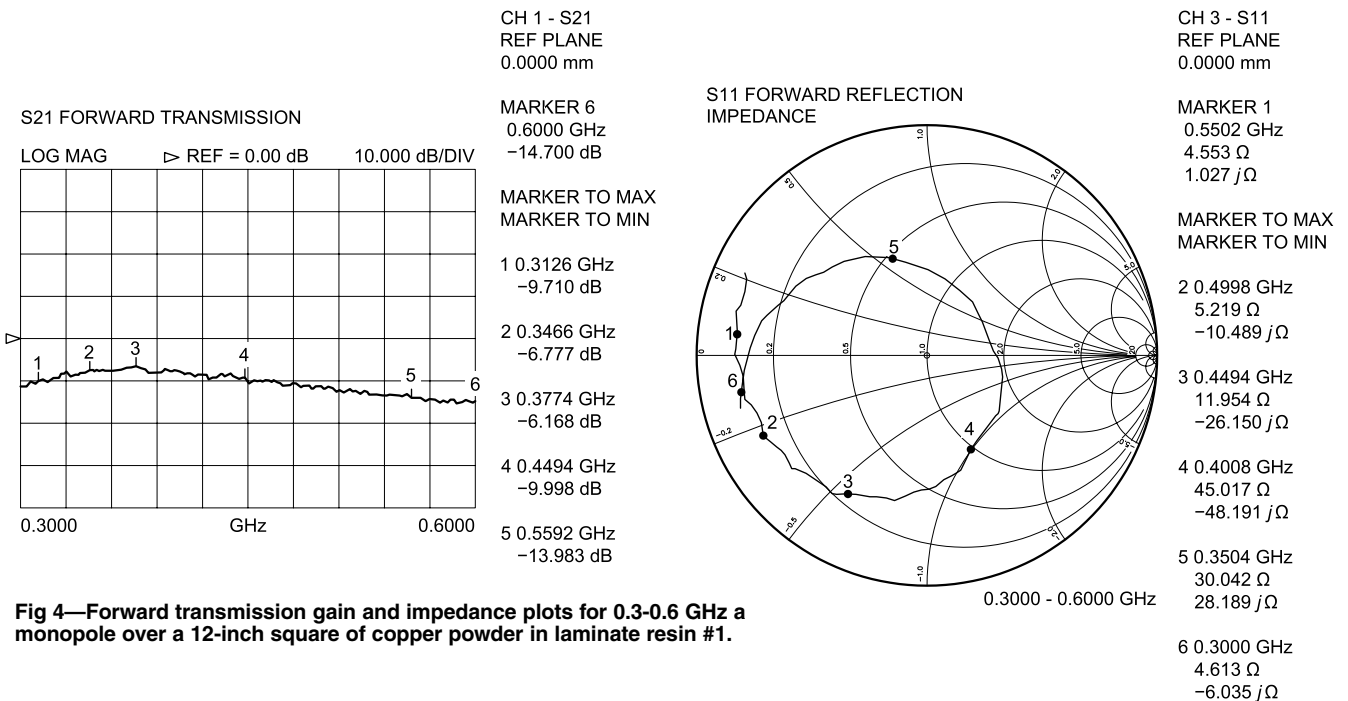
6 0.3000 GHz
4.613 Ω
−6.035 jΩ

Fig 4—Forward transmission gain and impedance plots for 0.3-0.6 GHz a monopole over a 12-inch square of copper powder in laminate resin #1.

The test samples were constructed by Merganser Aircraft Corporation on January 10, 2003. The gain and impedance tests were performed on January 17, 2003 in the Astron Wireless test facility in Sterling, Virginia.

Sample Calculations

For a λ/4 monopole at 440 MHz:

$$\lambda = \frac{c}{f} = \frac{300\left(10^6\right)\text{m/s}}{450\left(10^6\right)\text{Hz}} = 0.681818\,\text{m}$$

$$\frac{\lambda}{4} = 0.17045\,\text{m}$$

$$0.17045\,\text{m} \times 39.37\,\frac{\text{inches}}{\text{meter}} = 6.71\,\text{inches}$$

Distance from center to corner for a 12" sqaure

$$r = 6"\times\sqrt{2} = 8.48"$$

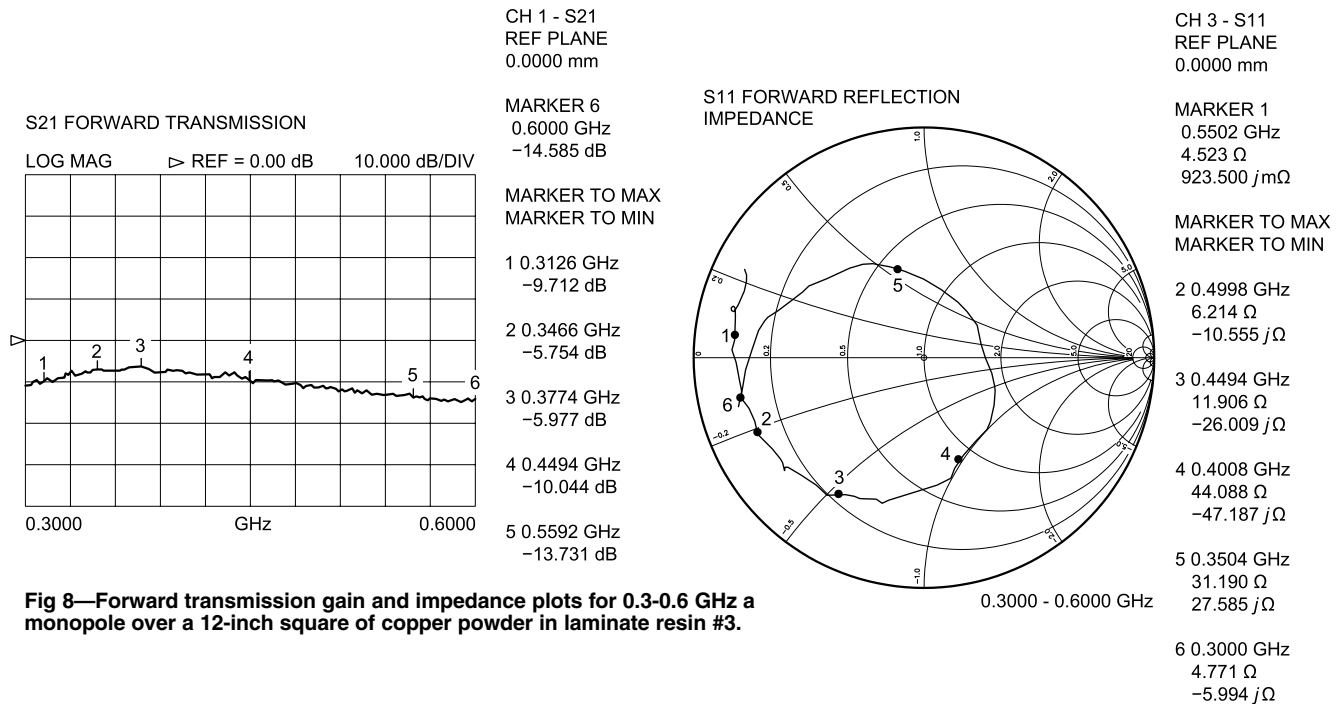$$8.48" > 6.71" = \frac{\lambda}{4}$$

Summary

The greatest power-out (Po) to power-in (Pi) ratio was 0.1022. The least *Po* to *Pi* was 0.0927. Thus, the greatest *Po/Pi* ratio exceeded the least *Po/Pi* ratio by 10% as shown in the spreadsheet (Fig 12).
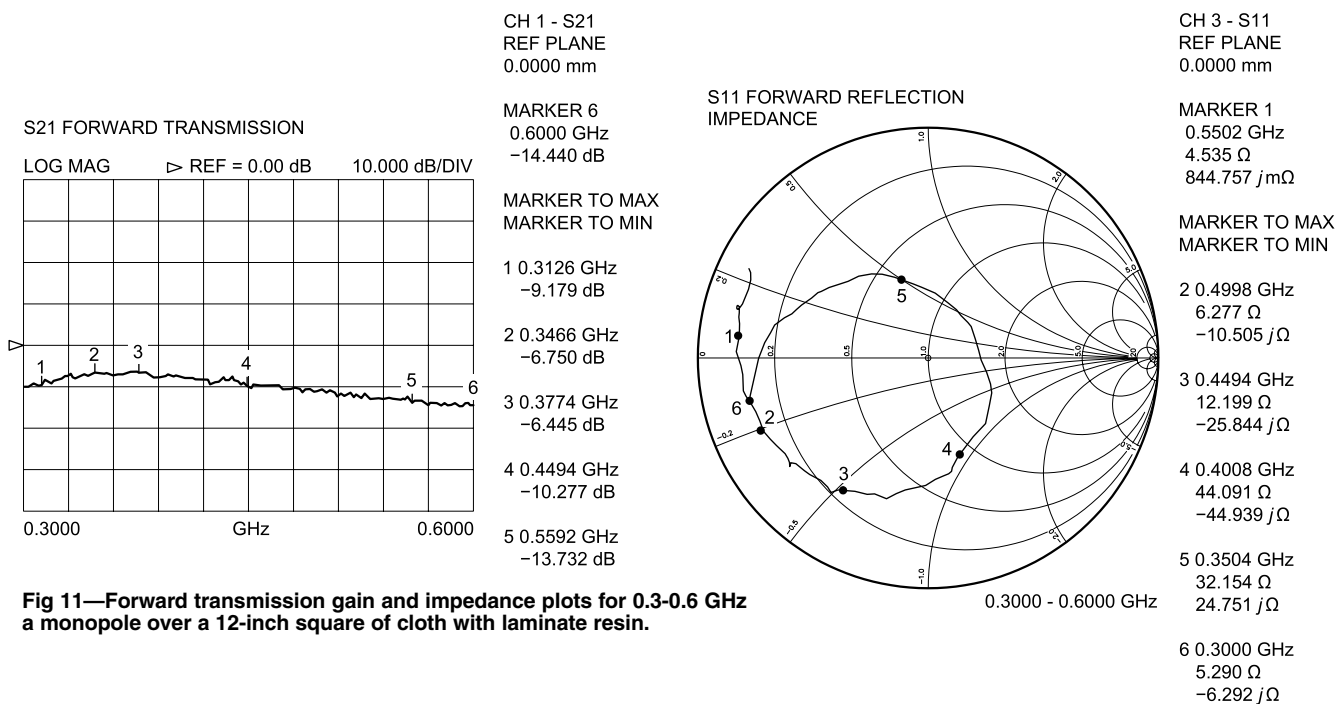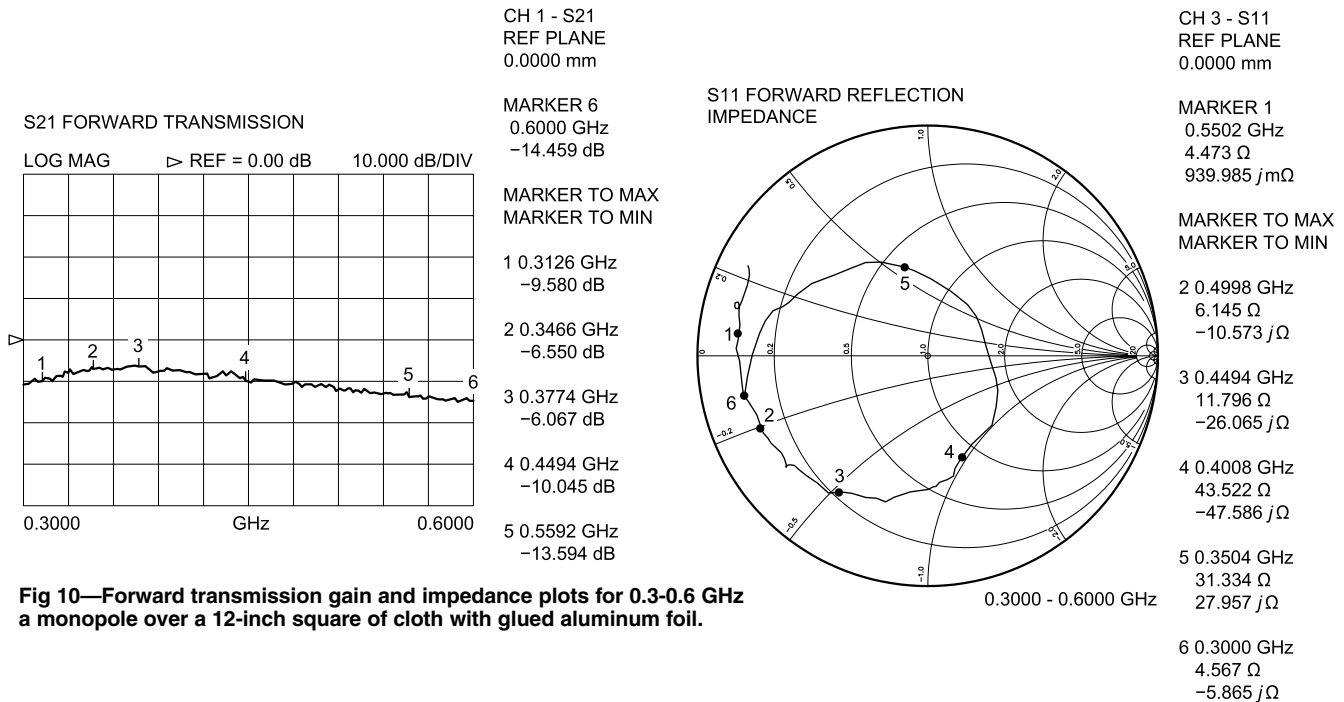
Acknowledgments

Fig 5—Forward transmission gain and impedance plots for a monopole over a 12-inch square of aluminum powder in latex paint coating.

Fig 6

S21 FORWARD TRANSMISSION

LOG MAG   ▷ REF = 0.00 dB   10.000 dB/DIV

0.3000   GHz   0.6000

CH 1 - S21
REF PLANE
0.0000 mm

MARKER 6
0.6000 GHz
−14.720 dB

MARKER TO MAX
MARKER TO MIN

1 0.3126 GHz
−9.565 dB

2 0.3466 GHz
−6.731 dB

3 0.3774 GHz
−5.018 dB

4 0.4494 GHz
−10.035 dB

5 0.5592 GHz
−13.764 dB

S11 FORWARD REFLECTION
IMPEDANCE

0.3000 - 0.6000 GHz

CH 3 - S11
REF PLANE
0.0000 mm

MARKER 1
0.5502 GHz
4.570 Ω
1.178 jΩ

MARKER TO MAX
MARKER TO MIN

2 0.4998 GHz
5.255 Ω
−10.317 jΩ

3 0.4494 GHz
11.945 Ω
−25.898 jΩ

4 0.4008 GHz
44.404 Ω
−47.180 jΩ

5 0.3504 GHz
30.653 Ω
27.830 jΩ

6 0.3000 GHz
4.665 Ω
−5.885 jΩ

Fig 6—Forward transmission gain and impedance plots for 0.3-0.6 GHz a monopole over a 12-inch square of copper powder in laminate resin #2.

Fig 7

S21 FORWARD TRANSMISSION

LOG MAG   ▷ REF = 0.00 dB   10.000 dB/DIV

0.3000   GHz   0.6000

CH 1 - S21
REF PLANE
0.0000 mm

MARKER 6
0.6000 GHz
−14.720 dB

MARKER TO MAX
MARKER TO MIN

1 0.3126 GHz
−9.565 dB

2 0.3466 GHz
−6.779 dB

3 0.3774 GHz
−5.970 dB

4 0.4494 GHz
−9.945 dB

5 0.5592 GHz
−13.516 dB

S11 FORWARD REFLECTION
IMPEDANCE

0.3000 - 0.6000 GHz

CH 3 - S11
REF PLANE
0.0000 mm

MARKER 1
0.5502 GHz
4.559 Ω
962.162 jmΩ

MARKER TO MAX
MARKER TO MIN

2 0.4998 GHz
5.211 Ω
962.162 jmΩ

3 0.4494 GHz
11.940 Ω
−26.125 jΩ

4 0.4008 GHz
44.564 Ω
−47.642 jΩ

5 0.3504 GHz
30.595 Ω
27.814 jΩ

6 0.3000 GHz
4.683 Ω
−6.000 jΩ

Fig 7—Forward transmission gain and impedance plots for 0.3-0.6 GHz a monopole over a 12-inch square of aluminum wire co-woven.

S21 FORWARD TRANSMISSION

LOG MAG ▷ REF = 0.00 dB 10.000 dB/DIV

0.3000 GHz 0.6000

CH 1 - S21
REF PLANE
0.0000 mm

MARKER 6
0.6000 GHz
−14.585 dB

MARKER TO MAX
MARKER TO MIN

1 0.3126 GHz
−9.712 dB

2 0.3466 GHz
−5.754 dB

3 0.3774 GHz
−5.977 dB

4 0.4494 GHz
−10.044 dB

5 0.5592 GHz
−13.731 dB

S11 FORWARD REFLECTION
IMPEDANCE

0.3000 - 0.6000 GHz

CH 3 - S11
REF PLANE
0.0000 mm

MARKER 1
0.5502 GHz
4.523 Ω
923.500 jmΩ

MARKER TO MAX
MARKER TO MIN

2 0.4998 GHz
6.214 Ω
−10.555 jΩ

3 0.4494 GHz
11.906 Ω
−26.009 jΩ

4 0.4008 GHz
44.088 Ω
−47.187 jΩ

5 0.3504 GHz
31.190 Ω
27.585 jΩ

6 0.3000 GHz
4.771 Ω
−5.994 jΩ

Fig 8—Forward transmission gain and impedance plots for 0.3-0.6 GHz a monopole over a 12-inch square of copper powder in laminate resin #3.

S21 FORWARD TRANSMISSION

LOG MAG ▷ REF = 0.00 dB 10.000 dB/DIV

0.3000 GHz 0.6000

CH 1 - S21
REF PLANE
0.0000 mm

MARKER 6
0.6000 GHz
−14.952 dB

MARKER TO MAX
MARKER TO MIN

1 0.3126 GHz
−10.088 dB

2 0.3466 GHz
−7.192 dB

3 0.3774 GHz
−5.499 dB

4 0.4494 GHz
−10.327 dB

5 0.5592 GHz
−14.188 dB

S11 FORWARD REFLECTION
IMPEDANCE

0.3000 - 0.6000 GHz

CH 3 - S11
REF PLANE
0.0000 mm

MARKER 1
0.5502 GHz
4.334 Ω
1.267 jΩ

MARKER TO MAX
MARKER TO MIN

2 0.4998 GHz
6.006 Ω
−10.373 jΩ

3 0.4494 GHz
11.685 Ω
−26.013 jΩ

4 0.4008 GHz
44.382 Ω
−47.477 jΩ

5 0.3504 GHz
31.616 Ω
27.101 jΩ

6 0.3000 GHz
4.942 Ω
−5.813 jΩ

Fig 9—Forward transmission gain and impedance plots for 0.3-0.6 GHz a monopole over a 12-inch square of commercial conductive paint.

Figure 10

S21 FORWARD TRANSMISSION

LOG MAG   ▷ REF = 0.00 dB   10.000 dB/DIV

0.3000   GHz   0.6000

CH 1 - S21
REF PLANE
0.0000 mm

MARKER 6
0.6000 GHz
−14.459 dB

MARKER TO MAX
MARKER TO MIN

1 0.3126 GHz
−9.580 dB

2 0.3466 GHz
−6.550 dB

3 0.3774 GHz
−6.067 dB

4 0.4494 GHz
−10.045 dB

5 0.5592 GHz
−13.594 dB

S11 FORWARD REFLECTION
IMPEDANCE

0.3000 - 0.6000 GHz

CH 3 - S11
REF PLANE
0.0000 mm

MARKER 1
0.5502 GHz
4.473 Ω
939.985 jmΩ

MARKER TO MAX
MARKER TO MIN

2 0.4998 GHz
6.145 Ω
−10.573 jΩ

3 0.4494 GHz
11.796 Ω
−26.065 jΩ

4 0.4008 GHz
43.522 Ω
−47.586 jΩ

5 0.3504 GHz
31.334 Ω
27.957 jΩ

6 0.3000 GHz
4.567 Ω
−5.865 jΩ

Fig 10—Forward transmission gain and impedance plots for 0.3-0.6 GHz a monopole over a 12-inch square of cloth with glued aluminum foil.

Figure 11

S21 FORWARD TRANSMISSION

LOG MAG   ▷ REF = 0.00 dB   10.000 dB/DIV

0.3000   GHz   0.6000

CH 1 - S21
REF PLANE
0.0000 mm

MARKER 6
0.6000 GHz
−14.440 dB

MARKER TO MAX
MARKER TO MIN

1 0.3126 GHz
−9.179 dB

2 0.3466 GHz
−6.750 dB

3 0.3774 GHz
−6.445 dB

4 0.4494 GHz
−10.277 dB

5 0.5592 GHz
−13.732 dB

S11 FORWARD REFLECTION
IMPEDANCE

0.3000 - 0.6000 GHz

CH 3 - S11
REF PLANE
0.0000 mm

MARKER 1
0.5502 GHz
4.535 Ω
844.757 jmΩ

MARKER TO MAX
MARKER TO MIN

2 0.4998 GHz
6.277 Ω
−10.505 jΩ

3 0.4494 GHz
12.199 Ω
−25.844 jΩ

4 0.4008 GHz
44.091 Ω
−44.939 jΩ

5 0.3504 GHz
32.154 Ω
24.751 jΩ

6 0.3000 GHz
5.290 Ω
−6.292 jΩ

Fig 11—Forward transmission gain and impedance plots for 0.3-0.6 GHz a monopole over a 12-inch square of cloth with laminate resin.

Fig 12—A spreadsheet of the investigation results.

□□

How Antenna Aperture Relates to Gain and Directivity

"Aperture" is a rare term in amateur literature, but it's common in professional antenna discussions. This discussion helps bridge the gap between the two realms.

By Robert J. Zavrel Jr, W7SX, ARRL Technical Advisor

O ver the past few years, I have become increasingly aware of a gap between material presented in Amateur Radio antenna literature and academic texts on the subject. Such texts as *The ARRL Antenna Book* represent 64 years of evolution and as such, contain an unequalled reservoir of information for practical applications of antenna technology. However, the theoretical treatment in this book is, by necessity, somewhat restricted. Although the theoretical treatment is usually adequate to provide a basic understanding for practical projects, those who wish to pursue their knowledge to a higher level are, for the most part, confronted with academic texts requiring a technical degree. This article attempts to bridge that gap.

149 Treehill Loop
Eugene, OR 97405
w7sx@aol.com

While presenting lectures on antenna theory, I am often struck by confusion that is easily remedied by some basic theory beyond amateur publications. For example, the relationship between frequency and path loss is often quite confusing. Without an understanding of the concept of antenna aperture and its various derivations, it is easy to see why this confusion exists. Therefore, I attempt to bridge this gap with a review of some basic concepts. I will also attempt to relate these concepts back to a more common understanding of amateur antennas and provide a few examples. The math will be kept as simple as possible—just algebra and for decibel notation, log functions—and I will attempt to explain each equation verbally as we go. I'll take some simple examples from optics, since radio waves are identical to light waves except for their wavelengths. Optics is, by definition, easier to "visualize."

Inverse Square-Law and Antenna Aperture

Imagine a light bulb located in free space. Assume this light bulb emits light at equal intensity in all directions and is, thus, an *isotropic* source. The light propagates away from the bulb at the speed of light, in the shape of an expanding sphere. In a pure vacuum, there is no absorption of the light; therefore all the power emitted by the light bulb will be evenly distributed over the area of the sphere.

As we observe farther away from the source, the surface of the sphere becomes larger and the energy density (W/area) on the sphere's surface becomes less. If we think of a receiving antenna as representing a very small percentage of the total area of the sphere, we can calculate the actual percentage of total radiation "gathered" by the receptor. This small percentage, or effective area of the receiving antenna is defined as

the *aperture* of the antenna.

The surface area of a sphere is $4\pi R^2$, where R is the radius of the sphere. Therefore, the ratio of power captured by the receive antenna with aperture A to the total power distributed over the area of the sphere is simply calculated using the ratio of the antenna aperture to the area of the sphere, or:

$$\frac{A}{4\pi R^2} \qquad \text{(Eq 1)}$$

You can think of A as being a small part of the sphere's surface.

The relationship between power received and power transmitted is:

$$P_r \quad \frac{A}{4\pi R^2} P_t \qquad \text{(Eq 2)}$$

where P_r is the power received and P_t is the power radiated by the source or transmitter.

Since the radius of the sphere and the distance from the transmitter to receiver (D) are equivalent, we can see that the inverse-square law is derived from spherical geometry. That is, the power in free space, at a distance R from a source is proportional to $1/R^2$ or the more familiar expression $1/D^2$.

For example: A light bulb emitting 100W of light is seen by an observer on a clear night at a distance of 10 miles. His eye's iris has an aperture of 0.01 square inches. How much light power enters his eye? What is the path loss, in decibels, between the light bulb and his eye? Answer: The area of the sphere with radius of 10 miles is about 1,257 square miles or 5.045×10^{12} square inches.

Neglecting atmospheric absorption, his eye receives only about 1.98×10^{-13} W from the light bulb, or –97 dBm. This corresponds to a path loss of about 147 dB (100 W is equivalent to +50 dBm). The actual attenuation of visible light through Earth's atmosphere is quite a bit greater than that because of molecular resonances, but you get the idea.

Another example, switching to metric units: At Earth's surface in full sunlight, we can measure about 750 W per square meter when the Sun is directly overhead. Again neglecting atmospheric effects, and knowing that the Sun is 151,000,000 km from the Earth, what is the total power output of the Sun? The area of the sphere where R is the Sun-Earth distance is 2.87×10^{23} square meters. So the total power output from the Sun must be at least (750 W) $(2.87\times10^{23}) = 2.15\times10^{26}$ W! (Because the Sun also emits energy in forms that do

not reach the ground, its total power output is actually a bit higher than that; but our answer is within a factor of two of the known value.)

Calculation of free-space radio propagation follows exactly the same principles as the optic examples above. *All* antennas have an equivalent aperture, although an antenna's aperture will vary in different directions. Also, antenna gain is directly proportional to aperture; but an understanding of aperture *per se* permits more subtle understanding of the behavior and theory of antennas.

In the above examples, the eye is used as a receive antenna. In humans, the eye is a highly *directional* receptor. Also, our square-meter panel must also be oriented perpendicular to the sun's rays for maximum response. However, it will be very useful to define a reference antenna aperture with *no* directionality—an antenna that receives equally well from all directions. Such an antenna can then be used to compare any possible directional response, from either a transmitting or a receiving antenna. If we use an antenna that radiates equally in all directions (the isotropic antenna introduced above), it will also receive equally well in all directions. A fundamental equation from antenna theory links the aperture of an isotropic antenna to the wavelength of operation:

$$A \quad \frac{\lambda^2}{4\pi} \qquad \text{(Eq 3)}$$

where λ is the wavelength and A is the aperture of the antenna in the same units as λ.

Please note the heavy dependence of isotropic-antenna aperture on the wavelength of operation. *The derivation of Eq 3 is often an exam question in physics electromagnetism courses. The reader may be encouraged to hear that I only received partial credit for my answer!*

When λ is expressed in meters, $\lambda \approx 300/f$, where f is the frequency in megahertz. So, aperture measured in square meters is:

$$A \cong \frac{7.16\times10^3}{f^2} \qquad \text{(Eq 4)}$$

Now combining Eqs 2 and 3, we can write the free-space path-loss equation between two isotropic antennas.

$$P_r \quad P_t\left(\frac{=\lambda}{4\pi\,R}\right)^2_{=} \qquad \text{(Eq 5)}$$

where

$$\left(\frac{=\lambda}{4\pi\,R}\right)^2_{=}$$

is derived from the aperture of an isotropic antenna divided by the area of the sphere at distance R or

$$\frac{\dfrac{\lambda^2}{4\pi}}{4\pi R^2}$$

By rearranging terms and converting to decibels, we have:

$$L_B(dB) \quad -32.4 - 20\log(f) - 20\log(R_{km}) = \qquad \text{(Eq 6)}$$

where L_B(dB) is the basic path loss for free space between two isotropic antennas. This simple equation can be used in first-approximation calculations of path losses.

Directivity and Gain

No real antennas exhibit a perfect isotropic response. All antennas respond better in some directions at the expense of other directions, as does the human eye. The variation in the directional response of an antenna is defined as its *directivity*. For example, if we place a mirror near the light bulb, a shadow will be cast in one direction, but twice the light intensity will be cast in the opposite direction. The radiating system now has a directivity of two in the lit direction, but the total emitted power remains the same with or without the mirror. Therefore at some distance away on the surface of the sphere, some parts of the sphere will receive more light than other parts.

The next important antenna parameter is *gain*. Gain is simply the product of directivity and antenna efficiency. *Unless otherwise stated, in this article efficiency is taken as 100%, therefore directivity and gain are assumed to be equal.* Many antenna systems indeed approach 100% efficiency, especially when the antenna's physical dimensions approach or exceed $\lambda/2$. In other words, the difficulty of maintaining antenna efficiency increases when the antenna size decreases, particularly below $\lambda/2$.

Ohmic resistance, as it becomes more significant than the radiation resistance, is the usual culprit in efficiency degradation, especially in small (relative to a wavelength) antennas.

Radiation resistance values can become very low in small antennas, thus a significant portion of the applied or incident power will be dissipated as heat rather than delivered to a receiver front end or radiated from a transmitter. This radiation efficiency is defined as:

$$RE = \frac{R_r}{R_r + R_l} \qquad \text{(Eq 7)}$$

where R_r is the radiation resistance and R_l is the ohmic resistance of the antenna. Two examples illustrate attempts to increase antenna efficiency (RE) by decreasing R_l. Amateur Radio mobile installations using 8-foot whip antennas are often used in the 75 m band—an antenna much smaller than $\lambda/4$. In this application, good efficiency has been achieved by using 3 inch copper pipe for the first four feet of length to reduce ohmic losses to a minimum. In such antennas, radiation resistance can be a small fraction of an ohm. Again, when using very small antennas (relative to the wavelength), efficiency must be achieved by lowering ohmic resistance, and copper pipe has low ohmic resistance.

Antenna efficiency is almost always critical in transmission systems. Suppose we have an antenna that is only 10% efficient. If we apply 100 W to it, only 10 W will be radiated. This is a large waste. However, low efficiency is sometimes acceptable in receive antennas, where directivity might be more desirable. For receivers at lower frequencies in particular, directivity is often more desirable than efficiency, because losses in the receive antenna are small relative to atmospheric noise. In effect, antenna losses increase the effective noise figure of a *receiver system*. Yet relatively high noise figures will not degrade performance at lower frequencies, such as 1.8, 3.5 and 7 MHz. Some examples of highly directional but inefficient antennas commonly used for low-frequency receivers are the Beverage and small loops. This is the reason that these antennas are usually referred to as *receive antennas*. The Beverage is a highly directional antenna with a low elevation-angle response when installed close to the Earth. Even with –10 dBi gain in the desired direction (very inefficient), it makes a very effective receive antenna for these low-frequency bands.

Solution to the Frequency versus Path-Loss Riddle

The path loss between two isotropic antennas was derived in Eq 5. We can see that loss is proportional to the square of the frequency: When frequency doubles, the loss quadruples. However, if the transmitting and receiving antennas have more or less gain than the isotropic, we can compensate for the power gains by adding the proper gain terms to Eq 5.

$$P_r = G_r G_t P_t \left(\frac{\lambda}{4\pi R} \right)^2 \qquad \text{(Eq 8)}$$

where G_r and G_t are the power gains of the receiver and transmitter antennas respectively, or in decibel notation Eq 8 becomes Eq 9 (below), where L_{path} is the actual path loss.

Thus we can relate antenna *gain* (over an isotropic) to an isotropic *aperture*, $\lambda^2/4\pi$, by a simple coefficient N. This relationship is simple to understand intuitively. If we double the aperture of an antenna, we double the power gain, or twice the gathering "area," which results in twice the power recovered. Doubling the aperture implies $N = 2$, or $10 \log(2) \approx 3$ dBi.

Antenna power gain is thus related to antenna aperture by:

$$G_{(p)isotropic} = N \qquad \text{(Eq 10)}$$

$$G_{dbi} = 10 \log N \qquad \text{(Eq 11)}$$

Perhaps the best antenna type to illustrate the concept of aperture is the parabolic antenna. The parabolic antenna is analogous to the reflecting optical telescope. The incoming electromagnetic radiation is reflected by the parabolic surface and converges at the focal point. A feed antenna is situated at the focal point to recover all the energy reflected by the parabola over the area of the dish —its aperture.

In the optical case, an eyepiece is placed at the focal point and the light gathered by the parabolic mirror is focused at the eye's retina. In the optical as well as the radio examples, the gain and aperture of the antenna are all proportional to the *cross-sectional area* of the parabolic reflector. Again, in real parabolic antennas, the parabolic surface, feed-point efficiency and other issues contribute to a difference between the directivity and gain.

In Eq 3 we saw that the aperture of an isotropic antenna is a function of the square of the wavelength. However, the power *gain* (again assuming 100% efficiency) of a parabolic antenna is also a function of wavelength (or simply the ratio of the parabolic area to the area of the isotropic reference), or:

$$G_{parabola} = \frac{\pi (R_{parabola})^2}{\dfrac{\lambda^2}{4\pi}} \qquad \text{(Eq 12)}$$

where the denominator is the aperture of the reference isotropic and the numerator is the aperture of the parabola, or

$$G_{parabola} = \left(\frac{\pi D}{\lambda} \right)^2 \qquad \text{(Eq 13)}$$

where D is the diameter of the parabola ($2 \times R$). Notice that for a dish or parabolic antenna, the gain *increases* as the frequency squared.

If we substitute $G_{parabola}$ for G_r (since we're using the parabola as a receive antenna) from Eq 8 we get:

$$P_r = G_t \left(\frac{\pi D}{\lambda} \right)^2 P_t \left(\frac{\lambda}{4\pi R} \right)^2 \qquad \text{(Eq 14)}$$

or

$$P_r = G_t P_t \left(\frac{D}{4 R} \right)^2 \qquad \text{(Eq 15)}$$

Consequently, for a given EIRP (for example an isotropic source) and a fixed receiver aperture (a fixed parabolic diameter, D), λ cancels indicating the path-loss *independence* of the wavelength or frequency term. The important point of this result is that although the isotropic gain *drops* as the square of the frequency, the gain of a parabolic (or any constant-aperture antenna) *increases* at the square of the frequency. Therefore the frequency (or wavelength) term cancels, and the path loss becomes frequency-independent.

In a final derivation, we assume fixed apertures at *both* the transmitter and receiver, for both G_r and G_t. The aperture-gain relationship holds true for both receive and

---

$$L_{path}(dB) = \frac{P_t}{P_r}$$
$$= 32.4 - 10 \log(G_t) - 10 \log(G_r) + 20 \log(f) + 20 \log(R_{km}) \qquad \text{(Eq 9)}$$

transmit antennas. Substituting

$$\left(\frac{\pi D}{\lambda}\right)^2$$

for both G_r and G_t in Eq 8 we get:

$$P_r = \left(\frac{\pi D}{\lambda}\right)^2\left(\frac{\pi D}{\lambda}\right)^2 P_t\left(\frac{\lambda}{4\pi R}\right)^2 \quad \text{(Eq 16)}$$

or

$$P_r = P_t\left(\frac{D}{4R}\right)^2\left(\frac{\pi D}{\lambda}\right)^2 \quad \text{(Eq 17)}$$

or

$$P_r = P_t D^4\left(\frac{\pi}{4R\lambda}\right)^2 \quad \text{(Eq 18)}$$

Here, the apertures of the receive and transmit antennas are equal. We can rearrange this equation to show different apertures for the transmitter and receiver, where aperture is:

$$A = \pi\left(\frac{D}{2}\right)^2 \quad \text{(Eq 19)}$$

Therefore Eq 18 becomes:

$$P_r = P_t\frac{A_r A_t}{R^2\lambda^2} \quad \text{(Eq 20)}$$

This discussion has resulted in the derivation of the *Friis Transmission Formula*, named for H. Friis who first published this fundamental equation.

Therefore, we can now state three conclusions relating to operating frequency, antenna aperture and link budget:

1. If isotropic antennas are used at the transmitter and receiver, then the link budget *increases* (more loss) by λ^2. In other words, if you double the operating frequency, the link budget increases by 6 dB (λ^2 in the numerator).
2. If the transmitter uses an isotropic antenna (EIRP remains constant) but the receive antenna aperture remains constant, then the link budget *remains constant* for all frequencies (λ^2 cancels).
3. If the transmitter and receiver both use fixed apertures, then the link budget actually *decreases* by λ^2 (λ^2 in the denominator).

One word of caution: These equations imply that if the gains of the receive and/or transmitter are made arbitrarily large, then it would be pos-

sible to receive more power than was transmitted, which is impossible. Therefore the physical constraint must be: $P_r \le P_t$. Received power may actually approach transmitted power in laser systems.

Some Practical Examples

The parabolic antenna was used as an example because of its obvious relationship to aperture. It is convenient that *any* antenna can be defined as having an equivalent aperture and gain at a given frequency. In addition, the above equations relating gain, aperture, wavelength and range hold for any antenna in use at the transmitter and receiver.

Indeed, the aperture of an antenna can be calculated if its decibel gain over isotropic is known. For example, a 40 m isotropic antenna will have an aperture of $40^2/4\pi$ or about 127 square meters. A half-wave 40-m dipole has a maximum gain of 2.14 dBi broadside to the dipole, or a power gain of about 1.64. Since the aperture is directly proportional to the power gain, the aperture of a 40-m dipole is about (127×1.64) or about 208 square meters. An good approximation for finding the aperture of a dipole is $(\lambda/2)\times(\lambda/4)$. The actual aperture of a dipole takes more the shape of an oval centered on the dipole element, "looking" broadside at the dipole. Of course, the power gain off the end of the dipole is zero, thus the aperture is also zero. Again using the intuition of visualizing an aperture oval drawn around a dipole, we can also visualize the gain of multi-element antennas.

If the spacing of two in-line dipoles (a colinear array) fed in-phase is close to zero, the gain of the antenna is about 1.6 dBd. However, if the spacing between the dipoles is increased,

the gain increases to about 3 dB. Since we are doubling the antenna size, we expect to see a 3 dB increase. However, when the two antennas are closely spaced, some of the apertures of both dipoles are duplicated, therefore the gain is reduced. When the two dipoles are separated, their individual apertures also separate until they actually do double the aperture of a single dipole.

A similar argument can be made for broadside arrays. Here maximum broadside gain, about 3 dB as expected, occurs at about $5/8 \lambda$ separation. A Yagi antenna can exhibit significant gain over a dipole. In effect, the dipole oval increases in size proportional to the power gain. A 6-dBd gain Yagi would result in an aperture area four times that of a dipole. Therefore, to achieve a full 3 dB gain by doubling the number of Yagis implies a minimum spacing between the Yagis greater than the $5/8 \lambda$ dipole requirement.

However, it should be mentioned that additional gain is not the common incentive for stacking HF Yagis. The incentive is usually to fill in radiation nulls created by ground reflections, which is beyond the scope of this discussion. Yet, gains less than 3 dB are achieved by stacking are caused by sub-optimum spacing. For VHF arrays, the incentive is usually to achieve more forward gain. Therefore, more effort is put into optimum spacing (and less of a mechanical challenge) to achieve maximum effective aperture in stacked VHF arrays.

References

1. R. D. Straw, N6BV, Editor, *The ARRL Antenna Book*, 17th ed. (Newington, Connecticut: ARRL, 1994).
2. J. D. Kraus, *Antennas* (New York: McGraw Hill, 1950).
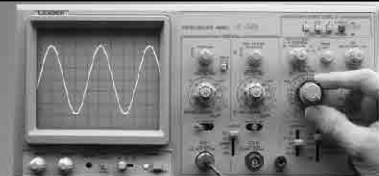
The Uncoder: An Automatic Universal CTCSS Tone Encoder/Decoder

---

Here's an accessory to revive older VHF equipment.

By Chris Sieg, WA3LDI

I hate to let any piece of equipment go to waste, but what can you do with those old 2-m FM rigs that have no CTCSS tone capability? Well, you add it, of course! While "big-knob" tone encoders have been available from several sources, their downside has been having to know the tone of the repeater you would like to use and the need to turn the knob every time you change repeaters. Wouldn't it be nice to have an add-on tone encoder and decoder that "sniffs" the PL from the repeater just like those fancy new rigs? Plus, as an added convenience and safety feature, remember what the tone was for each repeater? Imag-

ine not having to take your eyes off the road to rotate a knob just to change the PL. Now you can have all this and more with the Uncoder (see Fig 1).

The details of a universal encoder/decoder, or Uncoder for short, really started to gel when I decided to resurrect a couple of 2-m rigs that had been lying around the shop, unused for quite a while. One of the rigs was a Kenwood TS-700A (see Fig 2) all-mode base-station transceiver, and the other was a TR-7400A mobile that I wanted to use with some of the local PL-required repeaters. I wanted a device that was intuitive to use: Simply tune the transceiver to the repeater and let the Uncoder worry about the tone setup. The best solution would be a tone encoder/decoder that could detect the operating frequency and set the tone frequency appropriately. Once

given the CTCSS tone information for a particular frequency, the Uncoder should be able to remember the setting and automatically set the tone as I tune my radio to various repeaters. To accomplish this task, the Uncoder needed to incorporate a frequency counter, along with tone encoding/decoding and the appropriate microcontroller circuitry.

About the Circuit

The selection of a microcontroller chip for the heart of a design is an important decision. The microcontroller needs to have enough memory, I/O pins and system resources to support the work it needs to perform. Although there are many fine microcontroller products available in the market, I have always been a fan of Atmel's line of flash-programmable

PO Box 123
Hillsboro, NH 03244-0123
PIEXX@conknet.com

devices. One great feature of many in Atmel's line of microcontrollers is the ability to serially program the flash code memory space in the chip while it is installed in the circuit. With that feature, you can make changes in the program and then download the new code to the microcontroller without removing or changing any of the components on the circuit board. This is a great advantage while debugging your code. The device I chose for the project was the ATmega8 microcontroller. The Atmega8 incorporates 8 kB of program flash, 512 bytes of EEPROM to hold the frequency/tone lists, 1 kB of RAM, several internal counters/timers with input capture facilities as well as serial ports and an 8-channel A/D converter. Although I didn't use all of the Atmega8's features, some really helped simplify the design of the Uncoder.

The ATmega8's input capture feature, along with its associated timers, allows the microcontroller to accurately measure the period of a waveform. An input transition on the Input Capture pin (U2 pin 12) causes the microcontroller to record the value of one of its internal counters that is being continuously incremented by the processor's crystal-controlled clock.

This action performs most of the functions of the frequency-counter portion of the Uncoder. The transceiver's local oscillator is brought into the Uncoder at spring pin P1. The local-oscillator signal is coupled to the input (pin 8) of U7 an LMX1501 frequency-synthesizer. Although the LMX1501 is intended to be a frequency generation device, in the Uncoder U7 is used to amplify the local-oscillator signal and divide the frequency so that its period can be measured by the microcontrollers input-capture circuitry.

The Uncoder uses a tone encoder/decoder chip intended for FRS and GMRS radio equipment. The CMX808A, U6, incorporates a CTCSS tone generator, a fast-acting tone detector and various signal-conditioning components. The CMX808A can detect and decode a sub-audible tone in 150 ms. The highly integrated features of this device help keep the component count down in the Uncoder. Interface to the CMX808A is made through a clocked serial interface. The required 4-MHz clock for U6 is borrowed from the microcontroller's crystal oscillator via C22. The output tone from U6 is routed to the tone level pot, R26, and then is buffered and filtered by op amp U5 and its associated circuitry.

I used a four-digit, seven-segment

LED display on this project. The display is multiplexed, which means that each display digit is briefly illuminated one digit at a time, with the full four-digit indication being scanned across the LED device. Since the digits are scanned quickly, about 30 times

a second, all of the digits appear to be illuminated at once. This display-multiplexing scheme affords a simplified circuit; the digit segments are parallel connected so that the four digits require only a single driver. The segment drive is generated by U3, an

Fig 1—A completed Uncoder. This is the goal.

Fig 2—An Uncoder installed on top of a Kenwood TS-700A 2-meter transceiver.

eight-output shift register. The choice of a shift register for an output port was made for economy. With the shift register, you can generate eight outputs from a single 16-pin chip while employing only three I/O connections to the processor. Since other devices in the design share the clock and data lines, there is only one extra output line: OLD, an output load strobe, required from the processor to generate the eight segment outputs for the display. The LED display also uses five digit-select lines to select each of the four display digits plus a digit select for the mode displays. These digit select lines are generated by the microcontroller and buffered by transistors Q2, Q3, Q5 and Q6.

The Uncoder uses microcontroller I/O pins for the three push buttons, the rotary encoder, the Xmit and Off Hook interface inputs and a Tone Detect output that is buffered by transistor Q4. D1 and D2 are used to block voltages greater than Vcc, +5 V dc, on the Xmit and Off Hook interface inputs. J1 allows connection of an inexpensive programmer to the Uncoder for program updates. An eight-position modular jack, J2, connects most of the Uncoder's signals to the host transceiver. I chose the modular jack because of its easy availability. These jacks are commonly used for CAT5 network wiring.

Construction

The components used in the Uncoder required this to be a surface-mount project. Although many people seem uncertain about their ability to build projects that employ surface mount components, it is actually easier to use these devices. This, coupled with the fact that through-hole parts are becoming more difficult to obtain, requires the modern ham to spend the few hours of time learning surface-mount construction techniques. Although it isn't the intention of this article to provide a step-by-step tutorial in surface-mount construction techniques, I will provide a few pointers that I feel may be helpful in constructing the Uncoder.

Surface-Mount Assembly Notes

A mentor of mine once told me that cleanliness is next to godliness, except in soldering where cleanliness is next to nothing. This particularly holds true with soldering surface-mount components. Obtain a variable-temperature soldering station and make sure you keep the tip clean and tinned. You will definitely need to have a wet sponge on which to wipe the tip regularly. I

also suggest regularly dipping the tip of your iron in tinning flux. I put a teaspoon or so of Oatey #95 tinning flux in a bottle cap and dip the soldering iron tip into it when the tip gets dry. The Oatey product is available among the plumbing supplies at many hardware stores.

Apply a small quantity of rosin paste flux, Kester SP-44 for example, to the circuit board pads before placing the components. Don't use too much and try to keep it on the solder pads. If you use too much, there will be more to clean after assembly.

Install the surface-mount components first. That way, your board will sit flat on your workbench as you build it.

When soldering the components, apply the soldering iron and solder to the solder pad, not the component lead. This will help to keep the component from moving.

Tack solder one lead of ICs then check to make certain that the rest of the component leads are centered over their PC pads before completely soldering all of the leads. It is a lot easier to reposition a component when only a single lead is soldered.

When you need to install ICs with closely spaced leads, like the CMX808A, a technique that works quite well is to:

1. Apply a fair amount of solder to the tip of your iron.
2. Dip the tip into the tinning flux.
3. Draw the wetted bead of solder across the PC board/component leads.

This is a kind of poor man's wave soldering. If you end up with bridged pads, clean the soldering iron tip on your sponge, dip it into the tinning flux, and then try to draw the solder from the bridged pads with the wetted iron. If you need to, you can always use some solder wick to remove a solder bridge.

Clean the flux residue from your board with a commercial flux remover or alcohol. Don't use rubbing alcohol, it's mostly water and won't do a very good job.

Always carefully inspect your work after you complete the assembly. Use a strong lamp and a magnifier if needed. Sometimes it is easier to inspect a board if you shine the lamp through the board from the backside.

Uncoder Assembly Notes

The three push-button switches need to be mounted 1/16 of an inch above the topside of the PC board so that they will extend above the sheet metal front panel. Use a small PC board spacer

between the switches and the main PC board to accomplish this.

Note that pin 1 on each of the ICs is located closest to the reference designator "U" silk-screened on the PC board for that IC.

Make sure that the polarized caps and diodes are oriented properly. Double-check their orientation with the assembly drawing before soldering these components.

Fig 3 (pp. 42 & 43)—A schematic diagram of the Uncoder.
C1—1000 µF, 16 V
C2, C3, C5, C6, C12, C14, C15, C20, C21, C25—0.1 µF 1206
C4—100 µF, 16 V
C8, C7—39 pF 1206
C10, C11, C18, C19, C24—10 µF, 16 V
C13—47 µF, 6 V
C16, C30—1 µF 1206
C9, C17—0.001 µF 1206
C22—39 pF 1206
C23—22 pF 1206
D1, D2, D4, D5—1N914 1206
D3—1N4001 SM
JP2, JP3, JP4—PJUMP solder jumper
J1—6-pin header
J2—8P8C Modular jack
P2, P1—Spring connector
Q2, Q3, Q4, Q5, Q6—2N4401 SOT23
R1, R5, R12, R23, R33—100 kΩ 1206
R4, R6, R8, R9, R10, R11, R13, R15—470 Ω 1206
R7, R14—4.7 kΩ
R16, R17, R18, R19, R20, R21, R22, R24, R27, R29—2 kΩ
R25—1 kΩ
R26, R37—POT 47 kΩ
R28—68 kΩ
R30—330 kΩ
R31—82 kΩ
R32—47 kΩ
R34—1 kΩ
R36—1 kΩ 0603
S1, S2, S3—SWPCMNT
S4—RENCODE-CTS
U1—LM78L05 voltage regulator
U2—AtMega8-16AC
U3—74HCT595D
U4—LTC8710HR 7-segment display
U5—LM321
U6—CMX808A
U7—LMX1501AM
Y1—4.00ECSZ Crystal Parallel 22 pF
Misc
CAS1—Case Assembly with mounting bracket
PCB—Printed circuit board
Cable—Interface cable assembly

J2 Cable Colors (Standard Cable)

1	Red (ribbon)	+12 V
2	Red (shielded)	Audio In
3	Black (ribbon)	Xmit
4	White (shielded)	Audio Out
5	White (ribbon)	Hook
6	Yellow (shielded)	Tone Out
7	Black	Ground
8	Shields	

U1
LM78L05

REG
In   Out
Gnd

V_{CC}

D3
1N4001

C1 1000 µF 16 V
C2 0.1
C3 0.1
C4
C5 0.1
100 µF 16 V

V_{SS}

Except as indicated, decimal values of capacitance
are in microfarads (µF); others are in picofarads
(pF); resistances are in ohms;
k = 1,000, M = 1,000,000.

J1
CON6AP

$\overline{RESET}$ 1   2 MOSI
3   4 MISO
V_{CC} 5   6 CLK

U2
ATmega8

7 OSC1 IN   SCK PB5 17
MISO PB4 16
MOSI PB3 15
SS PB2 14
OC1 PB1 13
ICP PB0 12
8 OSC2 OUT   AIN1 PD7 11
AIN0 PD6 10
T1 PD5 9
T0 PD4 2
29 $\overline{RESET}$ INT1 PD3 1
INT0 PD2 32
PD1 TXD 31
PD0 RXD 30 HOOK SWITCH
ADC7 22 AUDIO DETECT
ADC6 19
V_{CC} ADC5 SCL PC5 28 XMIT DETECT
18 AVCC   ADC4 SDA PC4 27
20 AREF   ADC3 PC3 26
ADC2 PC2 25
ADC1 PC1 24
21 AGND   ADC0 PC0 23

C7 39
C8 39
Y1 4.00 MHz

V_{CC}
R5 100 k

D1 1N914
R7 4.7 k

V_{CC}
R12 100 k

D1 1N914
R14 4.7 k

J2
8P8C
1   2 AUDIO IN
XMIT 3   4 AUDIO OUT
OFF HOOK 5   6 TONE OUT
7   8

JP2 PJUMP
JP3 PJUMP
JP4 PJUMP

TONE DETECT   R20 2 k
R21 2 k
Q4 2N4401SOT23

V_{CC}
C12 0.1
C13 47 µF 6 V

U6
CMX808A

CLK 3 SCLK   SUB AUDIO OUT 18
ODAT 4 SDI   TX AUDIO IN 15
SDO 5 SDO   TX AUDIO OUT 16
SCE 6 $\overline{SCE}$ RX AMP IN 12
SINT 7 $\overline{IRQ}$ RX AMP OUT 13
1 XTAL OUT   RX AUDIO OUT 14
VOLUME IN 17
R36 1 M/0603   VOLUME OUT 19
C22 33
2 XTAL IN
VBIAS   GND   A/D CAP
11   10   9
C20 0.1   C21 0.1

V_{CC}
R23 100 k
R26 47 k
C15 0.1
R28 68 k
U5 LM321
1
5
4
3
2
R25 1 k
C10 10 µF 16 V
C11 10 µF 16 V
C9 0.001
R30 330 k
C14 0.1
R31 82 k
R32 47 k
C16 1 µF
R33 100 k
C17 220
R37 47 k
C30 1 µF
C18 10 µF 16 V
C19 10 µF 16 V
R34 RSM
R1 100 k

Except as indicated, decimal values of capacitance are in microfarads (µF); others are in picofarads (pF); resistances are in ohms; k = 1,000, M = 1,000,000.

C1, the 1000 µF 16 V capacitor is mounted on the rear of the board and parallel to it, so as not to extend above J2. Study the assembled Uncoder picture to ascertain this orientation before soldering C1 into the circuit.

Make sure you properly orient the display in the PC board before soldering. The decimal points are closest to J1.

The **RFIN** connection point and the associated ground lead located to its right are made to accept solderless spring pins. Install these pins with their open sides on the side of the board with the silk-screened markings. Carefully solder these pins so that you don't fill the open side with solder. These solderless spring pins are designed to accept a solid or tinned #24-#28 AWG wire lead.

For normal operation, install solder jumper JP2. This connects interface connector pin 8 to signal ground.

Generally, I make the interface cable that mates with J2 from a three-pair shielded cable for the audio connections; a twisted three-wire cable for V+, the Xmit and Hook switches and a #22 AWG power ground lead. The standard cable configuration is indicated on the schematic in Fig 3. These wires are all crimped into a standard RJ-45 plug and then glued to form a strain relief. Figs 4 and 5 show the completed circuit board.

You can either purchase a preprogrammed microcontroller or program this device in circuit.[1] If you decide to program the device in circuit, there are several sources for the programming cable and associated software. The hardware required to program the Uncoder via a PCs parallel (printer) port is shown below (Fig 6). One good source for the programmer software is: **www.lancos.com/prog.html**.

Connection to Transceiver

The pinout for J2, the modular 8-pin interface connector is as follows:

1. +12 VDC In
2. Audio In
3. Xmit
4. Audio Out
5. Hook Switch
6. Tone Out
7. Power Ground
8. Signal Ground.

Depending on the intended use and the locations of solder jumpers on the board, you may not need to connect all of the signals. For most of the installations that I have done, I have connected

the Uncoder to provide both transmit and receive CTCSS functionality.

The power required for the Uncoder is +9 to +15 V dc at approximately 50 mA. The power lead, pin 1 of J2,

should be connected to a convenient switched supply within your transceiver. The return connection for the power is on J2 pin 7.

For the Uncoder to operate in a
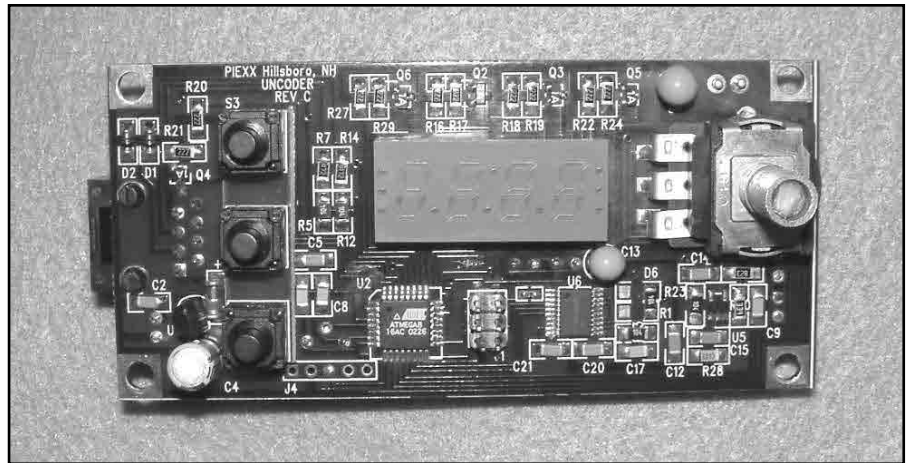
Fig 4—A top-side view of a finished Uncoder board.
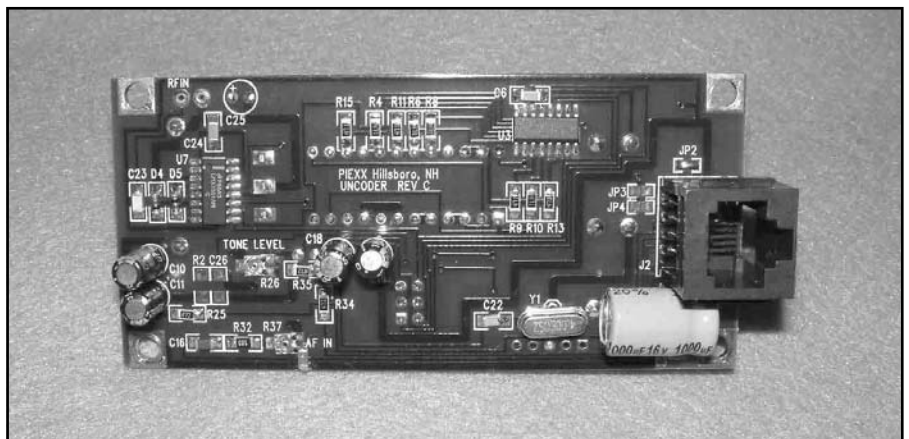
Fig 5—A bottom-side view of a finished Uncoder board.
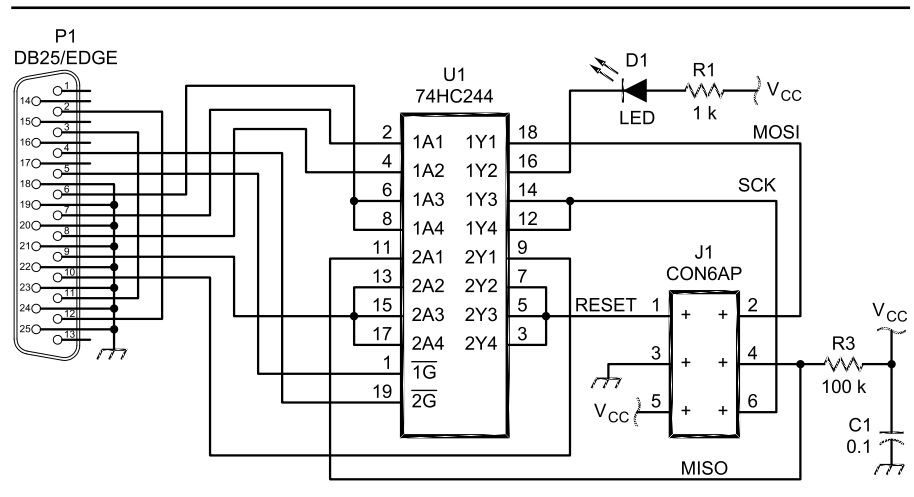
Fig 6—A schematic of a parallel-port adapter for programming the microcontroller inside the Uncoder.

[1]You can download code for this project from the ARRL Web **www.arrl.org/qexfiles/**. Look for 0405Sieg.zip.

tone-squelch mode, it needs to sample the detected audio and provide a way to disable the audio path in the squelched condition. The Uncoder provides an open-collector transistor output that can be connected into your transceiver's circuitry to enable or disable the audio path. An easier way to take care of both the tone input and squelch requirements is to connect the Uncoder's audio in (J2 pin 2) and audio out (J2 pin 4) in series with the hot lead of your rig's volume pot.

The CMX808A chip has an audio switch in line with its audio path, and this switch is deactivated by the Uncoder firmware when the tone squelch is activated and the correct tone signal is not seen. The connection in a typical transceiver is outlined in the schematic shown in Fig 7. If you have no need for tone squelch, simply connect J2 pin 2 to the high side of the volume control and leave J2 pin 4 unconnected. If you do not connect the audio in signal to the Uncoder, the device will not be able to detect and report the CTCSS tone being used with its FIND mode.

The tone output is available from the Uncoder on J2 pin 6. If your rig has a connection point for a tone generator, you should connect the tone output to it. Otherwise, connect J2 pin 6 to a point in the transceiver close to the modulator and beyond the microphone conditioning circuitry. The tone output level from the Uncoder can be adjusted to about 1 V rms if necessary. The high side of the deviation control is often a good point to inject the tone output. If you must connect the tone output to a point in the transceiver near the microphone input, you may need to install a series resistor to reduce the tone's signal level so that it won't swamp the modulator.

The Uncoder needs to detect when your transceiver switches to the transmit mode. P2 pin 3, the Xmit detect line, should be connected to either the PTT line on your mic plug, the trans-

mit indicator light or a switched Xmit power connection. Don't worry about the polarity of the signal; it can be switched in one of the setup menus.

J2 pin 5, Hook Switch, is an input to the Uncoder indicating that the microphone has been taken out of its holder. If you have a holder that is switched, connect this line to J2 pin 5; when you unhook the microphone, the tone squelch will be defeated allowing you to hear channel activity.

For the Uncoder to work in the automatic mode, it must be able to determine the transceiver operating frequency. Frequency detection is accomplished by installing a coax connection from the RFIN connection point on the Uncoder to the receiver local-

oscillator output of your transceiver. Most transceivers have a shielded cable running from a buffered VCO output on their synthesizer (or PLL) circuit board to the receiver first-mixer input. This usually makes for a convenient connection point to the Uncoder's RFIN frequency-counter input. With some transceivers, the local oscillator is sufficiently strong to be sampled by simply positioning the center lead of a coax from the Uncoder's RFIN input in the vicinity of the oscillator. If this method is employed, be sure to secure the shield lead so that its sense lead won't shift position during normal operation of the transceiver. Alternatively, a very small coupling capacitor (1-5 pF) may be used.
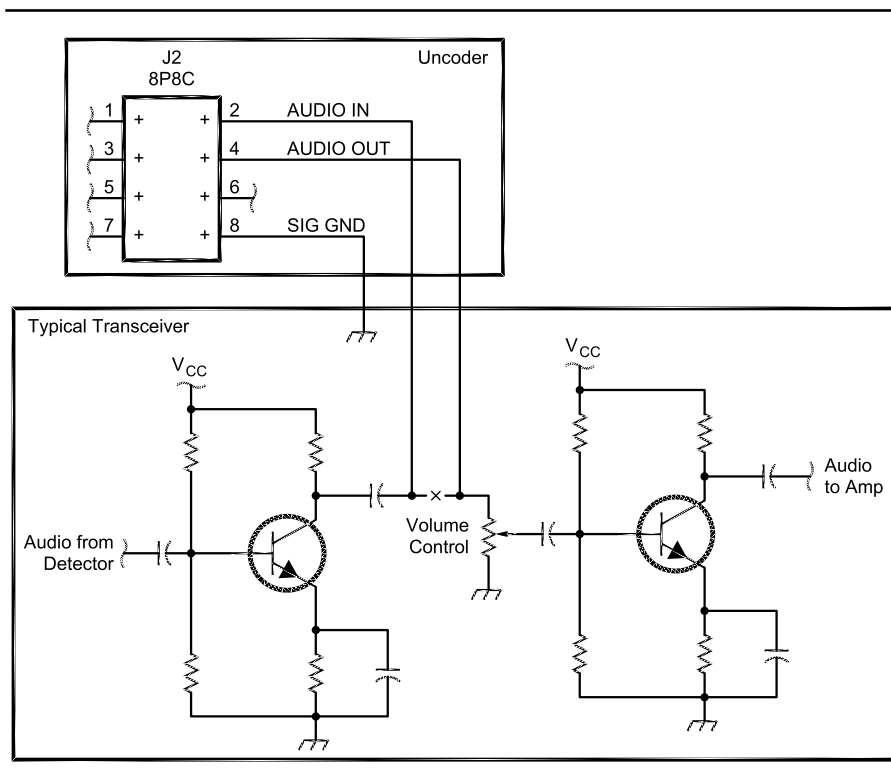
Fig 7—Uncoder receive-audio connections to a typical receiver.

Table 1

Available from WA3LDI

Assembled and tested Uncoder with Interface cable assembly	$129
A complete set of parts including the sheet metal case and interface cable	$99
Semiconductor kit including all ICs, transistors, diodes, LED display and preprogrammed microcontroller	$37
PC board kit including main and switch spacer PC boards	$17
Switch Kit including Rotary encoder & 3 push buttons	$6.50
Painted and silk-screened sheet metal case w/mounting bracket and LED lens	$19
Interface Cable assembly	$10
Parallel Port Adapter for AtMega8 Programming	$19

Make your connection to the transceiver as short and direct as possible. Avoid excessive cable length for all connections.

Setup

After you have installed the Uncoder and applied power, the display should light and show different information depending on how the Uncoder has been set up. If the display shows CRC, then the Uncoder's channel/setup memory is undefined and must be reset. To do so, press and then release, all three front-panel buttons. Press the XMIT button first and hold it while you simultaneously press and hold the RCV and AUTO buttons. When the display shows CLR, release the buttons. This procedure clears the channel memory and resets the setup parameters to their default states.

You will need to adjust the setup parameters to match your hardware configuration. To enter the setup mode, press and hold the XMIT button for about ½ second until the first setup parameter appears. Once in the setup mode, you can cycle through the various parameters by pressing the XMIT button. Each time you press it, the program cycles to the next setup parameter. Rotating the encoder knob will change the value of a parameter. All parameters, except the *A* (audio level) parameter, can be set to one of four possible states: 0, 1, L or h. The audio-level parameter can be set to a value between 0 and 31. The setup parameters are defined as follows:

Td—Tone Detect Output State

0—steady-state low (Q4 always on).
1—(default) steady-state high (Q4 always off).
L—high, will go low (Q4 on) if the tone squelch is enabled and the correct CTCSS tone is detected.
h—low, will go high (Q4 off) if the tone squelch is enabled and the correct CTCSS tone is detected.

tP—Transmit Detect Input Polarity

0, 1—input is ignored; the CTCSS tone, if selected, will appear on J2 pin 6.
L—(default) The Uncoder will go to the transmit mode when the Xmit signal on J2 pin 3 goes to a low state, less than 0.5 V dc.
h—The Uncoder will go to the transmit mode when the Xmit signal on J2 pin 3 goes to a high state, greater than 3 V dc.
When the Uncoder goes into the Xmit mode, the CTCSS tone that is

selected will be output on J2 pin 6 and the automatic frequency scanning algorithm will be suspended if the AUTO mode is enabled.

hP—Hook Switch Input Polarity.

0, 1—If the **hP** parameter is set to 0 or 1, the input is ignored**.**
L—The off-hook condition is detected when the Hook Switch signal on J2 pin 5 goes to a low state, less than 0.5 V dc.
h—(default) The off-hook condition is detected when the Hook Switch signal on J2 pin 5 goes to a high state, greater than 3 V dc.
When the Uncoder detects the off-hook state, the tone squelch, if selected, will be disabled. This allows you to hear, when you pick up the microphone, all stations operating on a frequency even if they aren't using a CTCSS tone.

Audio Level

In addition to an audio switch, the CMX808A also has a level control in the audio path. When the Uncoder's tone squelch is open, the audio level, as seen at J2 pin 4, is set according to the **A** value. An **A** value of 0 effectively turns off the audio channel. The maximum audio is achieved when **A** is set to 31.

PU—Power Up State

1—If the **PU** parameter is set to 1, the Uncoder will enter the automatic mode when it is powered up. Any other **PU** value will cause the Uncoder to power up in the normal Tone mode. The default state of **PU** is 0.

SU—Set Up

The Set Up parameter is not really a parameter setting but a way to access various calibration routines. Selecting a value with the knob and then entering the selected routine by pressing the RCV button enters the calibration routines. Depending on the value selected, four possible calibration routines can be executed:
0—This routine shows the frequency that the Uncoder is currently detecting. The display will continuously update until the operator, again, presses the RCV button.
This routine calibrates the Uncoder frequency counter. For 2 m operation, the receive frequency should be set for 146.520 MHz prior to selecting this calibration routine. After the calibration takes place the routine enters the frequency display mode and the display will continuously update until the operator, again, presses the RCV button.
This routine only calibrates the fre-

quency counter. Since you normally would want to set the IF offset frequency before calibration, using the **L** routine is generally the more appropriate calibration routine to use.

L—This routine allows the operator to preset the IF offset frequency and then calibrates the Uncoder frequency counter. For 2 m operation, the receive frequency must be set for 146.520 MHz prior to selecting this calibration routine. When this routine is entered, the IF will be shown with the display cycling between the megahertz digits and kilohertz digits. By turning the knob, you can adjust the IF offset frequency to that of your transceiver. Once the IF offset is correctly set, press the RCV button to enter the value and continue with the calibration. After the calibration takes place, the routine enters the frequency display mode and the display will continuously update until the operator, again, presses the RCV button.

H—The last calibration routine is used to set receive audio level provided to the tone decoder chip. When this routine is selected, the display will show a continuously updated three-digit reading that is proportional to the audio level. R37, marked AF IN on the bottom side of the Uncoder board, is used to adjust the audio level presented to the circuitry. Although the Uncoder is capable of working with a broad range of input levels, it is best to adjust R37 so that the LED display shows audio peaks in the 100-150 range. Generally, the unsquelched receiver noise will provide the greatest readings on the display and should be used to make this adjustment.

You can exit the setup parameter menu by either pressing the RCV button or executing one of the four calibration routines.

Operation

The Uncoder has two operating modes: normal and automatic. The automatic mode of operation is indicated by illumination of the right-most decimal point, directly above the front-panel silk-screen marking AUTO. You can switch from normal to automatic mode by pressing the AUTO button. Switching from the auto mode to the normal mode is accomplished by pressing any of the buttons.

Normal Mode Operation

In normal mode, you can set the transmit and receive tone frequencies manually or use the Uncoder's automatic tone-detection feature to find the frequency of a CTCSS tone being

received. To set the transmit tone, press the XMIT button and then rotate the knob to select the desired transmit CTCSS tone. If a transmit tone is selected, the XMIT led indicator will light.

To set the receive tone, press the RCV button and then rotate the knob to select the desired receive CTCSS tone. If a receive tone is selected, the RCV LED indicator will light. Selecting a receive tone will enable the tone squelch system, assuming that the Off-Hook switch isn't active, and the transceiver audio will be muted. When a received tone matches that to which the Uncoder is currently set, the DET LED will light and the tone squelch will open allowing you to hear the signal.

To find the tone being transmitted by a station, simultaneously press the XMIT and RCV buttons. The RCV LED will blink, indicating that the Uncoder is operating in the FIND mode and is searching for a tone. If no tone is detected, the display will show four dashes in its numeric field. The dashes will change to a valid tone frequency if a CTCSS tone is detected. You can exit the FIND mode in two ways:

If you simultaneously press the XMIT and RCV buttons, the Uncoder will automatically set both the transmit and receive tones to the detected tone frequency before exiting the FIND mode.

Pressing any other key will cause the Uncoder to exit the FIND mode without retention of the detected tone.

Automatic Mode Operation

In the automatic mode, the Uncoder samples the transceiver's receive frequency and compares this to a user-defined table of frequencies. If a match is detected, the Uncoder will automatically set both transmit and receive tones to the values retrieved from the table. For this process to proceed, the user must define the operating conditions for those frequencies to which he wishes the Uncoder to respond.

To add a frequency to the Uncoder's search list, simply tune your transceiver to the frequency of interest, set the transmit and receive tones as necessary for proper operation on that channel, then save the information by simultaneously pressing the RCV and AUTO buttons. To remove a channel from the list, follow the same procedure, but set both tones to off before saving the channel. If a channel is saved with the tones set to the off condition, its frequency is removed from the list. Similarly, a channel's tone data may be modified by saving new tone information at the same frequency. This will cause the table entry for that frequency to be overwritten with the new data.

Once a frequency list is created, you can start automatic mode operation by pressing the AUTO button. In the automatic mode, the AUTO LED will light and the last four digits of the frequency will show on the display. As you tune your transceiver, you will see the XMIT and RCV LEDs change states as you tune through frequencies that you have entered in the channel list. If you key your transceiver the automatic mode, the frequency scanning algorithm will be suspended until you return to the receive mode. Frequency scanning is suspended on transmit so that the Uncoder won't see the transmit frequency as a different entry in the channel table and modify the tone data inappropriately.

Conclusion

I think it is a blast to figure out ways to improve on older equipment with current technology. The Uncoder lets you breathe some new life into some of your older, high-quality FM equipment that has been shelved because it lacks tone features. By incorporating a frequency counter, tone encoder/decoder and the appropriate microcontroller based "glue," the Uncoder adds tone features to your older rig that perform as well or better than current production equipment. I hope that some of the design ideas employed in the Uncoder may act as a catalyst for other, future radio-upgrade designs. Expanding microcontroller product lines and the large quantity of LSI peripheral devices that appear every year lend themselves nicely to ham radio and open doors for a wide range of entrepreneurial endeavors.

*Chris Sieg, WA3LDI, has been a ham since 1968 and received his Extra class license in 1994. He owns and operates Piexx Company in Hillsboro, New Hampshire, where he designs and builds special electronic products. You can view his ham products at **www. piexx.com**.* □□

An Optimized Reduced-Height Vertical Array

Would you like a wire antenna that performs well at low heights without radials? This two-loop array may be the answer.

By Andrew Roos, ZS1AN

There are many occasions when it is not feasible to erect an antenna half a wavelength above ground as is necessary for horizontally polarized antennas like dipoles and Yagis to achieve good DX performance. This article describes a simple vertically polarized parasitic array that provides effective low-angle radiation with the top of the antenna as low as 0.2 λ above ground. Computer-optimized dimensions are provided for 80-, 40- and 20 m versions of the array, as well as practical construction details of the prototype.

The idea for the design comes from L. B. Cebik's excellent articles on "Self-

PO Box 350
Newlands, 7725, South Africa
zs1an@qsl.net

Contained Vertically Polarized Wire Antennas."[1] The antennas he describes are self-contained in that they do not require a ground connection to complete them electrically, so they do not require a buried radial system or "ground-plane" radials. Amongst the antennas Cebik describes, the Rectangular Self-Contained Vertical[2] ("Rectangular SCV") provides an attractive combination of high gain and low height.

The Rectangular SCV consists of a 1 λ rectangle approximately 1/8 λ high and 3/8 λ wide that is fed in the center of one of the vertical sides. It exhibits a bidirectional pattern similar to other 1 λ loops, giving a maximum gain of 3.7 dBi with the base 0.2 λ above average soil.[3] Radiation from the horizontal wires largely cancels so the antenna

[1]Notes appear on page 54.

functions as a broadside array of two in-phase vertical radiators, the vertical sides of the rectangle. The feed-point impedance is low so the antenna can be fed directly from a 50-Ω source.

Although L. B. notes in passing that "... all of the SCVs can be arrayed in pairs (or triplets) aligned broadside for either phased or parasitical operation,"[4] I have not found any detailed analysis of the optimum dimensions for such arrays or the performance that can be expected from them. The idea of using two rectangular elements was also suggested to me by the similarity of this arrangement to the driven four-element rectangular array described in *The ARRL Antenna Book*.[5] The book claims a gain of 6.8 dB over a single element for that array; and since the points of maximum current in both antennas are spaced and

phased similarly, I hoped that this design would achieve similar performance without the need for a phasing network.

The Rectangular SCV Array

The Rectangular SCV Array consists of two rectangular 1 λ loops, one a driven element and the other a parasitic reflector, spaced approximately λ/4 apart. Fig 1 shows an EZNEC[6] model of a Rectangular SCV Array. Wires 1 through 4 comprise the driven element, while the reflector consists of wires 5 through 8. Notice the position of the feed point, which is represented by the circle halfway up wire 1. The direction of maximum radiation is in line with the X-axis. The addition of a parasitic reflector results in a unidirectional pattern with a maximum gain of 6.4 dBi when mounted

with the base 0.2 λ above ground. This is 2.7 dB better than the basic Rectangular SCV, although in practice, we will have to be satisfied with somewhat less gain from both antennas if

we mount them close to ground to minimize the height required overall.

The addition of a reflector also raises the feed-point impedance.[7] Although it is possible to design for a
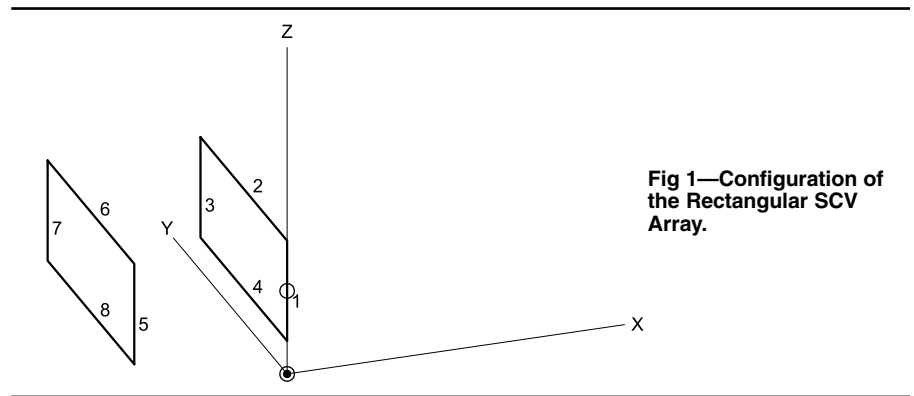
Fig 1—Configuration of the Rectangular SCV Array.
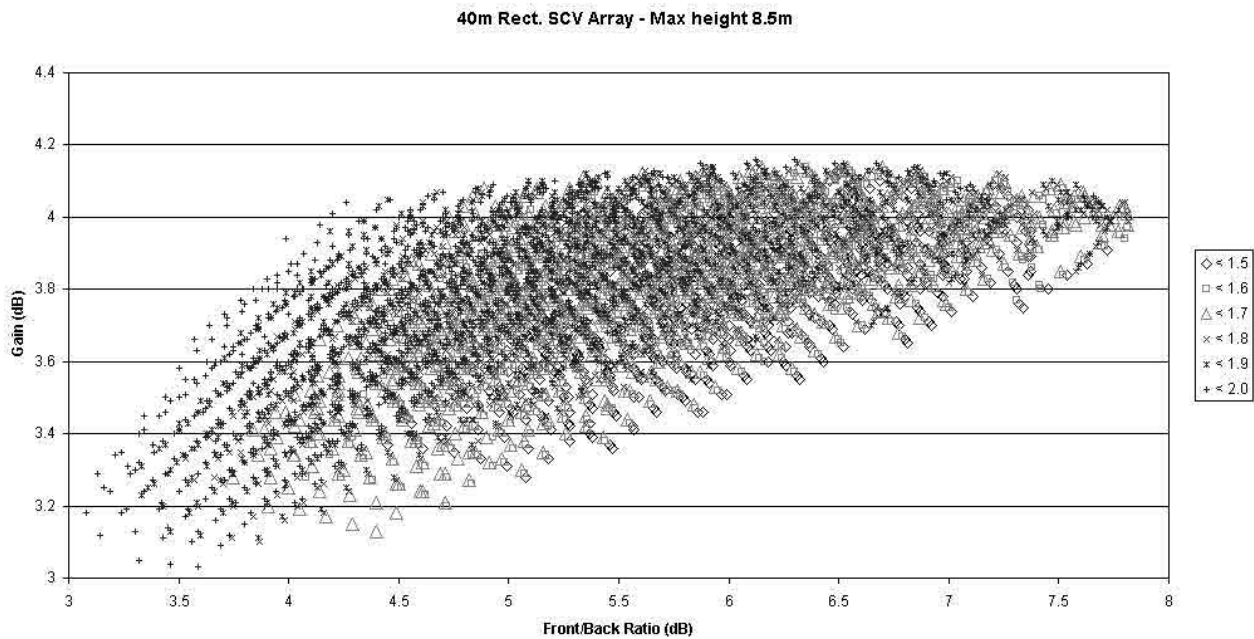
Fig 2—Scatter plot showing gain, F/B and SWR for one optimization run (40 m, maximum height 8.5 m).

Table 1

"Optimum" designs of Rectangular SCV Arrays

Band	Maximum Height(m)	Element Height(m)	Driver Width(m)	Reflector Width(m)	Element Space(m)	Base Height(m)	Match Length(m)	Minimum Gain(dB)	Minimum F/B(db)	Maximum SWR
20	4.2	3.10	7.85	7.90	4.80	1.10	3.44	4.6	9.1	1.3
20	6.3	3.70	7.35	7.45	4.50	2.60	3.44	5.3	10.2	1.4
40	8.5	6.80	14.80	14.95	9.80	1.70	6.82	4.1	7.5	1.6
40	12.8	7.80	14.10	14.35	8.00	5.00	6.82	4.6	7.8	1.7
80	16.4	15.00	26.45	27.30	18.00	1.40	13.36	3.5	5.3	2.4
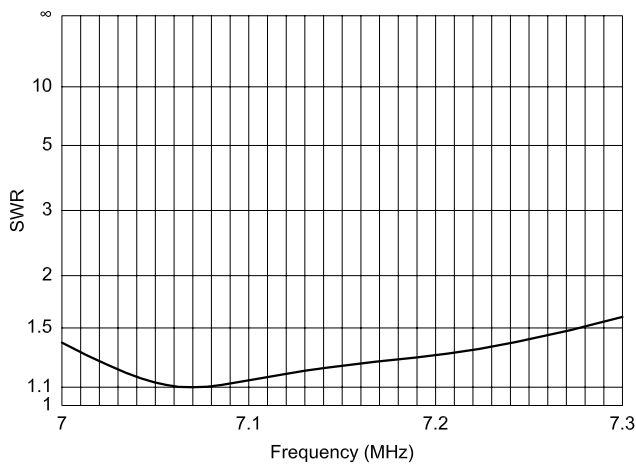
Fig 3—SWR of the 40 m SCV Array.
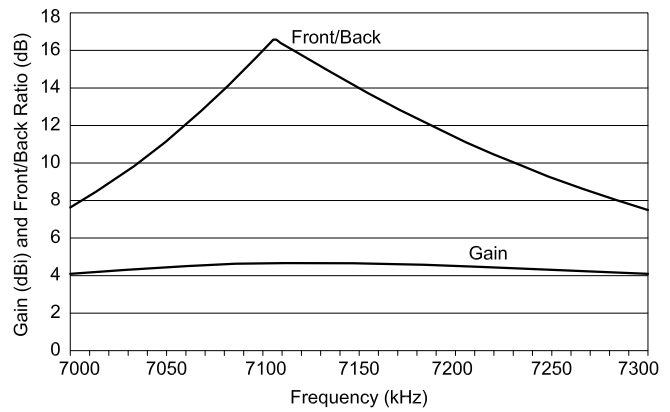
Fig 4—Gain and F/B versus frequency for the 40 m Rectangular SCV Array 8.5 m high.

direct match to 50 Ω, this compromises either the gain or the F/B. A better approach is to design for a feed-point impedance of 113 Ω, which can be matched to a 50-Ω source using a λ/4 matching section of 75-Ω coax.

This also slightly increases the SWR bandwidth of the antenna, since at frequencies above the design frequency the additional inductive component of the feed-point impedance is partially compensated by the matching section being—at the higher frequency—slightly longer than a λ/4. Similarly, below the design frequency the additional capacitive reactance of the antenna is partially compensated by the matching section's now being slightly shorter than a λ/4.

Computer Optimization

To see what was possible from this design, I wrote optimization software that steps through a number of values for each of the design parameters, constructed an *NEC-2* model of the resulting antenna (including the matching section) and then recorded the SWR, gain and F/B of each of the designs. I then analyzed the results using a spreadsheet to determine the optimum design.

In fact, there are many "optimums," since an improvement in one characteristic may result in a trade-off in another. I found the best way to locate my preferred combination of characteristics was to display the designs as points on an X-Y "scatter" chart, with the X axis representing F/B, the Y axis representing gain and the points color-coded according to SWR. Fig 2 shows an example. Notice that the gain, F/B and SWR figures represent worst-case values over the entire band.

During each optimizing run to generate a set of results like the one dis-
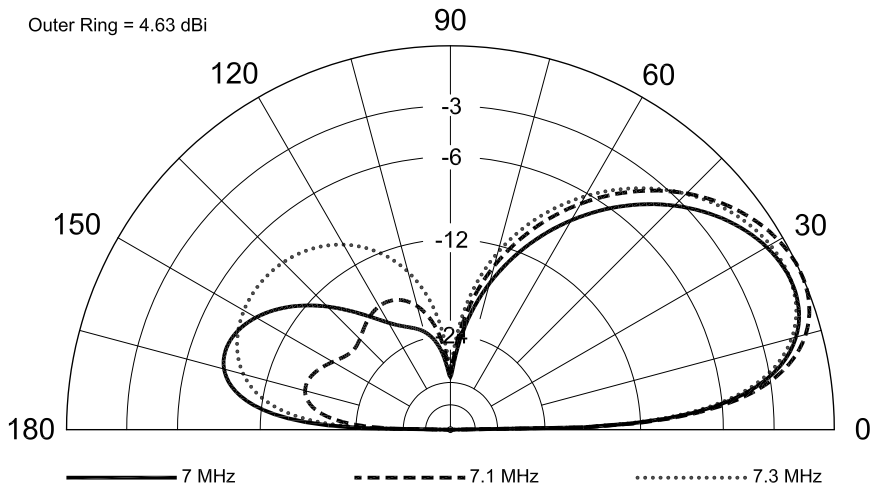
Fig 5—Elevation patterns of the 40 m Rectangular SCV Array at 7.0, 7.1 and 7.3 MHz.
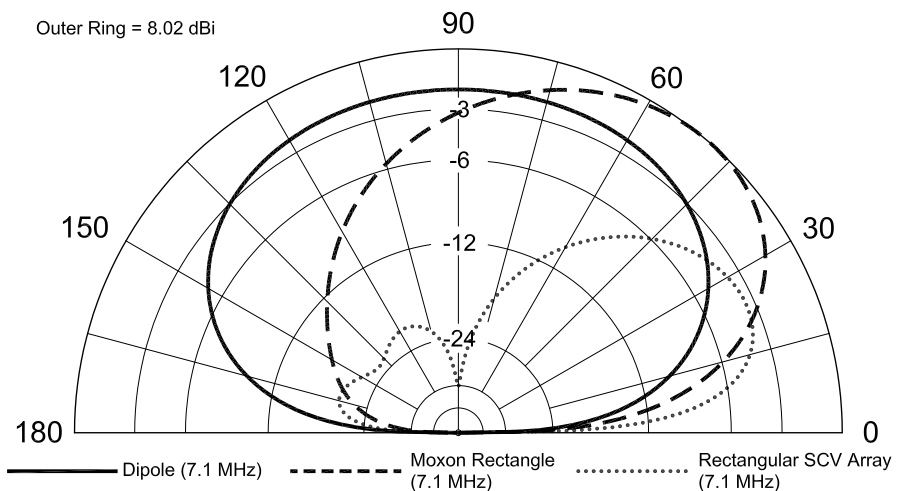
Fig 6—Elevation patterns of the 40 m Rectangular SCV Array, dipole and Moxon Rectangle.

played in Fig 2, the following parameters were varied:

- Height of the driven element and reflector.
- Width of the driven element.
- Width of the reflector.
- Spacing between the driven element and the reflector.

Each computer run generated and evaluated up to 10,000 designs, taking about 12 hours on my 600-MHz laptop. I did several runs optimizing designs for different bands and different maximum heights above ground. As Moxon warned, "... antenna problems such as this seem to be a high-risk area for those with computers."[8]

Because one of the key advantages of this antenna is its ability to achieve good performance at low heights above ground, one of the constraints I placed on the optimizing process was the maximum allowable height above ground for the highest part of the antenna. This is better than setting the height of the base above ground, which causes the optimization process to select taller, narrower designs that place the current concentrations in the center of each vertical side as high above ground as possible. Since this rather defeats the object of designing antennas for low heights, I chose instead to limit the maximum height of the highest part of the antenna, which favors wider, lower designs.

The optimization was run for three bands: 80 m, 40 m and 20 m. The inclusion of the 20-m band may seem surprising due to the widespread use of Yagis on this band. It was included for three reasons: First, although many amateurs can raise antennas to the 10 m or so required for effective Yagi performance, others cannot. Second, because of the advantage enjoyed by vertically polarized antennas over highly conductive ground mediums like salt water, the Rectangular SCV Array would be an excellent choice for an island DXpedition. Third, because it is a good band on which to inexpensively test a prototype.

For the 20-m and 40-m bands, I settled on two designs: a low design with a maximum (top) height of 0.2 λ and a medium-height design with a maximum height of 0.3 λ above ground. Although raising the maximum height to about 0.4 λ would further improve performance, this was considered unlikely in the face of the increased competition from horizontally polarized antennas at this height. For the 80-m band, I only optimized the 0.2-λ-high model, as the overall height of nearly 25 m required for the 0.3-λ version is

excessive for most amateurs.

An important consideration for computer modeling is the number of segments used in each wire. Convergence testing of early designs showed that 11 segments in the vertical wires and 30 segments in the horizontal wires converged to within a couple of hundredths of a decibel for all measurements while permitting reasonable computation times. All models were constructed using copper wire with a diameter of 2 mm (#12 AWG) and were evaluated over Sommerfeld-Norton ground with "medium" (0.005, 13) conductivity.

Optimum Designs

The designs in Table 1 were selected as optimum. The columns in the table should be interpreted as follows:

Band: the amateur band wavelength, in meters. The Region-1 allocations of 3.500-3.800 MHz and 14.000-14.350 MHz were used for the 80- and 20-m bands. The Region 2 allocation of 7.000-7.300 MHz was used for the 40-m band to make the

results more useful to American amateurs and in anticipation of the increased 40-m allocation for Region 1 as agreed at the WRC-03 conference in Geneva.

Maximum Height: The maximum height of any part of the antenna above ground. The lower value for each band is 0.2 λ, the higher value is 0.3 λ. On 80 m, the only value is for 0.2 λ.

Element Height: The height of the vertical sides of the driver and reflector.

Driver Width: The width of the horizontal sides of the driver.

Reflector Width: The width of the horizontal sides of the reflector. The height of the reflector was kept the same as the height of the driver to make it easier to stay within the maximum overall height constraint.

Element Spacing: The spacing between the driver and reflector.

Base Height: The height of the bottom of the driver and reflector above ground. Provided for convenience, this equals Maximum Height – Element Height.

Outer Ring = 4.63 dBi

7 MHz   7.1 MHz   7.3 MHz
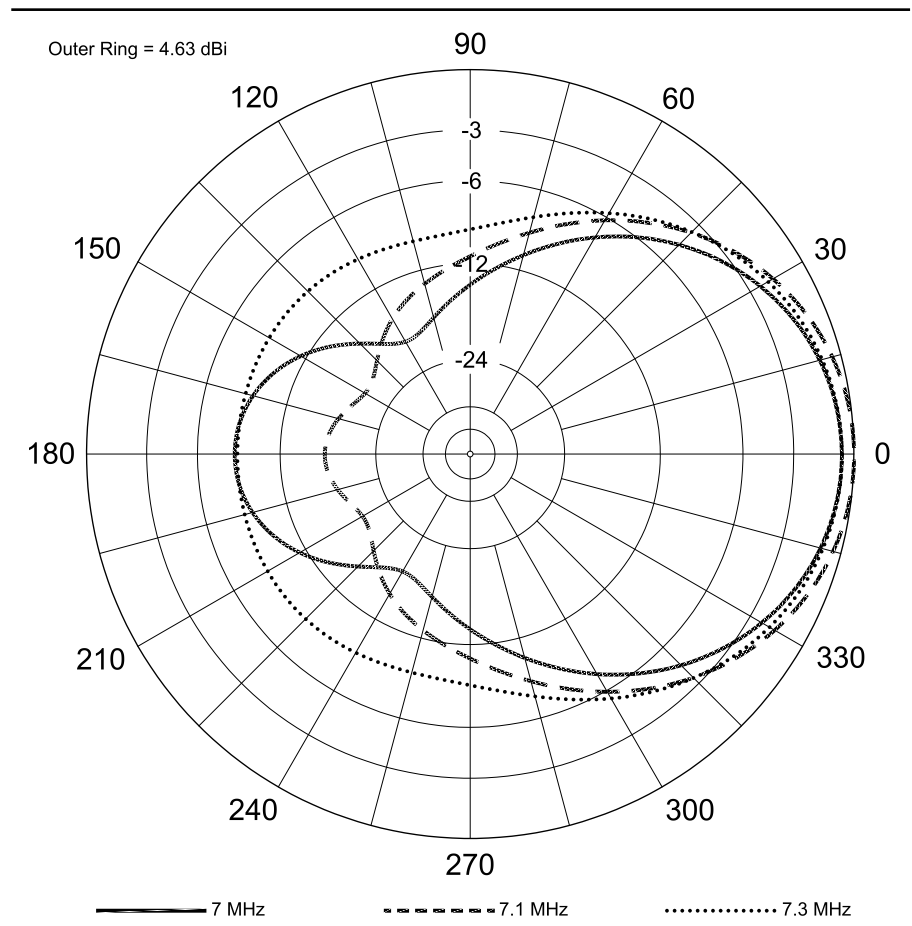
Fig 7—Azimuth patterns of the 40 m Rectangular SCV Array at 7.0, 7.1 and 7.3 MHz.

Match Length: The physical length of a $\lambda/4$ matching section if it is comprised of coax with a velocity factor of 0.65. This is the nominal velocity factor of RG-59B; however, because of variations in the actual velocity factor of purchased coax, it is recommended that matching sections be cut to size using a grid-dip oscillator or SWR analyzer.

Minimum Gain: The minimum gain achieved anywhere within the design band, in dBi.

Minimum F/B: The minimum F/B achieved anywhere in the design band, in dB.

Maximum SWR: The highest SWR anywhere in the design band.

All dimensions are in meters.

Performance

This section looks at the performance of one of the optimum designs, the 40-m array with a maximum height of 8.5 m above ground. The results for the other low designs are similar. First, let's get the basics out of the way with a plot of the antenna SWR, which appears as Fig 3. The SWR is below 1.5:1 over most of the band, so there should be no problem driving it directly from a solid-state rig without an ATU.

The graph in Fig 4 shows how the gain and F/B of the array vary with frequency. The gain is fairly constant between 4.1 and 4.7 dBi across the whole band, while the F/B peaks at 16.6 dB at 7.106 MHz and drops to about 7.5 dB at the band edges. This shows why the worst-case F/B drops fairly rapidly as the required bandwidth is increased, while gain is only slightly affected. It is also a caution about the antenna performance figures quoted by manufacturers, which often do not specify whether gain and F/B are specified for a single optimum frequency or are guaranteed across the entire band.

Turning next to the elevation pattern, Fig 5 shows the far-field elevation patterns at the band edges and at the frequency of the optimum F/B.

One plot is at 7.0 MHz, the second at 7.1 MHz and the other at 7.3 MHz. Notice that the elevation angles for maximum radiation are below 25° for all frequencies. At an elevation angle of 10°, the antenna still provides between 1.7 and 2.6 dBi gain.[9]

To see how this compares with horizontally polarized antennas at the same height, I plotted patterns of the Rectangular SCV Array, a Moxon Rectangle[10] and a dipole at 8.5 m above ground in Fig 6. Although the Moxon Rectangle has greater maximum gain than the Rectangular SCV Array (8.0 dBi as opposed to 4.8 dBi), its maximum gain is at an elevation angle of 50°. At an elevation angle of 10°, which is more useful for DX, the gain of the Moxon falls to –0.9 dBi compared with 2.6 dBi from the Rectangular SCV Array, giving the array a 3.5 dB advantage. The array is also superior to the dipole for all elevation angles below 35°, with an advantage of 7.4 dB at 10° elevation.

That supports the contention that a vertical array is a better choice for DX communication than a horizontally polarized antenna at low heights. Horizontally polarized antennas can be expected to outperform vertical arrays even at low angles of radiation when mounted half a wavelength or more above ground, unless the ground medium is unusually conductive (for example, salt water). The lower response of the array to high-angled radiation should also reduce QRM from nearby stations, provided they are out of ground-wave range.

Fig 7 shows the azimuth patterns

Outer Ring = 4.63 dBi

——— Phased Array (7.1 MHz)   ▪ ▪ ▪ ▪ ▪ Rectangular SCV Array (7.1 MHz)
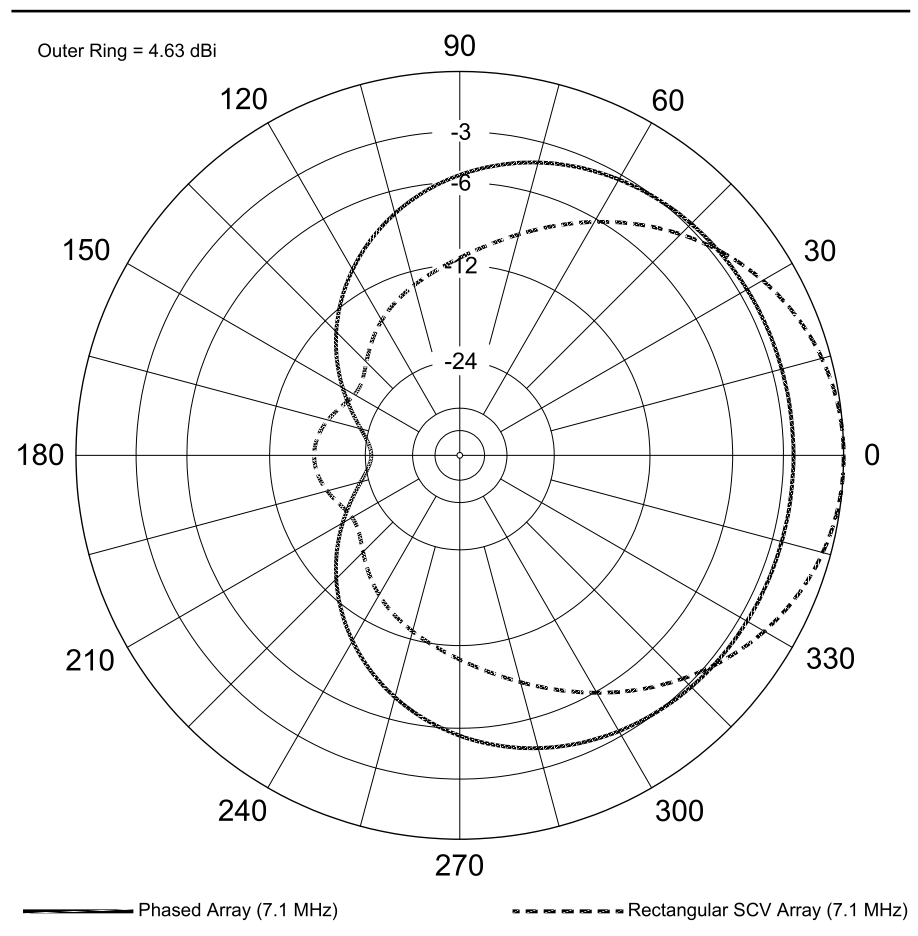
Fig 8—Azimuth patterns of the Rectangular SCV Array and a two-element phased array.

Table 2

Dimensions of the prototype

Band	Maximum Height(m)	Element Height(m)	Driver Width(m)	Reflector Width(m)	Element Space(m)	Base Height(m)	Match Length(m)	Minimum Gain(dB)	Minimum F/B(dB)	Maximum SWR
20	3.6	2.80	8.10	8.10	5.80	0.80	3.44	4.2	8.0	1.4

for the Rectangular SCV Array at frequencies of 7.0, 7.1 and 7.3 MHz. All plots are for an elevation angle of 24°. The –3dB beamwidth increases with frequency, ranging from 77° at 7.0 MHz to 90° at 7.3 MHz. It is interesting to compare the azimuth pattern with that of another common vertical array consisting of two vertical elements spaced λ/4 apart and fed 90° out of phase, as shown in Fig 8. The pattern of the Rectangular SCV Array has greater gain and is noticeably tighter than the cardioid pattern of the two-element phased vertical array. This is because each element of the Rectangular SCV Array is effectively acting as a broadside array of two in-phase radiators, so the pattern is closer to that of a four-element phased array.

Let us conclude by seeing how close we have gotten to the performance of the four-element rectangular array from *The ARRL Antenna Book* that inspired the journey. Fig 9 compares the azimuth patterns of the Rectangular SCV Array and the Four-Element Rectangular Array. The driven array has a tighter pattern with a beamwidth of 65° as opposed to 82° for the Rectangular SCV Array. It also has a somewhat higher gain of 6.1 dBi, as opposed to 4.8 dBi, an advantage of 1.3 dBi. However, this comes at the cost of more complex construction and the need to accurately phase the four separate elements.

An 80-M Design

The 80-m version also warrants some attention. It was not possible to keep the SWR under 2:1 for the whole of the 80-m band from 3.5 to 3.8 MHz. However, the graph in Fig 10 shows that the chosen design does keep the SWR below 2:1 from 3.500 to 3.740 MHz, a bandwidth of 6.6% of the center frequency.

Although it appears that raising the center frequency slightly could improve the SWR, this would be at the expense of both gain and F/B. I think it worthwhile to trade a small sacrifice in SWR, which can easily be corrected by an ATU, to keep as much gain and F/B as possible. Fig 11 shows the gain and F/B across the band. The best F/B is 15.7 dB at 3.596 MHz.

Outer Ring = 6.1 dBi

— 4 Element Rectangular Array (7.1 MHz)   – – – – Rectangular SCV Array (7.1 MHz)
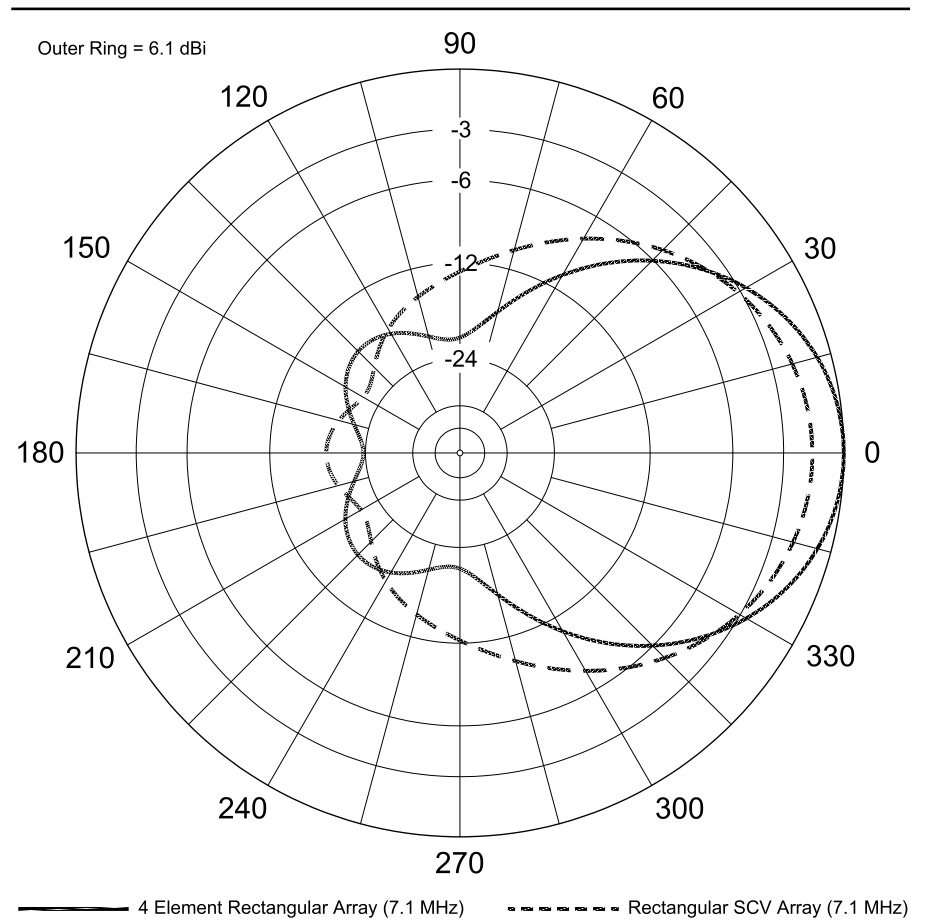
Fig 9—Azimuth patterns of the Rectangular SCV Array and the Four-Element Rectangular Array.
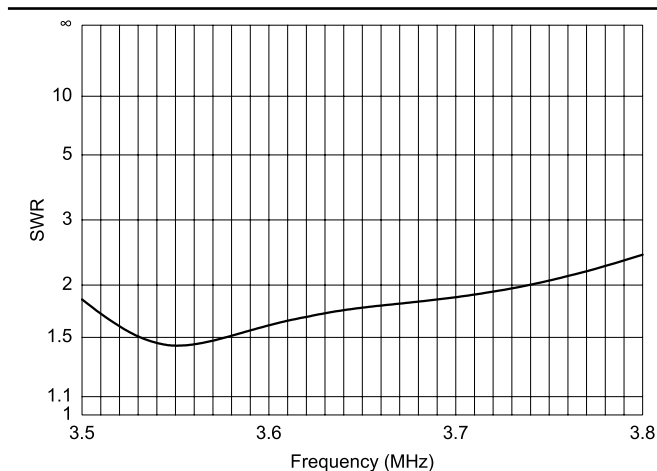
Fig 10—SWR of the 80-m Rectangular SCV Array.
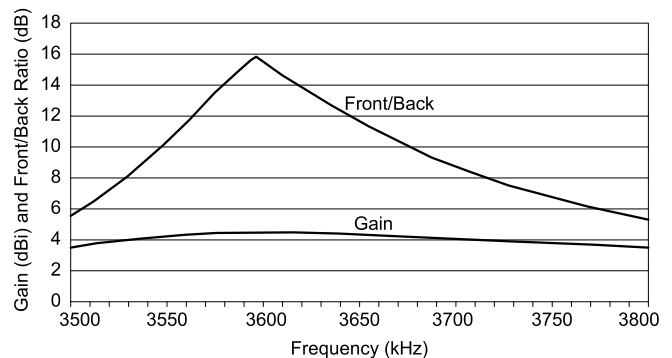
Fig 11—Gain and F/B versus frequency for the 80-m Rectangular SCV Array (maximum height 16.4 m).

Construction of a Prototype

I originally planned to construct a prototype of the 0.2-λ maximum height 20-m design, which stands 4.2 m off the ground. However, a trip to the local builder's yard showed that the most suitable supports in stock were only 3.6 m long, so I designed an even lower 20-m version with the dimensions shown in Table 2.

I bought four 3.6-m poles and drilled a hole in the bottom of each along the axis of the pole, into which I glued a spike made from a sawn-off tent peg to prevent the base of the pole from slipping. The driver and reflector were made out of 2.5 mm² stranded bare copper earth wire, which has a diameter of about 2 mm. They were each suspended between two of the poles using short lengths of nylon "ski rope." Two guy wires supported each of the poles. The resulting structure was fairly robust and quite suitable for a temporary Field Day or DXpedition antenna. The matching section was made from RG-59B coax, cut to length using a dip meter.

The SWR was as expected without any pruning. The antenna was erected to favor the path to Europe, and performance on that path was indistinguishable from a flattop dipole 10 m above ground and oriented in the same direction. Although I was initially disappointed—after all, my carefully planned and constructed beam was performing only as well as a dipole—comparison of the patterns predicted by *EZNEC* showed that this was expected, both antennas having a gain of 1.9 dBi at 10° elevation. The dipole had the advantage of being considerably higher than the array; and this again demonstrated that if you can raise even a simple horizontal antenna λ/2 above ground, then in most situations this is the better option.

One noticeable difference between the Rectangular SCV Array and the dipole was that the array picked up more local electrical interference, which meant that the signal-to-noise ratio was often below that of the dipole, even when the signal strengths were identical from both antennas. Notice also that the Rectangular SCV Array occupies quite a large area horizontally. The prototype took up a large portion of our garden and I am still trying to decide how I can fit a permanent 40-m array into it without upsetting my wife!

Conclusion

The Rectangular SCV Array is a useful alternative to horizontally polarized antennas when the maximum height of the antenna is restricted to significantly less than λ/2 above ground. This might be because of building restrictions or feasibility on the lower bands. For example, on the 80-m band, the 16.4 m supports needed for the array might be much more practical than a horizontally polarized beam mounted on top of a 40-m tower.

This antenna would be especially useful on island DXpeditions, where the high conductivity of a salt-water ground should give it a significant advantage over horizontally polarized antennas at any height. Compared to other vertically polarized arrays, the Rectangular SCV Array has a tighter pattern and more gain than a 90° spaced and phased array of two vertical elements. It comes close to the performance of a four-element rectangular array but with simpler construction and feeding. However, it does have the disadvantage that it is essentially a unidirectional antenna, there being no simple way to reverse the pattern as there is with driven arrays.

Notes

[1]L. B. Cebik, "Self-Contained Vertically Polarized Wire Antennas: A Family Album," **www.cebik.com/scv0.html**.

[2]Also known as the "Magnetic Slot" after Russell E. Prack, K5RP, "Magnetic Radiators—Low Profile Paired Verticals for HF," *The ARRL Antenna Compendium*, Volume 2 (Newington: ARRL, 1989), pp 39-41. However, since there is nothing especially "magnetic" about this antenna, I prefer Cebik's more descriptive name "Rectangular Self Contained Vertical."

[3]L. B. Cebik, "Part 3: The Rectangular Division," Figure 4, **www.cebik.com/scv3.html**.

[4]L. B. Cebik, "Part 1: The Group Picture," **www.cebik.com/scv1.html**.

[5]*The ARRL Antenna Book*, 19th edition (Newington, Connecticut: ARRL, 2002) p 8-27.

[6]*EZNEC* antenna modeling software is written by Roy Lewallen, W7EL. See **www. eznec.com**.

[7]In general, parasitic elements spaced closer than 1/8 λ will reduce the feed-point impedance, since the radiation from the parasitic element cancels out radiation from the driven element, even in the forward (desired) direction. However with more widely spaced elements the feed-point impedance is raised.

[8]L. Moxon, G6XN, *HF Antennas for All Locations*, second edition (Hertfordshire, England: RSGB, 1993) p 123.

[9]Of course this begs the question of which elevation angles are important for DX communication. Moxon suggests using 6° as representative of DX performance but cautions that "on the available evidence, however, it would be unwise to exclude higher angles up to at least 10° or so" (*op cit 8,* p 16). I have chosen to compare the performance of antennas for an elevation angle of 10°, which is a conservative choice, as the results for any lower angle would favor vertically polarized antennas even more.

[10]The Moxon Rectangle is a two-element horizontally polarized beam with the tips of the driven element and reflector bent inwards toward each other to increase coupling. The dimensions were calculated using the excellent computer program *MoxGen* written by AC6LA. It is available free from his Web site **www.qsl.net/ac6la/moxgen.html**. The algorithm used is from L. B. Cebik, "Designing Moxon Rectangles by Equation and by Model" at **www.cebik.com/moxgen.html**.

Andrew Roos has been a radio amateur since 2001. He has a Bachelor of Arts with Honors degree from Rhodes University and is the technical director and principal systems architect for a software development company in Cape Town, South Africa. His professional interests include the simulation and optimization of complex systems. The chairman of the Cape Town Amateur Radio Center, he regularly teaches courses for the Radio Amateur's Examination.

RF

By Zack Lau, W1VT

Why Homebrew 2-Meter Antenna Stacking Fails

Many hams stack 2-m beams in an attempt to get better signals. While the basic theory is quite easy to find on the Web and in antenna books, actual performance can be disappointing. In particular, the phasing networks don't seem to work quite right, so the SWR is considerably higher than expected—closer to 2:1 than 1:1. A 2:1 SWR is what you would expect from a kludge of a power divider—two equal lengths of 50 Ω cable connected to a T connector. In some cases, the pattern isn't even right, having two main lobes or a poor F/B. I'll show precisely why this happens and suggest techniques to insure success.

Fig 1 shows the typical installation for weak-signal SSB/CW use. The antennas are horizontally polarized and stacked on a vertical mast. Horizontal polarization is the convention for SSB/CW signals on all VHF and UHF bands. The elevation beamwidth is narrowed but not the azimuth, so it is easier to find weak signals. It can be a challenge to peak up weak signals

225 Main St
Newington, CT 06111-1494
zlau@arrl.org

with unknown beam headings. Cross polarization will result in a significant degradation of signal strengths. Because the radiating elements of the antenna are perpendicular to the mast, the interaction is negligible, given reasonable mast sizes. It can be a problem on 1296 MHz, where a typical mast becomes a significant fraction of a wavelength.[1]

Fig 2 shows the typical installation of stacked Yagis for FM and repeater use. The narrowing of the azimuth

[1]Notes appear on page 59.

beamwidth can be useful for selecting stations sharing the same frequency. The antennas are vertically polarized—as is the convention for amateur FM work on bands through 10 GHz, although horizontal polarization will often work on 10 meters. Long distance F2 and E-skip propagation modes found on 10 m scramble the polarization, so the signal could be horizontally polarized on receive, even though the transmit antenna was vertically polarized. The ionosphere is generally regarded as a good randomizer of polarization.[2] Jasik suggests
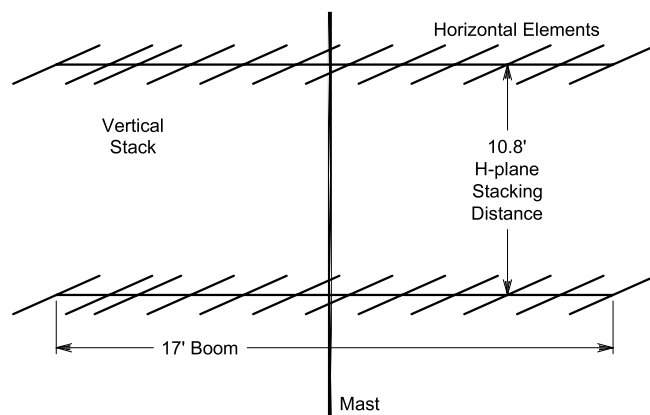
Fig 1—Horizontally polarized vertical stack used for weak signal SSB/CW.

choosing a polarization that will optimize radiation at the desired elevation angles.[3] A stacked pair offers a significant advantage over a single Yagi—it is very easy to design a rugged mechanical support structure that has a minimal effect on electrical performance. This is a serious problem with single-Yagi FM installations—a metal mast run up through the Yagi can seriously degrade performance.[4] Kent Britain, WA5VJB, did some experiments on a test range and saw gain degradations as high as 6 to 10 dB—nullifying the advantage of using a Yagi. A nonmetallic mast, such as fiberglass, can restore performance, if one doesn't mind the higher cost. A cross-boom structure can be useful for multiband arrays. I've often put 223 and 446 on opposite ends of a cross-boom array designed for FM simplex.

It is vitally important that the antennas be phased properly with both driven elements oriented the same way. If identical antennas are mounted mirror-image fashion, so that the feed points are closest to each other for minimum feedline length, they will be 180° out of phase. One of the driven elements must be "flipped" to maintain the proper phasing. An unexpected 180° phase shift is a quick recipe for failure. Fig 3 shows two ways of properly orienting stacked Yagis. Theoretically, one could add λ/2 of feedline to one antenna to restore proper phasing, but this looks to me like yet another path to disaster. Measurement of phase can be rather challenging at VHF. I prefer power splitting techniques that rely on balance and symmetry to maintain the proper phase relationship. There may also be complicated impedance issues to consider when designing asymmetrical phasing networks.

An unexpected 180° phase shift will result in a pattern null at the boresight of the antenna. This is easy to spot if you have a rotatable horizontal stack. Not only will the signal strength null at boresight, but signals will strongly peak on either side—you will have a beam with two major lobes. This isn't as easy to spot with a vertical stack used for SSB/CW, as the ground already introduces a pattern null at 0° elevation. Poor gain and F/B are signs that something is amiss. The main lobe will be difficult to examine unless you use the antenna for satellite and EME work; then the lobe is moved significantly skyward, off the horizon.

Fig 4 shows a typical power divider used to feed a pair of 2-m beams. The theory behind power dividers is quite
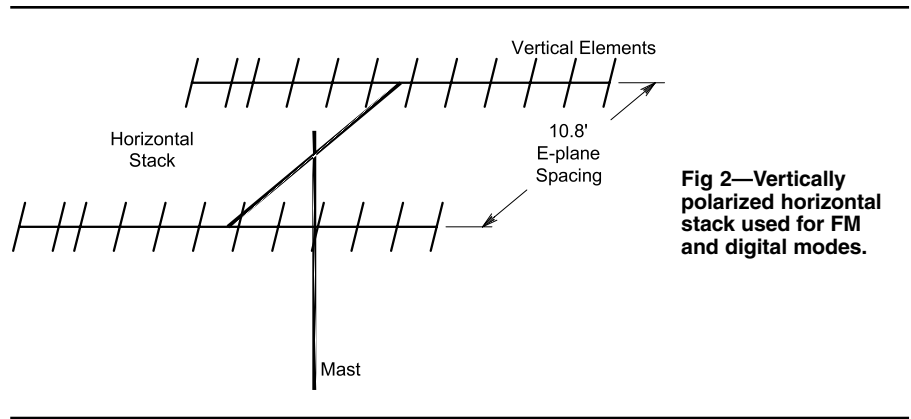
Fig 2—Vertically polarized horizontal stack used for FM and digital modes.
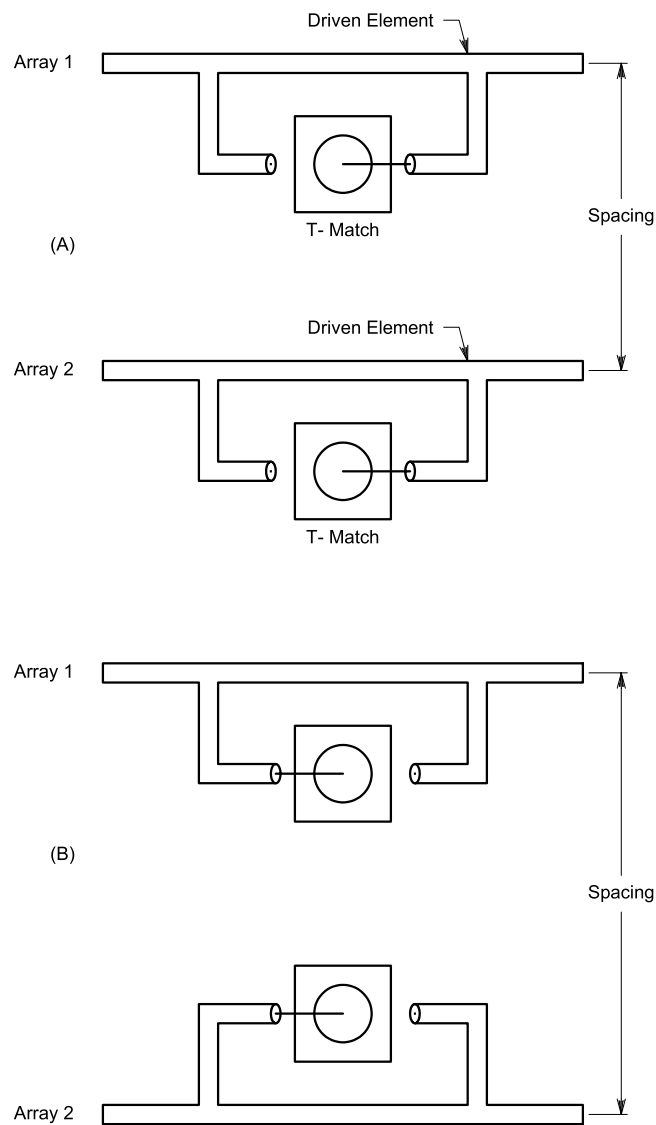
Fig 3—(A) The most straightforward way of mounting a pair of phased Yagis—they are translated in space by the stacking distance. (B) Mirror-imaged Yagis require a transposition of the driven element so the proper phase relationship is maintained. Note the connection of the center conductor of the coax connector to the driven element.

sound—an electrical quarter wavelength of 70-Ω coax is used to step up the impedance of a 50-Ω antenna to 100 Ω. Two 100-Ω loads in parallel form a 50-Ω load. In practice, 75-Ω cable is used instead of 70-Ω cable. This results in a step up impedance of Z_0^2/Z_{in} or 112.5 Ω. Parallel connecting two 112.5-Ω loads results in a 56.25-Ω load, which results in an SWR of 56.25/50 or 1.125. Not perfect, but this small a mismatch is difficult to measure, much less cause actual problems. In practice, quarter wavelength cables will be too short—you will need to add 50-Ω coax
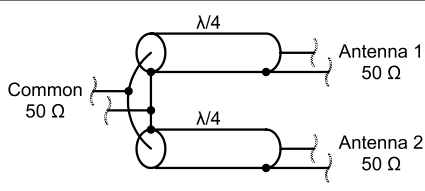
Fig 4—A simplistic power divider made out of 70-Ω coax.

Shield Connections not Shown
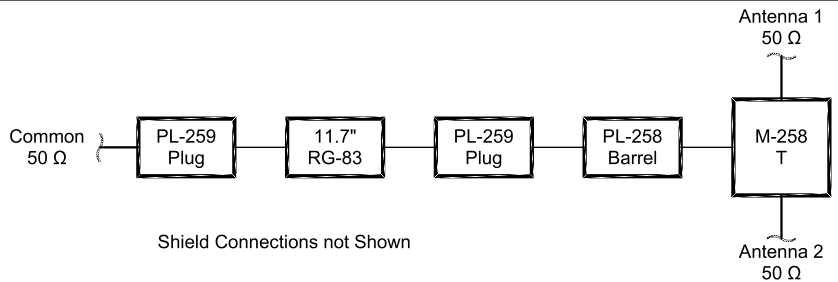
Fig 5—A power divider constructed out of RG-83 35-Ω coax. The tip-to-tip distance of the RG-83 cable with PL-259 UHF connectors is 11.7 inches.

Table 1
Microwave *Harmonica* Model of a 75-Ω Power Divider

```
*Design phasing harness using RG-11 and coaxial adapters.
Phasing: 6.8 in; distance between PL-259 connectors blk
CAB 1 10 DI=0.108in DO=0.28in p=0.75in er=2.3
CAB 10 11 DI=0.13in DO=0.34in p=0.1in er=3
CAB 11 12 DI=0.15in DO=0.45in p=0.25in er=3; PL259
CAB 12 13 DI=0.202 DO=0.469 P=1.1in er=3;PL 258 barrel
CAB 13 14 DI=0.156in DO=0.46in p=0.40in er=3 ;M358 Tee
CAB 14 20 DI=0.224in DO=0.454in p=0.82in er=3
CAB 14 40 DI=0.224in DO=0.454in p=0.82in er=3
CAB 20 21 DI=0.15in DO=0.45in p=0.25in er=3;PL259
CAB 21 22 DI=0.13in DO=0.34in p=0.1in er=3
CAB 22 24 DI=0.048in DO=0.32in p=0.75in er=2.3;RG-11 inside connector
CAB 24 25 DI=0.048in DO=0.32in p=phasing er=2.3
CAB 25 26 DI=0.048in DO=0.32in p=0.75in er=2.3;RG-11 inside connector
CAB 26 27 DI=0.13in DO=0.34in p=0.1in er=3
CAB 27 28 DI=0.15in DO=0.45in p=0.25in er=3;PL-259
CAB 28 29 DI=0.202 DO=0.469 P=1.1in er=3; PL-258 barrel
CAB 29 30 DI=0.15in DO=0.45in p=0.25in er=3;PL-259
CAB 30 31 DI=0.13in DO=0.34in p=0.1in er=3
CAB 31 32 DI=0.108in DO=0.28in p=0.75in er=3;RG-213 inside connector
res 32 0 r=50
CAB 40 41 DI=0.15in DO=0.45in p=0.25in er=3;PL259
CAB 41 42 DI=0.13in DO=0.34in p=0.1in er=3
CAB 42 44 DI=0.048in DO=0.32in p=0.75in er=2.3;RG-11 inside connector
CAB 44 45 DI=0.048in DO=0.32in p=phasing er=2.3
CAB 45 46 DI=0.048in DO=0.32in p=0.75in er=2.3;RG-11 inside connector
CAB 46 47 DI=0.13in DO=0.34in p=0.1in er=3
CAB 47 48 DI=0.15in DO=0.45in p=0.25in er=3;PL-259
CAB 48 49 DI=0.202 DO=0.469 P=1.1in er=3; PL-258 barrel
CAB 49 50 DI=0.15in DO=0.45in p=0.25in er=3;PL-259
CAB 50 51 DI=0.13in DO=0.34in p=0.1in er=3
CAB 51 52 DI=0.108in DO=0.28in p=0.75in er=3;RG-213 inside connector
res 52 0 r=50
divider:1por 1
end
freq
estp 140mhz 150mhz 50
end
```

Table 2
Power Divider made from 35-Ω RG-83 Coax and UHF Connectors

f (MHz)	Return Loss (dB)
110	18
120	20
130	24
132	25
136	27
138	28
140	30
142	31
144	31
146	31
148	31
150	30
152	29
156	27
160	24
170	20
175	19

Table 3
Power Divider made from RG-11 and UHF Connectors

f (MHz)	Return Loss(dB)
98	15
109	16
122	20
128	21
139	26
144	29
148	32
151	33
156	30
163	25
173	20

to reach the antenna feed points. Another suggestion is to add additional half wavelengths of 75-Ω coax.

Adding half wavelengths of 75-Ω coax works much better in theory than in practice at 2 m. Adding an extra wavelength of coax significantly narrows the bandwidth of the system, making it much more critical to cut the coax accurately. Thus, if a wavelength accuracy of 2% is acceptable, the tolerance may be 0.5% or less with a longer cable. The desire to measure the coax in physical, rather than electrical, units adds to the difficulty. This is done using the velocity factor, which is the ratio between the physical length and the electrical length. This can add another source of error—the velocity factor of low-loss foam coax can and does vary. Solid-dielectric polyethylene coax does have a rather reliable velocity factor of 0.66, but it has more loss. The frequency makes a big difference: 2% of a wavelength at 2 m is about an inch; at 70 cm it is just $1/3$ of an inch, while at 6 m it is three inches. I recommend sticking with λ/4 75-Ω phasing cables and using additional lengths of 50-Ω coax at 2 m. The situation may be different for a manufacturer, who can afford to set up custom jigs and electronic instrumentation to cut many cables to precisely the same electrical length.

The temperature coefficient of the coax is normally not a factor if you stick with λ/4 phasing lengths. Roger Norrod of the National Radio Astronomy Observatory measured temperature coefficients between 18 and 105 ppm/°C for ordinary braided coax.[5] It could be a problem with long phasing cables.

The stacking distance isn't that big of an issue. Most hams aren't going to stack antennas too far apart, as the distances are rather substantial. Too much distance won't hurt the gain; it just results in a pattern with excessive side lobes. Neither is stacking them a little closer than recommended a large problem: The gain goes down a bit and the pattern gets cleaner. It's not the sort of thing that results in system failure. Chapter 18 of *The ARRL Antenna book*, 20th edition, gives an example with a pair of 12-ft boom 2-m Yagis. The gain drops from 3.0 to 2.1 dB as the spacing is reduced from 10 ft to 5 ft.

The use of UHF connectors is a more insidious problem. They are barely acceptable at 2 m, adding a small low-impedance mismatch to the system. At 70 cm, they are bad enough to raise the SWR up to 1.5 to 1 when added indiscriminately to a matched

system. This becomes significant when you want to build a system out of higher impedance 75-Ω cable—such as the typical 75-Ω phasing network described in Fig 4. One solution is to skip the connectors and hard-wire the coax directly together. David Blaschke, W5UN, a famous 2-m EMEer, recommends this on a four-antenna phasing harness.[6] While this may not be a reliable long-term solution, it can be an effective technique for temporary stations.

A better solution is to use a power divider that is less sensitive to the low impedance of UHF connectors. Fig 5 shows an example using 35-Ω RG-83 coaxial cable. The effect of the coax connectors is much smaller—the length of the coax is much closer to the theoretical length when one ignores the effect of the connectors. A degree of tuning is also possible—you can "stretch" the λ/4 matching section with male and female UHF barrels. Thus, if the 35-Ω line section is cut too short, there may still be a quick way of tuning the system for a low SWR. This technique may also be useful with the 75-Ω system phasing system; adding some barrels may improve the match. I optimized the 35-Ω power divider by trial and error, varying the length of coax until I found the optimum length. Instead of soldering the shield to PL-259 connectors, I made temporary shield connections using setscrews threaded into the solder holes of the connector.[7]

How much cable to add or remove?

Table 4
Power Divider made from Square Aluminum and Round Brass Tubing

f (MHz)	Return Loss(dB)
136	22
138	23
140	24
142	26
143	26
144	27
145	28
146	29
147	30
148	30
149	30
150	31
151	31
152	31
153	30
155	29
157	28
160	25
165	22

Here are some rules of thumb. A half wavelength gets you completely around the Smith chart—back to where you started. There is no reason to vary a transmission line by more than a half wavelength for the purpose of impedance matching. A quarter wavelength gets you halfway around —this is as far away as you can get in terms of impedance transformation— thinking of a Smith chart as a map. I'd think of $1/16$ wavelength or less for small changes and more than $1/8$ for large changes. It is easier to remove cable than to add it.

RG-83 (35-Ω) coax is tough to find— the only source I have located in the last several years is the Wireman.[8] Expect to spend several bucks a foot. Many hams would still like to make a cheap phasing network out of 75-Ω cable and UHF connectors—if only someone else would design it. Therefore, I decided to model the 35-Ω phasing system with Microwave *Harmonica* and actual physical measurements of UHF connectors. With a good model of the system, I can go on to model other systems with UHF connectors. If the model is accurate, Microwave *Harmonica* should be able to predict the optimum coax lengths for a 75-Ω system.

I took apart UHF connectors and adapters to measure with a dial caliper. The M-358 T was easy—unscrew the center pin and the connector comes apart. I had to cut some other connectors apart with a band saw to make accurate measurements of the internal structure. They aren't totally complete—I ignored thin retaining rings as being insignificant at 2 m—why complicate the model with excessive detail? As you add more and more detail it becomes more difficult to spot errors. UHF connectors vary quite a bit—don't expect the connectors you buy at the next hamfest to match those in your junk box, much less the connectors that I used.

I then modified the 35-Ω power divider into one that uses a pair of 75-Ω coaxial cables. The effect of the UHF connectors is surprisingly large; the optimum length of the 75-Ω cables goes from a theoretical length of 15 inches to just 9.8 inches. This is the tip-to-tip distance of the cables, and it includes the length of the PL-259 connectors. The Microwave *Harmonica* model for this divider is shown in Table 1. Measured results for the two power dividers are shown in Tables 2 and 3. The performance of both is quite satisfactory. To make measurements, I substituted UG-146A/U adapters for the PL-258s. The Bird attenuators and

dummy loads in the ARRL Lab have N connectors—not UHF connectors. I also used a BNC to UHF adapter to connect the M-358 T connector to the female BNC of the return-loss coupler, a Mini-Circuits ZFDC-20-5.

Trying to get precise measurements with connectors that aren't the same impedance as the coax can be quite trying. You may optimize something in a test fixture, only to find mediocre performance when installed in the actual system. It may be more practical to empirically determine 75-Ω cable length. Trial-and-error methods can be surprisingly effective in optimizing antenna systems. Measure the frequency that results in the lowest SWR. If the frequency is too low, remove some cable. If it is too high, consider adding some UHF barrels or making the cable lengths longer. Modeling software presents a significant learning curve— I generally don't trust software until it begins to predict results that are verified with actual measurements. It can take quite a bit of time and effort to complete this loop. This method is especially practical with low-loss foam coax, which typically has a velocity factor that may vary. I've found that solid polyethylene coax typically comes very close to 0.66, but hams often want the lower loss of foam coax. Even better than an SWR meter is something that will measure impedance, such as an antenna analyzer or slotted line. The extra information provided may make the adjustment easier—an SWR meter just tells you how bad is the mismatch. This is analogous to knowing that you are five miles from your destination compared to knowing you are five miles due north of your destination. It can be quite comforting to know in which direction you should head, just as many hams want to know whether they need to remove or add cable. Who wants to wander around in SWR circles?

Yet another solution is to make a power divider out of aluminum and brass tubing. Square aluminum tubing is readily available at most hardware stores. Brass tubing comes in a wide variety of sizes so it is easy to select the one that will come close to the desired impedance. I presented a 70 cm design in the July 1999 *QEX*.[9] It can be easily scaled to 2 m by extending the length between coax connectors from 6.83 to 20.4 inches. You use the same brass and aluminum tubing sizes—just longer lengths. The measured return loss is shown in Table 3. Commercial power dividers constructed out of square aluminum tubing are manufactured by Directive

Systems.[10] They are willing to supply parts and materials to homebrewers.

It's hazardous to put too much trust in SWR/return-loss measurements. Can you optimize the length of a λ/4 power divider by measuring the optimum frequency for a λ/4 power divider and scaling it? The short answer is no. The uncertainties of typical dummy loads, SWR equipment and connectors is enough to make the calculation quite tenuous. For instance, according to Table 2, the optimum frequency is 151 MHz. Is this really an electrical λ/4 at 151 MHz, implying a velocity factor of 1.03? No, it is much more likely that the uncertainties involved resulted in an apparent return loss that maximized at 151 MHz.

While stacking Yagis can result in an extra 2.5 to 3 dB of gain, with more optimum antenna structures and patterns, it can be difficult to phase them properly. Hams have ruined perfectly good antenna arrays by "mirror-imaging" Yagis in an attempt to minimize coax length. They didn't realize that they were also inverting the phase of the driven elements. The popularity of UHF connectors is unfortunate—they significantly complicate efforts to stack Yagis at 2 m. They significantly skew the difference between simple theoretical calculations and reality. The situation gets even dicier when clever techniques are used, such as adding extra half waves of cable to

economize on connectors. While sophisticated engineering techniques could be used, it may be more practical for the average amateur to stick to more straightforward techniques, and use a little experimentation to optimize the system.

Notes
[1]C. Angle, N6CA, "Loop Yagis for 1296 MHz," *The ARRL Antenna Book*, 20th ed. (Newington, Connecticut: ARRL, 2003), pp 18-48 to 18-50.
[2]R. D. Straw, N6BV, Editor, *The ARRL Antenna Book*, 20th ed., page 23-7.
[3]H. Jasik, "Ionospheric Propagation," *Antenna Engineering Handbook*, (New York: McGraw Hill, 1961), p 33-21.
[4]K. Britain, WA5VJB, "Using Metal Booms to Support AMSAT Antennas," *Proceedings of the AMSAT-NA Eleventh Space Symposium and AMSAT Annual Meeting*, 1993, pp 56-58.
[5]R. D. Norrod, "Phase Stability Measurements versus Temperature for Several Coaxial Cable Types, National Radio Astronomy Observatory, Green Bank, West Virginia; **www.gb.nrao.edu/gbt/baseline/subpages/reports/MiscReports/cablePhaseStability.pdf**
[6] web.wt.net/~w5un/harness.jpg
[7]P. Karras, KE3FL, "More on Improved Connection to RG-6 CATV Coax," Hints and Kinks, *QST*, Nov 2001, p 61.
[8]**thewireman.com/who.html**; tel 800-727-WIRE (9473), fax 864-895-5811.
[9]Z. Lau, W1VT, "A 70-cm power divider," RF, *QEX*, July 1999, page 56-58.
[10]**www.directivesystems.com/**; tel 207-658-7758, fax 207-658-4337.   □□

Upcoming Conferences

ARRL TTF Forum at Hamvention

The ARRL's Technology Task Force (TTF) will hold its third Annual Forum at Dayton Hamvention on Sunday, May 16 from 10:15 AM to noon in Hara Arena. All Hamvention attendees are invited to attend.

TTF Chair and ARRL Central Division Vice Director Howard Huntington, K9KM, will moderate. All three of the TTF Working Groups will again be represented, including:
• 10:30 AM—High-Speed Multimedia (HSMM) Working Group: Mark Williams, AB8LN. Mark updates progress on merging Amateur Radio and networking technology via Radio Metropolitan Area Networks

(RMANs) using various node-connection methods.
• 11:00 AM—Digital Voice (DV) Working Group: Yoshikazu Nishimura, JA6UHL, AOR Japan and Matt Yellen, KB7TSE, of ICOM America. Yoshi will discuss ARD-9800 DV technical development and operating. Matt will talk about D-STAR DV development.
• 11:30 AM—Software-Defined Radio (SDR) Working Group: Gerald Youngblood, AC5OG, and Bob McGwier, N4HY. Gerald and Bob detail SDR advancements through open-source software development on the Flex Radio Systems SDR-1000.

Be there to learn about the latest in leading-edge Amateur Radio technology and what your League is planning for the future. Audience interaction is encouraged.—*Doug Smith, KF6DX; Chair, SDR Working Group*   □□

Letters to the Editor

Energy Conversion in Capacitors (Jul/Aug 2003)

Dear Doug:

I am rather disappointed that as the "Radio Amateurs Experimenter's" journal, neither yourself[1] nor any of your recent contributors[2, 3, 4] on the above topic mentioned the significance of electromagnetic radiation loss. In Note 3, you did not include some crucial works and the latest discussions in the *American Journal of Physics*.

Powell[5] in 1979 has essentially derived many of Warren Bruene's results (Note 4). More recently, Boykin[6] and myself[7] have also included radiation loss using point-dipole models. My paper has been accepted for the *American Journal of Physics* and is scheduled to appear in 2004.

The important points are:

1. According to the energy-partition theorem, which I have derived in Note 7, there is no breakdown of energy conservation.
2. In modeling, what you put in is what you get; so if you neglect radiation, as with the *PSpice* models used in Note 4, then you will still account for all the loss energy, but the physics is wrong.
3. In reality, radiation will account for some energy loss, either in the wires and even if your wires are of zero length then through the capacitors. Yes, capacitors are antennas (!) as I have shown in Note 7.

In the experiments of Jenkins, W5EU, as cited by Bruene, he would detect discrepancies between his measurements and Bruene's theory if component values were scaled down to the microhenries and picofarads range and the frequencies increased to megahertz and beyond. Perhaps he might want to do some proper experiments (which will involve some delicate RF measurements), to check the theory as published by Boykin and myself.

One interesting problem is the breakdown of the point-dipole approximation and thus the proper transient behavior (with radiation), which has not yet been solved. This seems to entail a more refined loop antenna model, such as those discussed by Chris Trask recently[8] in your journal.—*Tuck Choy, PhD, SMIEEE, MCIM; M0TCC/VK3CCA, Center for Materials Research, Department of Physics and Astronomy, University College London, United Kingdom;* tuckchoy@ieee.org

Notes
1. D. Smith, KF6DX, "Energy Conversion in Capacitors," *QEX*, Jul/Aug 2003, pp 52-54.
2. B. Kaune, "Letters to the Editor," *QEX*, Sep/Oct 2003, pp 58-59.
3. D. Smith reply to the above, *QEX*, Sep/Oct 2003, p 59.
4. W. Bruene, W5OLY, "Letters to the Editor," *QEX*, Nov/Dec 2003, pp 59-62.
5. R. A. Powell, "Two-capacitor problem: A more realistic view," *American Journal of Physics*, Vol 7 No 5, pp 460-462 (1979).
6. T. Boykin, D. Hite and N. Singh, "The Two-Capacitor Problem with Radiation," *American Journal of Physics*, Vol 70 No 4, pg 415-420 (2002).
7. T. C. Choy, "Capacitors Can Radiate: Further Results for the Two-Capacitor Problem," *American Journal of Physics*, to appear in Vol 74 (2004).
8. C. Trask, N7ZWY, "Active Loop Aerials for HF Reception Part 1: Practical Loop Aerial Design," *QEX*, Jul/Aug 2003, pp 35-42.

Dear Tuck,

Thanks for your unique contributions on this subject and for bringing those papers to the attention of our readers. In no way did I wish to imply that any breakdown in conservation of energy occurs in the two-capacitor problem. That is why I use the term conversion instead of loss. In an upcoming paper, I shall show that any real circuit resistance—including radiation resistance and the characteristic resistance of a transmission line or of free space—involves conversion of energy and *vice versa*. I believe I did mention in my article that radiation comes into play. The reference is at the top of the first column of p 53; but obviously, I did not quantify the effect. My sincere hope is that we will be able to show its significance precisely.—*Doug Smith, KF6DX, QEX Editor;* kf6dx@arrl.org

The Primary Source of Automotive RFI: Ignition Noise (Jan/Feb 2004)

Hi Doug,

I enjoyed this article very much, however, I cannot resist correcting his propagation of a great myth about Maxwell's equations. He states that Maxwell derived his four equations based on Faraday's work. This is both true and false.

Maxwell's great insight about the relationship between electricity and magnetism was one of the seminal events in classical physics. This relationship is as true today as it was in 1873 when he published "A Treatise on Electricity and Magnetism." He is justly famous. However, he did not derive the four equations we normally call Maxwell's equations. He arrived at a set of twenty equations of twenty variables in an obscure formulation of mathematical things called quaternions.

The man who first put these all together into four simple and powerful vector equations, in the form we know them today, was Oliver Heaviside. Among other things, this eccentric Victorian genius also was the first to derive what we now know as the "Telegrapher's Equation," which gives the relationship between voltage and current on transmission lines: The Smith chart is a graphical way of solving the Telegrapher's Equation. Since Heaviside also essentially invented the mathematical technique that we now call the Laplace Transform, he is undeservedly unknown.

There is an excellent biography of Oliver Heaviside titled *Oliver Heaviside: Sage in Solitude* written by Paul J. Nahin and published by the IEEE. I recommend it highly not only because it reveals the great influence this man had in the study of electromagnetism, but also because it is absolutely the best, most interesting biography I have ever read of a scientist—and I've read many. The book is just a terrific read; if you do read it, don't skip the preface!

Heaviside published most of his work in a rather obscure journal, now defunct, called *The Electrician* from about 1882 onwards. Many of these articles were collected together into a two-volume set titled *Electrical Papers*, published in 1892. Heaviside noted in his own diaries and journals—most of which still exist—that he had essentially done the transformation to what he called the "duplex" form of Maxwell's theory prior to 1885. By duplex, he meant the four symmetrical equations we now call Maxwell's equations. In Germany, Hertz did the same at about the same time. Some have claimed that Hertz did the work first, but Hertz himself acknowledged Heaviside's priority. Hertz and Heaviside were good friends through correspondence but they never met. Both Hertz and Heaviside did arrive at what is basically the modern differential form of those equations.

Subsequently, the equations were indeed usually referred to as the Hertz-Heaviside equations and much later, Einstein often called them the Maxwell-Hertz equations. It is only in the latter half of the 20th century that they have been called "Maxwell's equations," thereby depriving the others in this field some well-deserved credit.

This is not to denigrate the great work of Maxwell—he is one of my heroes because he broke the ground and

provided the insight. But he died before he could really refine his work and make it very useful. Heaviside tidied up the whole thing and introduced the use of vector calculus to replace the rather cumbersome quaternions that Maxwell used. An eminent Irish physicist, G. F. Fitzgerald, in 1893 wrote a review of Heaviside's *Electrical Papers* in which appears the following:

"Maxwell, like every other pioneer who does not live to explore the country he opened out, had not had time to investigate the most direct means of access to the country nor the most systematic way of exploring it. This has been reserved for Oliver Heaviside to do. Maxwell's treatise is encumbered with the debris of his brilliant lines of assault, of entrenched camps, of his battles. Oliver Heaviside has cleared these away, has opened up a direct route, has made a broad road and has explored a considerable trace of country. The maze of symbols, electric and magnetic potential, vector potential, electric force, current, displacement, magnetic force and induction, have been practically reduced to two, electric and magnetic force. Other quantities may be convenient, for the sake of calculation, to introduce, but they tell us little of the mechanism of electromagnetism."

"The duality of electricity and magnetism was an old and familiar fact. The inverse square law applied to both, every problem on one hand had its counterpart on the other. Oliver Heaviside has extended this to the whole of electromagnetism. By the assumption of the possibility of magnetic conduction, he has made all the equations symmetrical. Every mathematician can appreciate the value and beauty of this."

Regards—*Jim Koehler, VE5FP, 2258 June Rd, Courtenay, BC V9J 1X9;* **ve5fp@arrl.net**

Hi Jim,

Thanks for your note. I would have to say that Faraday, Gauss and Ampére also deserve credit for much of what Maxwell wrote, but Maxwell introduced the displacement field, essentially making his description of EM phenomena complete.—*Doug Smith, KF6DX,* QEX *Editor;* **kf6dx@arrl.org**

Hi Doug and Jim,

I enjoyed both of your comments very much. It's a real pleasure to learn more about the men who have brought about such scientific progress. I will have to read up more on Hertz and Heaviside—I know about Faraday and Maxwell, not to mention my idol Feynman. All the best,—*Stuart Downs, WY6EE, 11581*

Aspendell Dr, San Diego, CA 92131; **stuartdowns@earthlink.net**

Hi Doug,

I am disappointed with the article "The Primary Source of Automotive RFI: Ignition Noise." I feel the article is not at the technical level I expect in *QEX*. The author presents very little technical information, barely rising past the level suitable for an elementary auto-mechanics manual. He makes several sweeping statements without justification. His demonstrated use of test equipment is also at the beginner level.

The most disappointing part of the article is his final conclusion, stating that we must wait for the auto manufactures to fix the problem. This is a very bad attitude for any amateur publication to take, let alone the cutting edge experimentalist one. My experience is that the automobile companies have done an excellent job of reducing RFI to their installed AM/FM broadcast sets. They rightfully have little further interest in increasing their cost to help us. It is up to us, as it has always been, to find ways to make it better.

Going back at least to WW2, the ham literature is full of articles on shielding ignition systems. I had hoped there would be updated hints on further cleaning up the new systems without distributors. Stu waxes eloquently on the difficulty in being an experimentalist versus a theorist but then shows little evidence of experience with test equipment. In his spectrum displays, he leaves out the important settings of the analyzer bandwidth and sweep rate. Further, he doesn't distinguish what the background levels represent. Is it a quiet band or a neighbor running a California kilowatt? Without those parameters, his S/N measurements are meaningless.

Also glaring is the display of dc to 20 MHz, when we are only interested in a small band around 18 MHz and his inability to remove the display retrace. Similarly, his labeling in the caption is confused. The reference should be in dBm, not dB, and the scale in dB per division, not dBm per division. His "integration by grease pen" of the noise spectrum is simplistic and shows no appreciation for the nature of a repetitive impulse-noise source.

It is likely that a proper receiver IF filter and simple noise blanker could completely handle the noise shown. His call for a 40-dB improvement is completely unjustified. Not even the peaks of his displayed noise exceed 15 dB above his analyzer's noise floor anywhere near the 18-MHz ham band. His

theoretical bent is betrayed in his simplistic statements about magnetic versus electric field radiation and how RFI is dominated by the electric radiation. Where is his measurement? Where is his experiment?

He attempts to discourage the reader from the use of many well proven RFI shielding techniques by saying, "...no amount of grounding... will get rid of this type of noise...." Where is his evidence? After his early praise of Faraday (which seemed unrelated to the article), hasn't he ever heard of a Faraday shield? He should do some reading on grounding and shielding techniques, and then try some calculations on waveguides beyond cutoff. On all of my autos, I have found maintenance of the manufacturer's ground bonds (or adding some) has been very important to keeping an acceptable mobile radio environment.—*Steve Finberg, W1GSL, PO Box 397082, Cambridge, MA 02139-7082;* **w1gsl@mit.edu**

Doug,

I would refer Mr. Finberg, W1GSL, to the Jan/Feb 2000 issue of *QEX* or to **www.arrl.org/tis/info/pdf/ 001qex32.pdf**. The solution for ignition noise on new cars should be the same as that for older cars; that is, to shield (Faraday enclosure) the entire ignition system. The point of my article is the qualitative treatment of why and how ignition cables radiate—that's all! The solution has already been presented four years ago. Implementation may be different but the solution is the same. All the best —*Stu Downs*

A 200-W Power Amplifier (Jan/ Feb 2004)

Doug,

We thank Bob Miller, KE6F, for his comments (Letters to the Editor, Mar/ Apr 2004). In the schematic, Fig 3, as well as in the second paragraph on p 5, L2 should be T2, and L5 should be L2. T1 uses a binocular core (RF-400-0) with an integral center-tapped, single-turn winding, through which the primary is wound. L1 and L2 were wound on mandrels with the dimensions given and then removed from the mandrels. T2 has a center-tapped primary on the inside and the secondary on the outside. Each winding is one turn, with two pieces of copper tape in parallel. The varnish is removed from the inside top of the primary, where another piece of copper tape is soldered, forming the center tap. The inside edge of the primary is soldered to the board near C1; the outside of the secondary to

traces leading to ground and L2. Careful assembly is necessary to avoid shorts between the primary and secondary, while minimizing any gap that would reduce coupling. L3 and L4 are IF-transformer-type inductors that appear in the photo, as shiny square cans with round holes, on either side of T1.

If there are further questions, please e-mail Kent Potter at **potter@caltech.edu**. Also, we can provide copper tape for the transformers and a PC-board pattern.—*Takahiro Taniguchi, Kent Potter, KC6OKH and Dave Rutledge, KN6EK*

Tapped-Capacitor Matching Design (Mar/Apr 2004)

Doug,

Unfortunately, several errors and omissions occurred in my article. Fortunately, the *Excel* spreadsheet does the correct calculations. The following is a list of corrections in the article:

1. The article is missing the equation for *C2*. It is:

$$C2 \quad \frac{1}{\omega\,R2}\sqrt{\frac{R2 - Re3}{Re3}} \qquad \text{(Eq 1)}$$

2. The article is missing the equation for *Ce4*. It is:

$$Ce4 \quad C2\frac{(\omega\,R2\,C2)^2 + 1}{(\omega\,R2\,C2)^2} \qquad \text{(Eq 2)}$$

The line on the spreadsheet for $Q\mathrm{p}(Re2\|Ce2)$ should be labeled $Q\mathrm{pA}(Re2\|Ce2)$ and the equation on that line should be $Q\mathrm{pA} = Re2/(1/\ \omega\ *Ce2))$ for clarity. The line on the spreadsheet for $Q\mathrm{p}(R2\|C2)$ should be labeled $Q\mathrm{pBA}(R2\|C2)$ and the equation on that line should be $Q\mathrm{pB} = R2/(1/\omega\ *C2))$ for clarity. The equation on the spreadsheet for *Re3* should be $Re3 = Re2/(1 + Q\mathrm{pA}{}^\wedge 2)$. The equation on the spreadsheet for *Ce4* should be $Ce4 = C2/(Q\mathrm{pB}{}^\wedge 2)$.

The revised download file, 0403Evans.zip, contains a new version of the spreadsheet with the text errors corrected (the old spreadsheet correctly calculated the right answers).

The derivations for *Ce3* and *Ce4* are not in the original article, and I feel that a derivation is needed. Therefore, I've supplied a complete derivation that I hope is easier to follow. That too,

is a part of the updated download file. — *Randy Evans, KJ6PO, 2688 Middleborough Cir, San Jose, CA 95132;* **randallgrayevans@yahoo.com** ☐☐

Next Issue in QEX/Communications Quarterly

In the Jul/Aug issue, Tom McDermott, N5EG, and Karl Ireland bring us a nifty piece of test equipment for your shack: a low-cost 100-MHz vector network analyzer with a USB interface. Tom and Karl deftly present details of their instrument from conception to construction and alignment. Included in the discussion are certain design decisions they made along the way. The authors tell us how and why the thing works and what it can do for you.

Although not for the faint of heart, it is a project you can build! As few others do, this network analyzer gives you significant capabilities without breaking your bank account. ☐☐